ALMA MATER STUDIORUM
UNIVERSITÀ DI BOLOGNA

DEPARTMENT OF PHYSICS AND ASTRONOMY "A. RIGHI"

SECOND CYCLE DEGREE

PHYSICS

QUANTUM CIRCUIT EVOLUTION WITH FREE FERMIONS IN DISGUISE

Supervisor
Prof. Lorenzo Piroli

Co-supervisor
Dr. Dávid György Szász-Schagrin

Defended by
Daniele Cristani

Graduation Session / 12/2025

Academic Year 2024/2025

Abstract

The applications of free fermions in statistical physics and quantum computation have long been well established. In particular, the Jordan–Wigner (JW) transformation can map certain spin$-1/2$ chains to free fermionic systems, revealing their complete solvability. On the other hand, free fermionic systems are also classically simulable and therefore provide useful benchmarks for experimental implementations of quantum computers. Recently, Free Fermions in Disguise (FFD) have been introduced: these are new spin$-1/2$ chain models that can be mapped to free fermions, but not through the standard Jordan–Wigner transformation. In this thesis, we address the problem of constructing quantum circuits from Free Fermions in Disguise. This is challenging because not all circuits built from these models remain free fermionic, in contrast to the JW-diagonalizable case. We present a systematic approach to demonstrate that some circuits previously proposed in the literature are indeed free fermionic. We then study the circuit dynamics of certain observables expressible in terms of fermionic operators for small system sizes, performing an exact-diagonalization check comparing the spin and fermionic evolutions. These results raise new questions about the classical simulability of free fermions in disguise, which appears to be a more subtle issue than in standard JW-diagonalizable models.

Contents

Introduction

Free systems have always been useful models in physics. Indeed, working with non-interacting particles often ensures that the model can be solved exactly, making such systems powerful tools for approximating more complex theories or for exploring new phenomena in a simplified framework.

In particular, free fermionic systems play a major role in the context of statistical and many-body physics. They describe non-interacting fermionic particles and represent the standard models for free electrons, as well as effective descriptions of weakly interacting electronic systems. Their relevance also comes from their close relationship with spin systems, which were originally introduced to model ferromagnetism.

Already in 1928, Jordan and Wigner developed what is now known as the *Jordan–Wigner transformation* (JW) [1], a mapping that converts spin degrees of freedom into fermionic ones. This transformation has been extremely powerful in solving several spin$-1/2$ chains, particularly in one-dimension. For models such as the XX chain, the XY chain, and the Quantum Ising Model, the Jordan–Wigner mapping transforms the spin Hamiltonian into a free fermionic model, making a full analytical solution possible. This was first achieved in 1961 in [2] (see also [3, 4] for a more modern treatment). The same authors later showed in [5] that the transformation can also be used to analytically solve the two-dimensional classical Ising model.

Various generalizations of the Jordan–Wigner transformation have been proposed [6–12], but the first rigorous criterion for determining whether a given spin Hamiltonian can be mapped to a free fermionic one was introduced in [13] using graph-theoretic methods (see also [14]).

Free fermionic systems are also of great importance in quantum computation, largely because of their relation with classical simulability. Normally, simulating a quantum system on a classical computer requires resources that increase exponentially with the system size. However, some special quantum systems, called *classically simulable*, can be simulated using only polynomial resources. These kinds of systems are really useful as rare benchmarks for testing experimental implementation of quantum computers. Free fermionic models are a key example of such systems.

Indeed, an n-dimensional free fermionic system initialized in a *fermionic Gaussian state* [15–17], a special class of states that satisfy Wick's theorem [18–20], is fully characterized by a $2n \times 2n$ matrix of two-point correlators, known as the *correlation matrix*. This characterization makes such systems classically simulable. Furthermore, *matchgate circuits*, introduced in [21], are a class of efficiently simulable quantum circuits which makes use of two-qubit gates called matchgates, which can each be mapped to fermionic Gaussian operators through the Jordan-Wigner transformation [22–24]. In addition, as spin$-1/2$ chains are completely equivalent to qubit systems, it is straightforward to understand the relevance of chains with a free fermionic spectrum for quantum computation.

Starting from these premises, a natural question to ask is whether all spin$-1/2$ chains with a free fermionic spectrum can be mapped to free fermions through the Jordan–Wigner transformation or one of its extensions. The answer is no. Indeed, already in [25–27], models that have a free fermionic spectrum but are not Jordan–Wigner diagonalizable were studied.

Then, in [28], Fendley introduced the *Free Fermions in Disguise* (FFD) models, the main focus of this

thesis. These models admit a mapping to free fermions, but only in the case of open boundary conditions and through a highly non-linear and non-local transformation. A graph-theoretic solvability criterion for these models was introduced in [29], later extended to higher dimensions in [30] and generalized further in [31], for a chain defined as an interpolation between the FFD model of [28] and the chain studied in [26].

Free Fermions in Disguise are particularly interesting since they provide a novel alternative to the conventional JW–diagonalizable free fermionic spin chains. This naturally motivates the idea of building quantum circuits from these systems and investigating their classical simulability, to observe whether they behave in ways similar to the well-known JW examples.

In [32], an initial attempt at this was made. However, some unexpected difficulties not present in JW models appeared, as circuits derived from FFD models are not necessarily free fermionic quantum circuits, namely circuits represented in terms of a unitary operator generated by a free fermionic Hamiltonian. Losing this property would imply losing the free fermionic structure of the original models and, consequently, their most significant features. In [32], the free fermionic nature of a specific FFD-based circuit was established, while other circuit were conjectured to be free fermionic on the basis of numerical evidence, one of those shown to be free fermionic in [33].

On the other hand, [34] investigated for the first time the dynamics of Free Fermions in Disguise models by examining a particular infinite-temperature correlation function. They computed both the continuous-time evolution and a discrete-time evolution implemented through the free fermionic circuit introduced in [32]. However, this analysis also revealed additional challenges. One major issue is the inverse problem: rewriting spin operators in terms of fermionic ones. For JW-diagonalizable models this is relatively simple, but for FFD models it becomes much harder due to the complicated mapping and the exponential degeneracy of the energy spectrum. In [34], the authors managed to express some local observables in terms of fermionic operators, offering a first partial solution. Later, in [35], the full Hilbert-space structure of FFD models was determined, resolving the degeneracies entirely and providing a solid basis for a more systematic attempt at solving the inverse problem.

In this thesis, we further investigated the open questions regarding Free Fermions in Disguise. In particular, our analysis follows the results we presented in [36]. There, we established the free fermionic nature of some of the circuits introduced in [32], using a systematic method applicable to different circuit architectures. Notably, we proved for the first time the free fermionicity of a circuit with constant-depth, a feature that makes it more suitable for implementation on present-day noisy quantum devices [37].

Moreover, we examined the circuit dynamics of the edge operator, a specific local operator that naturally arises in the construction of fermionic operators for FFD models. This operator had already been shown in [34] to admit a fermionic representation in the Hamiltonian setting. Specifically, we generalized this construction for circuits and performed a form of exact-diagonalization check by comparing the time evolution of the edge operator computed in both the spin and fermionic representations.

Finally, we addressed the question of simulability: in [36] we proved that the dynamics of local observables expressible in terms of fermionic operators, such as the edge operator, can be efficiently simulated on a classical computer. However, we will not examine this aspect in detail in the present thesis.

The structure of this thesis is as follows. In Chapter 1, we introduce free fermionic systems, characterinzg them through their Hamiltonians and their spectra, discussing methods for their diagonalization. We then introduce spin chains and the Jordan–Wigner transformation, establishing the aforementioned connection between spin and fermionic systems. Finally, we present an example of a JW–diagonalizable model, specifically the XY chain.

In Chapter 2, we examine the relationship between free fermionic systems, classical simulability, and quantum computation. We begin by defining quantum circuits and introducing fundamental concepts of quantum simulation. We then study matchgate circuits, highlighting their connection to free fermions and

their classical simulability. Later, we discuss fermionic Gaussian states: we provide their definition and demonstrate how they can be fully characterized by the correlation matrix. Finally, we provide a precise definition of free fermionic quantum circuits and show that any circuit constructed from JW-diagonalizable models is necessarily free fermionic.

In Chapter 3, we provide an overview of the state of the art regarding Free Fermions in Disguise. We begin with an introduction to these models, then followed by a presentation of their solution and the construction of the mapping to free fermions. Next, we discuss the inverse problem, summarizing the previously known results of [34] and the full characterization of the Hilbert-space structure [35]. Finally, we introduce the circuits constructed from FFD models that were conjectured to be free fermionic in [32], including the proof provided there for one particular circuit.

To conclude, in Chapter 4 we present our new results on Free Fermions in Disguise. First, we show the proof of the free fermionic nature of the previously mentioned quantum circuits, as we established in [36]. We then focus on the dynamics of the edge operator, providing an exact-diagonalization check by comparing its fermionic evolution with its circuit evolution. Finally, we conclude with brief remarks on the classical simulability of these circuits.

Chapter 1

Free Fermionic Systems and the Jordan-Wigner transformation

Free fermionic systems are defined as collections of non-interacting fermionic particles. These models are of fundamental importance to many-body physics, with many applications across various subfields. Specifically, they provide an effective description for weakly interacting electrons and frequently arise as collective excitations within condensed matter systems [38]. An example is given by the Landau quasiparticles in Fermi liquids, which exhibit free-particle behaviour. Many properties of metals can be accurately described using the band theory of these collective electrons [39].

From an analytical perspective, the relevance of free fermionic models comes from their solvability and integrability. In particular, in one dimension they give the natural framework to describe several integrable spin chains, including the quantum Ising model, the XX chain, the XY chain and also the $2-$dimensional classical Ising model [2, 5]. This connection is established via the Jordan-Wigner transformation (hereafter JW) [1], a mapping that relates spin operators to fermionic creation and annihilation operators.

In this chapter we provide an introduction to free fermionic systems and the Jordan-Wigner transformation.

We start with Section 1.1 by providing mathematical and physical definitions of bosons and fermions and addressing the underlying differences in physical behaviour between these two classes of quantum particles. We then describe them employing the second quantization formalism, concluding with a discussion on free bosonic and fermionic systems. In Section 1.2, we define free fermionic systems, following two different approaches. Initially, we introduce and diagonalize the most generic quadratic fermionic Hamiltonian, and subsequently, we define the system through the characteristics of its energy spectrum. In Section 1.3, we introduce general spin chain models and show their connection to fermionic systems via the Jordan-Wigner transformation. Finally, in Section 1.4 we illustrate these concepts through the explicit example of the XY-chain. We utilize the JW trasformation to map it to an equivalent free fermionic system, which we then solve by diagonalizing the fermionic quadratic Hamiltonian.

1.1 Bosons and fermions

In quantum mechanics, we can distinguish two fundamental classes of particles: **bosons** and **fermions** [40]. At the most fundamental level, their difference lies in their spin. Indeed, bosons possess integer spin, whereas fermions have half-integer spin. However, the distinction between these particles becomes most apparent when considering many-particle systems, where their collective behavior plays a central role. In particular,

bosons and fermions exhibit different behaviors under particle exchange: the state vector of a system of bosons is symmetric, while that of fermions is antisymmetric. Let us discuss the particles' different statistics more in detail.

In classical mechanics, it is, in principle, possible to determine the exact trajectory of a set of identical particles if their initial positions, momenta, and equations of motion are known. This allows, at least conceptually, to track and distinguish individual particles over time. In contrast, quantum mechanics fundamentally prohibits this. Indeed, the Heisenberg uncertainty principle dictates that a particle's position and momentum cannot be simultaneously specified with arbitrary precision. As a result, quantum particles cannot move along a well-defined trajectory that could be followed deterministically and are therefore fundamentally indistinguishable, since their individual evolution cannot be tracked given some initial conditions. This indistinguishability, implies that moving around particles in a N particle system, should not change physical properties in any way [41].

Mathematically, we describe the state of a composite quantum system with a *state vector* $|\Psi\rangle$, which for an $N-$particle system can be written as $|\psi_1\psi_2\dots\psi_N\rangle$. Then, the invariance of the system's physical properties under a permutation P of the particles, implies that the state vector can at most acquire a global phase:

$$\left|\psi_{P(1)}\psi_{P(2)}\dots\psi_{P(N)}\right\rangle = e^{i\phi_P}\left|\psi_1\psi_2\dots\psi_N\right\rangle . \tag{1.1}$$

The set of all possible permutations of N objects is a group, called *permutation group* and denoted by S_N. Any permutation $P \in S_N$, can be decomposed as a product of elementary permutations (also called transpositions) σ_i, which consist in an exchange of neighboring elements:

$$\sigma_i : (1,\dots,i,i+1,\dots,N) \to (1,\dots,i+1,i,\dots,N) . \tag{1.2}$$

These transpositions have the following three properties:

$$\begin{aligned} &1)\ \sigma_i\sigma_j = \sigma_j\sigma_i \ \text{ if } \ |i-j|>2 , \\ &2)\ \sigma_i\sigma_{i+1}\sigma_i = \sigma_{i+1}\sigma_i\sigma_{i+1} , \\ &3)\ \sigma_i^2 = 1 . \end{aligned} \tag{1.3}$$

The *parity* of a permutation is defined as:

$$(-1)^P = \begin{cases} +1 & \text{if } P \text{ is given by an } \textit{even} \text{ number of transpositions} \\ -1 & \text{if } P \text{ is given by an } \textit{odd} \text{ number of transpositions} \end{cases} \tag{1.4}$$

While the decomposition of a given permutation into a product of elementary transpositions is not unique, all such decompositions share the same parity, which, therefore, constitutes an intrinsic property of the permutation itself.

Let us use a chosen decomposition of a permutation P in terms of transpositions $P = \sigma_{\alpha_1}\dots\sigma_{\alpha_k}$, to rewrite (1.1) as:

$$\begin{aligned} \left|\psi_{P(1)}\psi_{P(2)}\dots\psi_{P(N)}\right\rangle &= \left|\psi_{\sigma_{\alpha_1}\dots\sigma_{\alpha_k}(1)}\dots\psi_{\sigma_{\alpha_1}\dots\sigma_{\alpha_k}(N)}\right\rangle = \\ &= e^{i\phi_1}\left|\psi_{\sigma_{\alpha_2}\dots\sigma_{\alpha_k}(1)}\dots\psi_{\sigma_{\alpha_2}\dots\sigma_{\alpha_k}(N)}\right\rangle = \\ &= \dots = e^{i\phi_1}\dots e^{i\phi_N}\left|\psi_1\psi_2\dots\psi_N\right\rangle . \end{aligned} \tag{1.5}$$

The properties (1.3) imply the following conditions on the phases $\phi_1,\dots,\phi_N$:

$$\begin{aligned} &1)\ e^{i\phi_i}e^{i\phi_j} = e^{i\phi_j}e^{i\phi_i} \text{ for } |i-j|>2, \text{ which is always true} , \\ &2)\ e^{i\phi_i}e^{i\phi_{i+1}}e^{i\phi_i} = e^{i\phi_{i+1}}e^{i\phi_i}e^{i\phi_{i+1}} \text{ which holds iff } \phi_i=\phi_j=\phi,\ \forall i,j \\ &3)\ e^{i2\phi} = 1 \text{ which holds iff } \phi = 0,\pi . \end{aligned} \tag{1.6}$$

Therefore, we can conclude that there are two possible situations:

- $\phi = 0$, which implies $\phi_P = 0$ for any P: the state vector is completely invariant, or *symmetric* under any exchange of particles
$$\left|\psi_{P(1)}\psi_{P(2)}\dots\psi_{P(N)}\right\rangle = |\psi_1\psi_2\dots\psi_N\rangle \ . \tag{1.7}$$
This kind of particles are called **bosons**.

- $\phi = \pi$, which implies $\phi_P = 0, \pi$ depending on the parity of P: the state vector is *antisymmetric*, changing sign if the permutation is odd
$$\left|\psi_{P(1)}\psi_{P(2)}\dots\psi_{P(N)}\right\rangle = (-1)^P\,|\psi_1\psi_2\dots\psi_N\rangle \ . \tag{1.8}$$
This kind of particles are called **fermions**.

1.1.1 Bosons and Fermions in second quantization

The second quantization formalism offers a concise and convenient framework for describing systems of many identical particles, regardless of their statistics. Within this formalism, the distinction between bosons and fermions is entirely encoded by some algebraic relations.

This framework relies on the definition of *creation* and *annihilation* operators, which we denote by $a_i^\dagger$ and a_i when we are not specifying whether they are bosonic or fermionic. These operators act on a quantum state by creating or destroying a particle in state i. We can then construct the Hilbert space starting from the vacuum state $|0\rangle$, from which all other quantum states can be obtained through successive applications of the creation operators $a_i^\dagger$:

$$|\Psi\rangle = \mathcal{N}(a_1^\dagger)^{n_1}(a_2^\dagger)^{n_2}\dots(a_N^\dagger)^{n_N}\,|0\rangle \equiv |n_1 n_2\dots n_N\rangle \ , \tag{1.9}$$

where $\mathcal{N}$ is a normalization constant and $n_i \in \mathbb{N}_0$. Conversely, applying an annihilation operator a_i to the vacuum or to any state which does not have a particle in state i yields zero. $a_i^\dagger$ and a_i are defined to obey commutation or anticommutation relations for bosons or fermions respectively.

Bosonic operators, denoted here by $b_i^\dagger, b_i$, must satisfy the following *canonical commutation relations* (CCR):

$$[b_i, b_j^\dagger] = \delta_{ij}\,, \qquad [b_i, b_j] = [b_i^\dagger, b_j^\dagger] = 0\,, \tag{1.10}$$

where $[A, B] = AB - BA$ is the commutator. If we consider $b_i^\dagger$ as "creating" a boson in state i, it is clear that (1.10) imply the symmetry under exchange:

$$b_i^\dagger b_j^\dagger\,|0\rangle = b_j^\dagger b_i^\dagger\,|0\rangle \ . \tag{1.11}$$

This does not put any restrictions on the number of particles that can be in the same quantum state.

In the case of fermions, on the other hand, we must define the operators $c_i^\dagger, c_i$ such that they obey *canonical anticommutation relations* (CAR):

$$\{c_i, c_j^\dagger\} = \delta_{ij}\,, \qquad \{c_i, c_j\} = \{c_i^\dagger, c_j^\dagger\} = 0\,, \tag{1.12}$$

where $\{A, B\} = AB + BA$ is the anticommutator. It is easy to see that due to (1.12), particles created by these creation operators are now antisymmetric under exchange:

$$c_i^\dagger c_j^\dagger\,|0\rangle = -c_j^\dagger c_i^\dagger\,|0\rangle \qquad \text{if} \qquad j \neq k\,. \tag{1.13}$$

Furthermore, we recover the famous *Pauli exclusion principle*, which says that one cannot have two fermions in the same quantum state:

$$(c_i^\dagger)^2 \left|0\right\rangle = 0\,. \tag{1.14}$$

A critical observable constructed from the creation and annihilation operators is the number operator, defined for state j as $n_j = a_j^\dagger a_j$. This Hermitian operator counts the occupation number of particles in state j, with eigenvalues $0, 1, 2, \ldots$ for bosons and $0, 1$ for fermions.

For more details on second quantization in many-body systems, see [42].

Remark 1.1 (Majorana Operators). We can linearly combine the fermionic operators $c_k^\dagger, c_k$ to define the $2n$ hermitian and traceless *Majorana operators* γ_μ [16, 17]:

$$\gamma_{2j-1} = c_j + c_j^\dagger\,, \qquad \gamma_{2j} = -i(c_j - c_j^\dagger)\,, \tag{1.15}$$

with $j = 1, 2, \ldots, n$ while $\mu = 1, 2, \ldots, 2n$. The inverse relations are:

$$c_j = \frac{\gamma_{2j-1} + i\gamma_{2j}}{2}\,, \qquad c_j^\dagger = \frac{\gamma_{2j-1} - i\gamma_{2j}}{2} \tag{1.16}$$

In terms of these operators, the CAR (1.12) appear as:

$$\{\gamma_\mu, \gamma_\nu\} = 2\delta_{\mu\nu}\,. \tag{1.17}$$

The $\{\gamma_\mu\}$ generate a *Clifford Algebra* $\mathcal{C}_{2n}$. An arbitrary element $C \in \mathcal{C}_{2n}$ can be represented as a polynomial in $\{\gamma_\mu\}$, i.e.

$$C = \alpha\mathbb{1} + \sum_{p=1}^{2n} \sum_{1\le\mu_1<\cdots<\mu_p\le 2n} \alpha_{\mu_1,\ldots,\mu_p}\gamma_{\mu_1}\ldots\gamma_{\mu_p}\,. \tag{1.18}$$

Majorana operators are defined in the same way as position and momentum operators in the treatment of the quantum harmonic oscillator [40] and for generic bosonic systems [42].

1.1.2 Free Systems of Bosons and Fermions

A many-body system is free, if its constituents are non-interacting particles. When these particles are fermions, the system is referred to as a free fermionic system, while for bosons it is called free bosonic. Our next objective is to provide a mathematical description of these systems, specifying the form of their Hamiltonians and the structure of their energy spectra.

In the first quantization formalism, the Hamiltonian of a system of free particles consists exclusively of the kinetic energy of the individual particles and any one-body potential terms, such as gravitational, Coulomb, or other external fields acting on the whole system. In formulas, we have:

$$H = \sum_{i=1}^{N} \frac{p_i^2}{2m} + \sum_{i=1}^{N} V_1(r_i)\,, \tag{1.19}$$

where p_i and r_i are respectively the momentum and position operators of the i-th particle.

These Hamiltonians are simple *one-body operators*, which are defined as sums of operators acting on individual particles:

$$O = \sum_i O_1(r_i, p_i)\,. \tag{1.20}$$

Such operators can be conveniently expressed in the second quantization formalism as linear combinations of number operators [42]:

$$O = \sum_k \varepsilon_k a_k^\dagger a_k\,, \tag{1.21}$$

where ε_k are the eigenvalues of the one-body operator O. This formulation applies to both bosonic and fermionic systems, with the distinction between the two encoded in the commutation or anticommutation relations satisfied by the creation and annihilation operators.

More in general, it can be proven that any quadratic Hamiltonian of the form:

$$H = \sum_{i,j=1}^{n} \left(A_{ij} a_i^\dagger a_j + B_{ij} a_i a_j + C_{ij} a_i^\dagger a_j^\dagger + D_{ij} a_i a_j^\dagger \right) , \tag{1.22}$$

both fermionic and bosonic, can be diagonalized to something of the form (1.21) up to a constant term. In (1.22), n is the number of bosonic/fermionic mode. Different commutation relations and imposing the Hermitian property of the Hamiltonian will impose conditions on A, B, C, D. In the following, we will discuss the fermionic case. If interested, see [43] for the slightly more complex bosonic one.

When dealing with interacting systems, one typically encounters *two-body operators*, which depend on the positions or momenta of pairs of particles. In the second quantization formalism, such operators can be shown to be quartic in the creation and annihilation operators [42]. Operators involving higher-order interactions will be also of higher order in the fermions or bosons.

1.2 Free Fermionic Systems

Let us now focus on fermions, the particles of interest in this thesis. We will characterize free fermionic systems through their Hamiltonian and discuss a method for its diagonalization. Subsequently, we will provide an alternative characterization based on their energy spectrum, which is often a more accessible physical property.

1.2.1 Fermionic Quadratic Hamiltonians

We begin by introducing some notation. Throughout this subsection, Hamiltonian operators will be denoted by $\hat{H}$, while H will refer to the corresponding matrix defined in (1.26). For a system with n modes, we collect all creation and annihilation operators into the following $2n-$dimensional vectors:

$$\mathcal{C} = \begin{pmatrix} c_1 \\ \vdots \\ c_n \\ c_1^\dagger \\ \vdots \\ c_n^\dagger \end{pmatrix} , \qquad \mathcal{C}^\dagger = \begin{pmatrix} c_1^\dagger & \dots & c_n^\dagger & c_1 & \dots & c_n \end{pmatrix} . \tag{1.23}$$

The canonical anticommutation relations (CAR) can then be compactly written as $\{\mathcal{C}_\mu, \mathcal{C}_\nu^\dagger\} = \delta_{\mu\nu}$, where $\mu, \nu = 1, \dots, 2n$, and $\mathcal{C}_\mu$ and $\mathcal{C}_\nu^\dagger$ denote the $\mu-$th and $\nu-$th components of $\mathcal{C}$ and $\mathcal{C}^\dagger$, respectively. Greek letters will be used for indices ranging from 1 to $2n$. It is important to note that $\mathcal{C}$ is not a matrix, and therefore $\mathcal{C}^\dagger$ is not its Hermitian conjugate. This notation is introduced purely for convenience in expressing the vectors defined in (1.23).

We now proceed to characterize free fermionic Hamiltonians and discuss a method for their diagonalization, following primarily [17], [43], and [44].

The first step is to specialize (1.22) to the fermionic case. To this end, we impose the CAR (1.12) on the creation and annihilation operators and require the Hamiltonian to be Hermitian, $\hat{H} = \hat{H}^\dagger$. These conditions

lead to the following constraints:

$$\begin{aligned} D_{ij} &= -A_{ji} \qquad \text{and} \qquad A_{ij} = A_{ij}^\dagger\,, \\ B_{ij} &= -B_{ji}, \qquad C_{ij} = -C_{ji} \qquad \text{and} \qquad C_{ij} = -B_{ij}^*\,. \end{aligned} \tag{1.24}$$

Hence, the most general quadratic fermionic Hamiltonian can be written as:

$$\hat{H} = \sum_{i,j=1}^{n} \left(A_{ij} c_i^\dagger c_j - A_{ij}^* c_i c_j^\dagger + B_{ij} c_i c_j - B_{ij}^* c_i^\dagger c_j^\dagger \right)\,, \tag{1.25}$$

where A_{ij} must be elements of an Hermitian matrix $A = A^\dagger$ and B_{ij} of a skew-simmetric matrix $B = -B^T$. Defining the matrix:

$$H = \begin{pmatrix} A & -B^* \\ B & -A^* \end{pmatrix}\,, \tag{1.26}$$

the Hamiltonian (1.25) can be compactly expressed in terms of the vectors $\mathcal{C}$ and $\mathcal{C}^\dagger$ introduced in (1.23) as

$$\hat{H} = \mathcal{C}^\dagger H \mathcal{C}\,. \tag{1.27}$$

The next step is the diagonalization of a Hamiltonian of this form. To achieve this, we will employ a *canonical transformation*, which maps the original creation and annihilation operators onto new ones. In this specific case, these new operators must be chosen such that the Hamiltonian in Eq. (1.26) becomes diagonal.

Let us rewrite $\mathcal{C}$ as $\mathcal{C} = \mathcal{S}\tilde{\mathcal{C}}$, where

$$\tilde{\mathcal{C}} = \begin{pmatrix} \tilde{c}_1 \\ \vdots \\ \tilde{c}_n \\ \tilde{c}_1^\dagger \\ \vdots \\ \tilde{c}_n^\dagger \end{pmatrix}\,, \tag{1.28}$$

and $\tilde{c}_i, \tilde{c}_j^\dagger$ are the new fermionic operators. For the new operators to be genuinely fermionic, they must satisfy the canonical anticommutation relations given in Eq. (1.12). This implies the following:

$$\delta_{\mu\nu} = \{\mathcal{C}_\mu, \mathcal{C}_\nu^\dagger\} = \sum_{\sigma,\rho=1}^{2n} \{\mathcal{S}_{\mu\sigma}\tilde{\mathcal{C}}_\sigma, \tilde{\mathcal{C}}_\rho^\dagger \mathcal{S}_{\rho\nu}^\dagger\} = \sum_{\sigma,\rho=1}^{2n} \mathcal{S}_{\mu\sigma}\{\tilde{\mathcal{C}}_\sigma, \tilde{\mathcal{C}}_\rho^\dagger\}\mathcal{S}_{\rho\nu}^\dagger \overset{!}{=} \sum_{\sigma,\rho=1}^{2n} \mathcal{S}_{\mu\sigma}\delta_{\sigma\rho}\mathcal{S}_{\rho\nu}^\dagger = \sum_{\sigma=1}^{2n} \mathcal{S}_{\mu\sigma}\mathcal{S}_{\sigma\nu}^\dagger\,. \tag{1.29}$$

Hence, $\mathcal{S}$ is unitary ($\mathcal{S}\mathcal{S}^\dagger = \mathcal{S}^\dagger\mathcal{S} = \mathbb{1}$), and therefore invertible, with inverse $\mathcal{S}^{-1} = \mathcal{S}^\dagger$.

If we define $\boldsymbol{c}$, $\tilde{\boldsymbol{c}}$ and $\boldsymbol{c}^\dagger$, $\tilde{\boldsymbol{c}}^\dagger$ as the column vectors of annihilation and creation operators respectively, we can rewrite the canonical transformation $\mathcal{S}$ as:

$$\begin{pmatrix} \boldsymbol{c} \\ \boldsymbol{c}^\dagger \end{pmatrix} = \begin{pmatrix} U & V^* \\ V & U^* \end{pmatrix} \begin{pmatrix} \tilde{\boldsymbol{c}} \\ \tilde{\boldsymbol{c}}^\dagger \end{pmatrix}\,, \tag{1.30}$$

which in components is

$$\begin{aligned} c_i &= \sum_{k=1}^{n} \left(U_{ik}\tilde{c}_k + V_{ik}^*\tilde{c}_k^\dagger \right)\,, \\ c_i^\dagger &= \sum_{k=1}^{n} \left(V_{ik}\tilde{c}_k + U_{ik}^*\tilde{c}_k^\dagger \right)\,. \end{aligned} \tag{1.31}$$

The unitarity of $\mathcal{S}$ imposes the following conditions on U and V:

$$U^\dagger U + V^\dagger V = \mathbb{1}\,, \qquad\qquad U^\dagger V^* + V^\dagger U^* = 0\,. \tag{1.32}$$

Let us now define the operator $\mathcal{J}$ acting on $\mathbb{C}^{2n}$ as:

$$\mathcal{J}\begin{pmatrix}\mathbf{u}\\ \mathbf{v}\end{pmatrix} = \begin{pmatrix}\mathbf{v}^*\\ \mathbf{u}^*\end{pmatrix}\,, \tag{1.33}$$

where $\mathbf{u}, \mathbf{v} \in \mathbb{C}^n$. One can easily show that $\{H, \mathcal{J}\} = 0$ by applying the two terms of the anticommutator to a generic vector in $\mathbb{C}^{2n}$. Then, we can prove that if $\vec{x} \in \mathbb{C}^{2n}$ is an eigenvector of H with eigenvalue ε, also $\mathcal{J}\vec{x}$ will be an eigenvector of H, but with eigenvalue $-\varepsilon$:

$$H\vec{x} = \varepsilon\vec{x} \qquad \Longrightarrow \qquad H(\mathcal{J}\vec{x}) = -\mathcal{J}(H\vec{x}) = -\varepsilon(\mathcal{J}\vec{x})\,. \tag{1.34}$$

Hence, all eigenvalues of H lie symmetrically with respect to the origin.

Let $\vec{x}_1, \vec{x}_2, \ldots, \vec{x}_n$ be the n eigenvectors of H with non negative eigenvalues $\varepsilon_1, \varepsilon_2, \ldots, \varepsilon_n$, then if we choose $\mathcal{S}$ to be:

$$\mathcal{S} = \begin{pmatrix}\vec{x}_1 & \ldots & \vec{x}_n & \mathcal{J}\vec{x}_1 & \ldots & \mathcal{J}\vec{x}_n\end{pmatrix} = \begin{pmatrix}\mathbf{u}_1 & \ldots & \mathbf{u}_n & \mathbf{v}_1^* & \ldots & \mathbf{v}_n^*\\ \mathbf{v}_1 & \ldots & \mathbf{v}_n & \mathbf{u}_1^* & \ldots & \mathbf{u}_n^*\end{pmatrix} = \begin{pmatrix}U & V^*\\ V & U^*\end{pmatrix}\,, \tag{1.35}$$

we can diagonalize the matrix H:

$$H_D := \mathcal{S}^\dagger H \mathcal{S} = \mathrm{diag}(\varepsilon_1, \ldots, \varepsilon_n, -\varepsilon_1, \ldots, -\varepsilon_n)\,. \tag{1.36}$$

The full Hamiltonian can then finally be written in diagonal form as:

$$\hat{H} = \tilde{\mathcal{C}}^\dagger H_D\, \tilde{\mathcal{C}} = \sum_{j=1}^{n} \varepsilon_j \left(\tilde{c}_j^\dagger \tilde{c}_j - \tilde{c}_j \tilde{c}_j^\dagger\right) = \sum_{j=1}^{n} 2\varepsilon_j \left(\tilde{c}_j^\dagger \tilde{c}_j - 1/2\right)\,, \tag{1.37}$$

or, removing the hat and the $\sim$ for better readability:

$$H = \sum_{j=1}^{n} \varepsilon_j \left(c_j^\dagger c_j - c_j c_j^\dagger\right) = \sum_{j=1}^{n} 2\varepsilon_j \left(c_j^\dagger c_j - 1/2\right)\,. \tag{1.38}$$

This is exactly analogous to Eq. (1.21), with an added constant term which determines the ground-state energy.

Before moving on, let us make some considerations:

1. The Hamiltonian satisfies the following commutation relations with the diagonalizing creation and annihilation operators:

   $$[H, c_k^\dagger] = 2\varepsilon_k c_k^\dagger\,, \qquad\qquad [H, c_k] = -2\varepsilon_k c_k\,. \tag{1.39}$$

   These relations imply that acting with $c_k^\dagger$ or c_k on an eigenstate of H either annihilates the state or produces another eigenstate whose energy is shifted by $2\varepsilon_k$ or $-2\varepsilon_k$, respectively.

   Indeed, let $|E\rangle$ be an eigenstate of the Hamiltonian with energy E. Considering, for example, the creation operator, we find

   $$H c_k^\dagger |E\rangle = (c_k^\dagger H + 2\varepsilon_k c_k^\dagger)\,|E\rangle = (E + 2\varepsilon_k)(c_k^\dagger |E\rangle)\,. \tag{1.40}$$

   Hence, $c_k^\dagger |E\rangle$ is itself an eigenstate of the Hamiltonian with energy $E + 2\varepsilon_k$. We can therefore interpret $c_k^\dagger$ as creating particles with energy $2\varepsilon_k$, while c_k destroys such a particle.

2. The eigenvalues of the Hamiltonian (1.38) can be written as:

$$E = \sum_{k=1}^{n} \tau_k \varepsilon_k \,, \tag{1.41}$$

where $\tau_k = \pm 1$. We can label the eigenstates of the Hamiltonians using these τ_k, with $\tau_k = +1$ if mode k is occupied, while $\tau_k = -1$ if it is not. We see that this and the standard basis are equivalent

$$\begin{aligned} H\,|n_1 \dots n_n\rangle &= \sum_{k=1}^{n} 2\varepsilon_k \left(c_k^\dagger c_k - 1/2\right) |n_1 \dots n_n\rangle = \sum_{k=1}^{n} \varepsilon_k \left(2n_k - 1\right) |n_1 \dots n_n\rangle \,, \\ H\,|\tau_1, \dots, \tau_n\rangle &= \sum_{k=1}^{n} \varepsilon_k \left(c_k^\dagger c_k - c_k c_k^\dagger\right) |\tau_1, \dots, \tau_n\rangle = \sum_{k=1}^{n} \tau_k \varepsilon_k \,|\tau_1, \dots, \tau_n\rangle \,, \end{aligned} \tag{1.42}$$

and $2n_k - 1 = \tau_k$, since for $n_k = 0$ we get $2n_k - 1 = -1$, whereas for $n_k = 0$, $2n_k - 1 = 1$.

We will employ the different relabelling of the eigenstates of the Hamiltonian in Subsection 1.2.2.

Remark 1.2 (Hamiltonian using Majorana Operators). In Remark 1.1, we introduced the Hermitian Majorana operators γ_μ, defined in terms of the fermionic annihilation and creation operators c_j and $c_j^\dagger$ as in Eq. (1.15). Since the Majorana operators are linear combinations of these fermionic operators, it follows that any generic fermionic quadratic Hamiltonian (1.25) can be rewritten as a quadratic form in the Majorana operators. In particular, it can be expressed as:

$$H = i \sum_{\mu,\nu=1}^{2n} h_{\mu\nu} \gamma_\mu \gamma_\nu \,, \tag{1.43}$$

where, due to hermiticity and the canonical anticommutation relations for the Majorana operators (1.17), the $2n \times 2n$ matrix $h_{\mu\nu}$ must be real and skew-symmetric ($h_{\mu\nu} = -h_{\nu\mu}$). Note that Eq. (1.43) represents an element of the Clifford algebra introduced in Remark 1.1.

To relate the coefficients appearing in Eqs. (1.25) and (1.43), we can express the operators c_j and $c_j^\dagger$ in Eq. (1.25) in terms of the Majorana operators, using the inverse relations given in Eq. (1.16). By doing so, we obtain the following relations:

$$\begin{aligned} 4i\, h_{2j-1,2k-1} &= A_{jk} - A_{jk}^* + B_{jk} - B_{jk}^* \,, \\ 4i\, h_{2j-1,2k} &= i\left(A_{jk} + A_{jk}^* + B_{jk} + B_{jk}^*\right) \,, \\ 4i\, h_{2j,2k-1} &= i\left(-A_{jk} - A_{jk}^* + B_{jk} + B_{jk}^*\right) \,, \\ 4i\, h_{2j,2k} &= A_{jk} - A_{jk}^* - B_{jk} + B_{jk}^* \,. \end{aligned} \tag{1.44}$$

Let us now consider a canonical transformation acting on the Majorana operators. We rewrite $\gamma_\mu = \sum_\sigma \mathcal{O}_{\mu\sigma} \tilde{\gamma}_\sigma$, where $\{\tilde{\gamma}_\sigma\}$ denotes another set of Majorana operators. Then, we have:

$$2\delta_{\mu\nu} = \{\gamma_\mu, \gamma_\nu\} = \sum_{\sigma,\rho=1}^{2n} \{\mathcal{O}_{\mu\sigma}\tilde{\gamma}_\sigma, \mathcal{O}_{\nu\rho}\tilde{\gamma}_\rho\} = \sum_{\sigma,\rho=1}^{2n} \mathcal{O}_{\mu\sigma}\mathcal{O}_{\nu\rho}\{\tilde{\gamma}_\sigma, \tilde{\gamma}_\rho\} \overset{!}{=} 2 \sum_{\sigma,\rho=1}^{2n} \mathcal{O}_{\mu\sigma}\mathcal{O}_{\nu\rho}\delta_{\sigma\rho} = \sum_{\sigma=1}^{2n} \mathcal{O}_{\mu\sigma}\mathcal{O}^T_{\rho\nu} \,, \tag{1.45}$$

Therefore, we find that $\mathcal{O}\mathcal{O}^T = \mathcal{O}^T\mathcal{O} = \mathbb{1}$: the canonical transformations for Majorana operators are orthogonal rather than unitary.

The diagonal form of the Hamiltonian (1.37) can be rewritten in terms of the Majorana operators by using Eq. (1.16) to express the diagonalizing creation and annihilation operators $\tilde{c}_j^\dagger, \tilde{c}_j$ in terms of the corresponding diagonalizing Majorana operators $\tilde{\gamma}_\mu$. This yields:

$$H = i \sum_{j=1}^{n} \varepsilon_j \,\tilde{\gamma}_{2j-1}\tilde{\gamma}_{2j} \,. \tag{1.46}$$

1.2.2 Free Fermionic Spectrum

Let us now characterize a free fermionic system in terms of its spectrum. Why is this important? As discussed earlier, free fermionic systems often arise from spin systems. In some cases, however, the mapping from spins to fermions may not be immediately evident, as we will see in the Free Fermions in Disguise models. It is therefore useful to rely on an accessible property of the system to identify its fermionic nature. The energy spectrum appears to be a good fit for this purpose, since it can always be determined, at least numerically, through exact diagonalization methods. If the spectrum exhibits the characteristic structure of a free fermionic system, we can conclude that the original Hamiltonian is equivalent to a quadratic fermionic Hamiltonian in some auxiliary space.

Let us state the definition given in Ref. [32] for a free fermionic spectrum.

Definition 1.1 (**Free Fermionic Spectrum**)**.** A Hamiltonian H acting on Hilbert space $\mathcal{H}$ has a *free fermionic spectrum* in a finite volume L if the following are satisfied:

1. There are n real numbers ε_k, $k = 1, \ldots, n$ such that the distinct eigenvalues λ are of the form (1.41);

2. For generic values of ε_k every eigenvalue has the same degeneracy D in a chosen volume L.

These two criteria ensure the existence of fermionic creation and annihilation operators. Here, n denotes the number of fermionic eigenmodes within a volume L. When the energies ε_k are all distinct, there are 2^n distinct eigenvalues. In the case of a degeneracy $D > 1$, there is some flexibility in the definition of the fermionic operators. Note that Definition 1.1 is strict and excludes models which split into independent sectors with a free spectrum, such as the XY model with periodic boundary conditions (PBC), which we will discuss in the Section 1.4. This restriction is made because FFD models admit creation and annihilation operators only under open boundary conditions.

Let us construct the fermionic operators given the spectrum of Eq. (1.41), starting with the case $D = 1$. We denote the eigenstates as $|\tau_1, ..., \tau_n\rangle$, where $\tau_k = \pm 1$, such that the corresponding energy eigenvalues are given by Eq. (1.41), as discussed in the previous section. The creation operators $c_k^\dagger$, $k = 1, ..., n$ are then:

$$c_k^\dagger = \sum_{\tau_l = \pm 1,\, l \neq k} \left(\prod_{l=1}^{k-1} \tau_l \right) |\tau_1, \ldots, \tau_k = +1, \ldots, \tau_n\rangle \langle \tau_1, \ldots, \tau_k = -1, \ldots, \tau_n| \,, \tag{1.47}$$

while the corresponding annihilation operator:

$$c_k = (c_k^\dagger)^\dagger = \sum_{\tau_l = \pm 1,\, l \neq k} \left(\prod_{l=1}^{k-1} \tau_l \right) |\tau_1, \ldots, \tau_k = -1, \ldots, \tau_n\rangle \langle \tau_1, \ldots, \tau_k = +1, \ldots, \tau_n| \,. \tag{1.48}$$

We can use the following compact notation:

$$\Psi_{\pm k} = \sum_{\tau_l = \pm 1,\, l \neq k} \left(\prod_{l=1}^{k-1} \tau_l \right) |\tau_1, \ldots, \tau_k = \pm 1, \ldots, \tau_n\rangle \langle \tau_1, \ldots, \tau_k = \mp 1, \ldots, \tau_n| \,, \tag{1.49}$$

with $c_k^\dagger = \Psi_k$ and $c_k = \Psi_{-k}$. With this notation the canonical anticommutation relations of Eq. (1.12) have the following form:

$$\{\Psi_{\pm k}, \Psi_{\pm k'}\} = 0 \qquad \{\Psi_{\pm k}, \Psi_{\mp k'}\} = \delta_{kk'} \,. \tag{1.50}$$

This will be the main notation when dealing with Free Fermions in Disguise in Chapters 3 and 4.

Let us look at a simple example to justify the definition of Eq. (1.49).

Example 1.1. We choose $n = 3$ and $k = 2$. Then our creation and annihilation operators will be:

$$\begin{aligned}\Psi_{\pm 2} &= \sum_{\tau_1,\tau_3=\pm 1} \tau_1 \left|\tau_1, \pm 1, \tau_3\right\rangle \left\langle \tau_1, \mp 1, \tau_3\right| = \\ &= \left|1, \pm 1, 1\right\rangle \left\langle 1, \mp 1, 1\right| + \left|1, \pm 1, -1\right\rangle \left\langle 1, \mp 1, -1\right| - \left|-1, \pm 1, 1\right\rangle \left\langle -1, \mp 1, 1\right| - \left|-1, \pm 1, -1\right\rangle \left\langle -1, \mp 1, -1\right| \ .\end{aligned} \tag{1.51}$$

We can easily see that, when applied to eigenstates of the form $|\tau_1, \mp 1, \tau_3\rangle$, these operators produce the eigenstate with the opposite value of τ_2:

$$\Psi_{\pm 2} \left|\tau_1, \mp 1, \tau_3\right\rangle = \tau_2 \left|\tau_1, \pm 1, \tau_3\right\rangle \ . \tag{1.52}$$

The corresponding energy eigenvalue then increases or decreases by $2\varepsilon_2$, respectively, as if a particle with that energy were being created or annihilated. This behavior is precisely what one expects from fermionic creation and annihilation operators.

We can prove that creation and annihilation operators defined in Eq. (1.49) ensures the canonical anti-commutation relations (1.50). We can then rewrite the original Hamiltonian – which, in this context, does not need to be fermionic to begin with – from its general form into the free fermionic diagonal form as

$$H = \sum_{k=1}^{n} \varepsilon_k \left(\Psi_k \Psi_{-k} - \Psi_{-k} \Psi_k\right) \ , \tag{1.53}$$

which is identical to Eq. (1.38), but in the alternative notation.

Let us now prove the CAR (1.50). To show this, it is sufficient to compute the products $\Psi_{\pm k}\Psi_{\pm k'}$ and $\Psi_{\pm k}\Psi_{\mp k'}$ and then sum specific combinations of these.
First, let us focus on the case $k \neq k'$. We will choose $k' > k$ without loss of generality.

$$\begin{aligned}\Psi_{\pm k}\Psi_{\pm k'} = &\left[\sum_{\tau_l=\pm 1,\, l\neq k} \left(\prod_{l=1}^{k-1} \tau_l\right) \left|\tau_1, \ldots, \tau_k = \pm 1, \ldots, \tau_n\right\rangle \left\langle \tau_1, \ldots, \tau_k = \mp 1, \ldots, \tau_n\right|\right] \cdot \\ &\cdot \left[\sum_{\tau'_{l'}=\pm 1,\, l'\neq k'} \left(\prod_{l'=1}^{k'-1} \tau'_{l'}\right) \left|\tau'_1, \ldots, \tau'_{k'} = \pm 1, \ldots, \tau'_n\right\rangle \left\langle \tau'_1, \ldots, \tau'_{k'} = \mp 1, \ldots, \tau'_n\right|\right] \ .\end{aligned} \tag{1.54}$$

We end up with an inner product between the basis states, which results in a product of delta functions:

$$\delta_{\tau_1,\tau'_1} \ldots \delta_{\mp 1,\tau'_k} \ldots \delta_{\tau_{k'},\pm 1} \ldots \delta_{\tau_n,\tau'_n} \ . \tag{1.55}$$

Those will get cancelled by the sums over all the $\tau'_{l'}$ and over $\tau_{k'}$. The coefficient in front of each term then becomes simply $\tau'_k \ldots \tau'_{k'-1}$, since all other terms will square to one, and moreover we must impose $\tau'_k = \mp 1$, while $\tau'_j = \tau_j$, for any j. This yields:

$$\Psi_{\pm k}\Psi_{\pm k'} = (\mp 1) \sum_{\substack{\tau_l=\pm 1 \\ l\neq k,k'}} \tau_{k+1} \ldots \tau_{k'-1} \left|\tau_1, \ldots, \tau_k = \pm 1, \ldots, \tau_{k'} = \pm 1, \ldots, \tau_n\right\rangle \left\langle \tau_1, \ldots, \tau_k = \mp 1, \ldots, \tau_{k'} = \mp 1, \ldots, \tau_n\right| \ . \tag{1.56}$$

With very similar calculations, we get:

$$\begin{aligned}
\Psi_{\pm k'}\Psi_{\pm k} &= (\pm 1)\sum_{\substack{\tau_l=\pm 1\\ l\neq k,k'}} \tau_{k+1}\dots\tau_{k'-1}\,|\tau_1,\dots,\tau_k=\pm 1,\dots,\tau_{k'}=\pm 1,\dots,\tau_n\rangle\langle\tau_1,\dots,\tau_k=\mp 1,\dots,\tau_{k'}=\mp 1,\dots,\tau_n|\,,\\
\Psi_{\pm k}\Psi_{\mp k'} &= (\pm 1)\sum_{\substack{\tau_l=\mp 1\\ l\neq k,k'}} \tau_{k+1}\dots\tau_{k'-1}\,|\tau_1,\dots,\tau_k=\pm 1,\dots,\tau_{k'}=\mp 1,\dots,\tau_n\rangle\langle\tau_1,\dots,\tau_k=\mp 1,\dots,\tau_{k'}=\pm 1,\dots,\tau_n|\,,\\
\Psi_{\mp k'}\Psi_{\pm k} &= (\mp 1)\sum_{\substack{\tau_l=\mp 1\\ l\neq k,k'}} \tau_{k+1}\dots\tau_{k'-1}\,|\tau_1,\dots,\tau_k=\pm 1,\dots,\tau_{k'}=\mp 1,\dots,\tau_n\rangle\langle\tau_1,\dots,\tau_k=\mp 1,\dots,\tau_{k'}=\pm 1,\dots,\tau_n|\,,
\end{aligned} \tag{1.57}$$

and therefore $\{\Psi_{\pm k},\Psi_{\pm k'}\}=0$ and $\{\Psi_{\pm k},\Psi_{\mp k'}\}=0$ for $k\neq k'$.
Conversely, if $k=k'$, it is easy to see that $\Psi_{\pm k}\Psi_{\pm k}$ is given by a sum of terms of this form:

$$|\tau_1,\dots,\tau_k=\pm 1,\dots,\tau_n\rangle\langle\tau_1,\dots,\tau_k=\mp 1\dots,\tau_n\,|\tau_1,\dots,\tau_k=\pm 1,\dots,\tau_n\rangle\langle\tau_1,\dots,\tau_k=\mp 1\dots,\tau_n|=0\,, \tag{1.58}$$

which are all zero due to the inner product between orthogonal states present in the middle. Therefore $\{\Psi_{\pm k},\Psi_{\pm k}\}=0$. Finally, in $\Psi_{\pm k}\Psi_{\mp k}$ and $\Psi_{\mp k}\Psi_{\pm k}$, the products of the τ_l cancel completely. We therefore get:

$$\begin{aligned}
\Psi_{\pm k}\Psi_{\mp k} &= \sum_{\substack{\tau_l=\mp 1\\ l\neq k}} |\tau_1,\dots,\tau_k=\pm 1,\dots,\tau_n\rangle\langle\tau_1,\dots,\tau_k=\pm 1,\dots,\tau_n|\,,\\
\Psi_{\mp k}\Psi_{\pm k} &= \sum_{\substack{\tau_l=\mp 1\\ l\neq k}} |\tau_1,\dots,\tau_k=\mp 1,\dots,\tau_n\rangle\langle\tau_1,\dots,\tau_k=\mp 1,\dots,\tau_n|\,,
\end{aligned} \tag{1.59}$$

which summed give a resolution of the identity in the basis $|\tau_1,\dots,\tau_n\rangle$. Hence, $\{\Psi_{\pm k},\Psi_{\mp k}\}=\mathbb{1}$.

Now, consider a uniform degeneracy $D>1$. In this case, the creation and annihilation operators are not uniquely defined, as different choices can be made by selecting different basis within each degenerate level. We denote these basis vectors as

$$|\tau_1,\dots,\tau_n|a\rangle\,,\qquad \tau_k=\pm 1\,,\qquad a=1,\dots,D\,. \tag{1.60}$$

The fermionic operators can then be defined from Eq. (1.49), adding a summation over a:

$$\Psi_k=\sum_{a=1}^{D}\sum_{\tau_l=\pm 1,\ l\neq k}\left(\prod_{l=1}^{k-1}\tau_l\right)|\tau_1,\dots,\tau_k=+1,\dots,\tau_n|a\rangle\langle a|\tau_1,\dots,\tau_k=-1\dots,\tau_n|\,. \tag{1.61}$$

While these operators depend on the basis choice, they always satisfy the canonical anticommutation relations, Eq. (1.50). Furthermore, the combination $\Psi_k\Psi_{-k}-\Psi_{-k}\Psi_k$ in the Hamiltonian (1.53) remains well-defined, as rotations within the degenerate eigenspace leave it invariant.

In the FFD models introduced in Ref. [28], the freedom of choice of the fermionic operator is determined by the definition of the edge operator χ. We will discuss this further in Chapter 3.

1.3 Spin Chains and Free fermions: the Jordan-Wigner transformation

Spin chains are fundamental models in statistical physics. They were originally introduced to describe magnetic systems, which consist of particles carrying magnetic spins fixed at specific positions. A simple and intuitive way to model these systems is to consider a lattice in which each site hosts a spin particle.

Spin$-1/2$ chains are the simplest class of spin chains. Their Hilbert space is given by $\mathcal{H}_L \cong (\mathbb{C}^2)^{\otimes L}$, where L denotes the length of the chain. This space is equivalent to the Hilbert space of an $L-$qubit system. Its dimension is 2^L, and thus it grows exponentially with the system size, similarly to systems of bosons and fermions. However, contrary to those systems, spin$-1/2$ models with a quadratic Hamiltonian cannot be solved in general. Nevertheless, there exists a powerful method to relate spin chains to fermionic systems, known as the **Jordan–Wigner transformation (JW)**, first introduced by Jordan and Wigner in [1]. The following discussion will mainly follow [3] and [4].

Let us first consider a single spin$-1/2$ particle. As previously stated, its Hilbert space is isomorphic to $\mathbb{C}^2$. A basis of the space of hermitian operators acting on $\mathbb{C}^2$ is given by the Pauli operators X, Y, Z and the identity. We will denote the elements of this basis as σ^α, where $\alpha = 0, 1, 2, 3$ and $\sigma^0 = \mathbb{1}$, $\sigma^1 = X$, $\sigma^2 = Y$, $\sigma^3 = Z$. When we refer only to Pauli operators, we will use latin letters as indexes, e.g. $i = 1, 2, 3$. The standard matrix representation of X, Y and Z is:

$$X = \begin{pmatrix} 0 & 1 \\ 1 & 0 \end{pmatrix}, \qquad Y = \begin{pmatrix} 0 & -i \\ i & 0 \end{pmatrix}, \qquad Z = \begin{pmatrix} 1 & 0 \\ 0 & 1 \end{pmatrix}, \tag{1.62}$$

but they can be defined algebraically making use only of the commutation and anticommutation relations:

$$[\sigma^j, \sigma^k] = 2i \sum_{l=1}^{3} \epsilon_{jkl} \sigma^l \,, \qquad \{\sigma^j, \sigma^k\} = 2\delta_{jk} \mathbb{1} \,, \tag{1.63}$$

where ϵ_{jkl} is the Levi-Civita tensor. From (1.63), we can write the product of arbitrary Pauli matrices as:

$$\sigma^j \sigma^k = \delta_{ij} \mathbb{1} + i \sum_{l=1}^{3} \epsilon_{jkl} \sigma^l \,. \tag{1.64}$$

We will choose as a basis for our single spin Hilbert space $\{|\uparrow\rangle, |\downarrow\rangle\}$, eigenstates of Z with eigenvalues 1 and -1 respectively. From X and Y we can now construct two *ladder operators*, which map $|\uparrow\rangle$ to $|\downarrow\rangle$ and viceversa:

$$\sigma^\pm = \frac{X \pm iY}{2}, \qquad \sigma^+ |\downarrow\rangle = |\uparrow\rangle \,, \qquad \sigma^- |\uparrow\rangle = |\downarrow\rangle \,. \tag{1.65}$$

It is clear that $(\sigma^\pm)^\dagger = \sigma^\mp$ and that the standard Pauli matrices can be written in terms of them as:

$$X = \sigma^+ + \sigma^- \,, \qquad Y = -i(\sigma^+ - \sigma^-) \,, \qquad Z = 2\sigma^+\sigma^- - 1 \,. \tag{1.66}$$

The ladder operators satisfy the canonical anticommutation relations (1.50) for one fermionic mode:

$$\{\sigma^\mp, \sigma^\pm\} = 1 \,, \qquad \{\sigma^\pm, \sigma^\pm\} = 0 \,. \tag{1.67}$$

The Pauli operator basis is particularly well suited for describing spin$-1/2$ particles, since the spin operators S^j (with the same index convention used for σ^j) can be expressed in terms of the Pauli matrices as $S^j = \hbar\sigma^j/2$. Hence, a Hamiltonian describing interacting spins can be conveniently written as a linear combination of products of Pauli operators.

Let us now consider a one-dimensional lattice of size L. We will denote as σ_j^α an element of the Pauli basis acting on site j, meaning:

$$\begin{gathered} \sigma_j^\alpha = \mathbb{1} \otimes \cdots \otimes \sigma^\alpha \otimes \cdots \otimes \mathbb{1} \\ \uparrow \\ j \end{gathered} \tag{1.68}$$

Clearly, Pauli matrices acting on different sites commute, while those acting on the same site satisfy the algebra given in Eq. (1.63). As a consequence, the ladder operators $\sigma_j^{\pm}$ do not obey fermionic anticommutation relations at different sites, but instead satisfy bosonic commutation relations:

$$\begin{aligned} &\{\sigma_j^-, \sigma_j^+\} = 1 \,, \qquad\qquad \{\sigma_j^{\pm}, \sigma_j^{\pm}\} = 0 \,, \\ &[\sigma_i^-, \sigma_j^+] = [\sigma_i^-, \sigma_j^-] = [\sigma_i^+, \sigma_j^+] = 0 \qquad i \neq j \,. \end{aligned} \tag{1.69}$$

The ladder operators $\sigma_j^{\pm}$ can be identified with *hard-core bosonic operators* b_j and $b_j^\dagger$. These can be obtained by starting from the standard infinite-dimensional bosonic Hilbert space and truncating it to dimension two, imposing $(b_j^\dagger)^2 = 0$. This condition follows from the local anticommutation relations. Physically, such a truncation can be interpreted as introducing a very large – ideally infinite – on-site repulsion term in the bosonic Hamiltonian, preventing multiple bosons from occupying the same quantum state.

Explicitly, this correspondence is set up by identifying, at each site[1], $|0\rangle \leftrightarrow |\uparrow\rangle$ and $|1\rangle = b^\dagger|0\rangle \leftrightarrow |\downarrow\rangle$, which leads to the mappings $\sigma_j^+ \leftrightarrow b_j$ and $\sigma_j^- \leftrightarrow b_j^\dagger$. The standard Pauli matrices can then be written as:

$$X = b^\dagger + b \,, \qquad Y = i(b^\dagger - b) \,, \qquad Z = 1 - 2b^\dagger b \,. \tag{1.70}$$

The mapping to hard-core bosons is not particularly useful, since we do not have a method to diagonalize a quadratic hard-core bosonic Hamiltonian. However, in one-dimension the spins can still be mapped to spinless fermionic operators, using the aforementioned Jordan-Wigner transformation:

$$c_j = \exp\Big[-i\pi \sum_{k=1}^{j-1} b_k^\dagger b_k\Big] b_j \,, \qquad\qquad c_j^\dagger = b_j^\dagger \exp\Big[i\pi \sum_{k=1}^{j-1} b_k^\dagger b_k\Big] \,. \tag{1.71}$$

It is clear from (1.71) that $c_j^\dagger c_j = b_j^\dagger b_j = \sigma_j^- \sigma_j^+$, and therefore we can invert the transformation as:

$$b_j = \exp\Big[i\pi \sum_{k=1}^{j-1} c_k^\dagger c_k\Big] c_j \,, \qquad\qquad b_j^\dagger = c_j^\dagger \exp\Big[-i\pi \sum_{k=1}^{j-1} c_k^\dagger c_k\Big] \,. \tag{1.72}$$

The only difference between the original and the transformed operators is the phase factor $\exp\Big[\pm i\pi \sum_{k=1}^{j-1} c_k^\dagger c_k\Big]$. The value of this phase is determined by the number of fermions in modes $k = 1, ..., j-1$, since it is expressed in terms of the number operators[2] $c_k^\dagger c_k$. The phase takes the value $+1$ when there is an even number of occupied modes and -1 when the number is odd.

This phase factor, commonly referred to as the *Jordan-Wigner string*, is responsible for the non-local nature of the mapping. Indeed, it requires a specific ordering of the spin sites, which is straightforward in one-dimension but becomes more arbitrary in higher dimensions. This is precisely what makes the extension of the transformation to higher-dimensional systems nontrivial [6–8].

Since the number operators $n_j = \sigma_j^- \sigma_j^+ = c_j^\dagger c_j = b_j^\dagger b_j$ have the following properties:

$$[n_j, n_i] = 0 \,, \qquad (n_j)^k = n_j \text{ for } k \geq 1 \,, \qquad (n_j)^0 = 1 \,, \tag{1.73}$$

we can rewrite the Jordan-Wigner string as:

$$\begin{aligned} \exp\Big[\pm i\pi \sum_{k=1}^{j-1} c_k^\dagger c_k\Big] = \prod_{k=1}^{j-1} \exp\Big[\pm i\pi n_k\Big] = \prod_{k=1}^{j-1} \sum_{n=0}^{\infty} \frac{(\pm i\pi)^n}{n!} (n_k)^n = \prod_{k=1}^{j-1} \Big(1 + n_k \sum_{n=1}^{\infty} \frac{(\pm i\pi)^n}{n!}\Big) = \\ = \prod_{k=1}^{j-1} \Big(1 + n_k(e^{\pm i\pi} - 1)\Big) = \prod_{k=1}^{j-1} (1 - 2n_k) = \prod_{k=1}^{j-1} Z_k \,. \end{aligned} \tag{1.74}$$

[1] This identification is not unique, as the two states can be interchanged.

[2] Strictly speaking, one should first verify that the operators c_k and $c_k^\dagger$ satisfy the canonical anticommutation relations (1.12) before identifying $c_k^\dagger c_k$ as fermionic number operators. However, we can already interpret them as such for hard-core bosons, since $c_k^\dagger c_k = b_k^\dagger b_k$.

Now with this simpler expression we can easily prove some properties of $e^{\pm i\pi n_k}$:

$$\begin{aligned}
&1)\ [e^{\pm i\pi n_j}, b_i] = 0 \qquad \text{if} \qquad i \neq j\ , \\
&2)\ \{e^{\pm i\pi n_j}, b_j\} = \{1 - 2b_j^\dagger b_j, b_j\} = 2b_j - 2(b_j^\dagger (b_j)^2 + b_j^\dagger b_j b_j^\dagger) = 2b_j - 2(-(b_j^\dagger)^2 b_j + b_j) = 0\ , \\
&3)\ (e^{\pm i\pi n_j})^2 = (Z_j)^2 = 1\ .
\end{aligned} \tag{1.75}$$

By hermitian conjugation, the first two properties hold also for $b^\dagger$.

We can use (1.75) to finally prove the CAR (1.12) (let's choose $i < j$ without loss of generality):

$$\begin{aligned}
\{c_i, c_j\} &= b_i \left(\prod_{k=i}^{j-1} e^{\pm i\pi n_k}\right) b_j + b_j \left(\prod_{k=i}^{j-1} e^{\pm i\pi n_k}\right) b_i = b_i b_j \left(\prod_{k=i}^{j-1} e^{\pm i\pi n_k}\right) - b_j b_i \left(\prod_{k=i}^{j-1} e^{\pm i\pi n_k}\right) = 0\ , \\
\{c_i, c_j^\dagger\} &= b_i \left(\prod_{k=i}^{j-1} e^{\pm i\pi n_k}\right) b_j^\dagger + b_j^\dagger \left(\prod_{k=i}^{j-1} e^{\pm i\pi n_k}\right) b_i = b_i b_j^\dagger \left(\prod_{k=i}^{j-1} e^{\pm i\pi n_k}\right) - b_j^\dagger b_i \left(\prod_{k=i}^{j-1} e^{\pm i\pi n_k}\right) = 0\ , \\
\{c_i, c_i\} &= 2(b_i)^2 = 0\ , \\
\{c_i, c_i^\dagger\} &= \{b_i, b_i^\dagger\} = 0\ .
\end{aligned} \tag{1.76}$$

In principle, the Jordan–Wigner transformation can always be applied to one-dimensional spin$-1/2$ chains. However, it does not necessarily map a spin Hamiltonian to a free fermionic one, even when the original Hamiltonian is quadratic in the spin operators. Nevertheless, there exist several important models that can indeed be mapped to free fermionic systems and thus diagonalized and completely solved. Until recently, it was not fully understood under which conditions the JW transformation would yield a free fermionic model. This question was clarified in [13], where the problem was reformulated in terms of the graph-theoretic task of recognizing line graphs, a problem that can be solved optimally.

Remark 1.3 (JW for Majorana operators). If we linearly combine the fermionic operator defined in (1.71) to define Majorana operators as in (1.15), we get the following Jordan-Wigner transformation for Majorana operators:

$$\begin{aligned}
\gamma_{2j-1} &= (b_j + b_j^\dagger) \left(\prod_{k=1}^{j-1} Z_k\right) = X_j \left(\prod_{k=1}^{j-1} Z_k\right)\ , \\
\gamma_{2j} &= -i(b_j - b_j^\dagger) \left(\prod_{k=1}^{j-1} Z_k\right) = Y_j \left(\prod_{k=1}^{j-1} Z_k\right)\ .
\end{aligned} \tag{1.77}$$

We can therefore simply multiply the JW string to X_j and Y_j to get Majorana operators. The inverse transformation would look like, using (1.70):

$$\begin{aligned}
X_j &= (c_j^\dagger + c_j) \left(\prod_{k=1}^{j-1} Z_k\right) = \gamma_{2j-1} \left(\prod_{k=1}^{j-1} Z_k\right)\ , \\
Y_j &= i(c_j^\dagger - c_j) \left(\prod_{k=1}^{j-1} Z_k\right) = \gamma_{2j} \left(\prod_{k=1}^{j-1} Z_k\right)\ .
\end{aligned} \tag{1.78}$$

1.4 The example of the XY-chain

The most well-known examples of spin chains that can be mapped to free fermionic models are the XY-chain, the XX-chain, and the transverse-field Ising model (TFIM). All of these models can be derived as special

cases of the Hamiltonian for the transverse-field anisotropic XY chain:

$$H = -J \sum_{j=1}^{L} \left[\left(\frac{1+\gamma}{2} \right) X_j X_{j+1} + \left(\frac{1-\gamma}{2} \right) Y_j Y_{j+1} + h\, Z_j \right] . \tag{1.79}$$

This Hamiltonian describes a one-dimensional lattice of length L, with a three-dimensional spin variable at each lattice site. The spins interact with their nearest neighbors in an anisotropic manner, characterized by the *anisotropy parameter* $\gamma \in [0, 1]$. Interactions between the z-components are neglected, while each spin couples to an external magnetic field of strength h applied along the z-direction.

The aforementioned XX-chain is recovered in the absence of anisotropy ($\gamma = 0$):

$$H = -\frac{J}{2} \sum_{j=1}^{L} \left(X_j X_{j+1} + Y_j Y_{j+1} + h\, Z_j \right) , \tag{1.80}$$

while the TFIM is recovered for maximal anisotropy ($\gamma = \pm 1$, we write it for $\gamma = +1$):

$$H = -J \sum_{j=1}^{L} \left(X_j X_{j+1} + h\, Z_j \right) . \tag{1.81}$$

Let us now see the Jordan-Wigner transformation in action, by diagonalizing the XY-chain Hamiltonian of equation Eq. (1.79). This was firstly done in [2]. This discussion will, again, mostly follow [3] and [4].

Our first step will be to rewrite the Hamiltonian in terms of ladder operators $\sigma_j^{\pm}$, and therefore of hard-core bosonic operators $b_j, b_j^\dagger$:

$$\begin{aligned} H &= -J \sum_{j=1}^{L} \left[\sigma_j^+ \sigma_{j+1}^- + \sigma_j^- \sigma_{j+1}^+ + \gamma(\sigma_j^+ \sigma_{j+1}^+ + \sigma_j^- \sigma_{j+1}^-) + h(1 - 2\sigma_j^- \sigma_j^+) \right] = \\ &= -J \sum_{j=1}^{L} \left[b_j^\dagger b_{j+1} + b_{j+1}^\dagger b_j + \gamma(b_j^\dagger b_{j+1}^\dagger + b_j b_{j+1}) + h(1 - 2 b_j^\dagger b_j) \right] . \end{aligned} \tag{1.82}$$

We can then perform the JW transformation (1.71) to work with fermionic operators $c_j, c_j^\dagger$. We use that $\prod_{k=1}^{j-1} \left(e^{i\pi n_k} \right) \prod_{k=1}^{j} \left(e^{i\pi n_k} \right) = e^{i\pi n_j} = 1 - 2n_j$ and $c_j^\dagger n_j \left| 0 \right\rangle = c_j^\dagger n_j \left| 1 \right\rangle = 0$ for any $j = 1, \ldots, N$, to get

$$b_j^\dagger b_{j+1} = c_j^\dagger (1 - 2n_j) c_{j+1} = c_j^\dagger c_{j+1} , \qquad b_j^\dagger b_{j+1}^\dagger = c_j^\dagger (1 - 2n_j) c_{j+1}^\dagger = c_j^\dagger c_{j+1}^\dagger , \tag{1.83}$$

It is clear that the Hamiltonian will be quadratic in the fermionic operators. However, before rewriting it we have to make some remarks on boundary conditions.

The most standard choice for boundary conditions are **periodic boundary conditions (PBC)**, which require $\sigma_{j+L}^\alpha = \sigma_j^\alpha$, effectively representing the lattice as a ring. In terms of hard-core bosons, this condition translates to $b_{j+L} = b_j$ and $b_{j+L}^\dagger = b_j^\dagger$.

Before reformulating these conditions to fermions, it is important to note that (1.83) does not hold for the boundary terms. These terms are not quadratic in the fermionic operators, but they produce the following contribution

$$J\mathcal{P} \left(c_L^\dagger c_1 + c_1^\dagger c_L + \gamma\, c_L^\dagger c_1^\dagger + \gamma\, c_1 c_L \right) , \tag{1.84}$$

where $\mathcal{P} = \exp\left[\pm i\pi \sum_{k=1}^{L} c_k^\dagger c_k \right] = \prod_{k=1}^{L} Z_k$. This operator is the *parity operator*, since, as discussed earlier, the phase factor $\exp\left[\pm i\pi \sum_{k=1}^{L} c_k^\dagger c_k \right]$ takes the value $+1$ when acting on a state with an even number of

occupied modes, and -1 when the number is odd. Using this, the full Hamiltonian expressed in terms of fermionic operators becomes:

$$\begin{aligned} H = &- J \sum_{j=1}^{L-1} \left(c_j^\dagger c_{j+1} + c_{j+1}^\dagger c_j + \gamma\, c_j^\dagger c_{j+1}^\dagger + \gamma\, c_{j+1} c_j \right) + Jh \sum_{j=1}^{L} \left(2 c_j^\dagger c_j - 1 \right) \\ &+ J\mathcal{P} \left(c_L^\dagger c_1 + c_1^\dagger c_L + \gamma\, c_L^\dagger c_1^\dagger + \gamma\, c_1 c_L \right) . \end{aligned} \tag{1.85}$$

The Hamiltonian in Eq. (1.85) describes spinless fermions hopping on a lattice, with interactions that create or annihilate fermion pairs on neighboring sites. This can be seen as a simple one-dimensional analogue of the BCS model. When $\gamma \neq 0$, the interaction terms prevent the Hamiltonian from commuting with the total particle number operator $N = \sum_{k=1}^{L} n_k$ and therefore the particle number is not conserved. However, since fermions are always created or annihilated in pairs, the parity remains conserved, i.e., $[\mathcal{P}, H] = 0$. Consequently, the Hamiltonian can be decomposed into two independent sectors corresponding to positive and negative parity, using the projection operators $(1 \pm \mathcal{P})/2$:

$$H = \frac{1+\mathcal{P}}{2} H^+ + \frac{1-\mathcal{P}}{2} H^- , \tag{1.86}$$

where $H^\pm$ have the form of (1.85), but replacing $\mathcal{P}$ with its eigenvalues ± 1.

We can insert the boundary terms back in the sum if we impose appropriate boundary conditions: antiperiodic for the even sector, while periodic for the odd one ($c_{j+L}^{(\pm)} = \mp c_j^{(\pm)}$). The two Hamiltonians will then look like:

$$H^\pm = -J \sum_{j=1}^{L} \left(c_j^{(\pm)\dagger} c_{j+1}^{(\pm)} + c_{j+1}^{(\pm)\dagger} c_j^{(\pm)} + \gamma\, c_j^{(\pm)\dagger} c_{j+1}^{(\pm)\dagger} + \gamma\, c_{j+1}^{(\pm)} c_j^{(\pm)} - h\,(2 c_j^{(\pm)\dagger} c_j^{(\pm)} - 1) \right) . \tag{1.87}$$

Each sector is governed by the same Hamiltonian, but with a different Fock space due to different boundary conditions.

Another commonly used choice is **open boundary conditions (OBC)**. In this case, the chain ends at site L, with no additional sites beyond it. As a result, there is no term for site $L+1$, and the Hamiltonian reduces to:

$$H_{OBC} = -J \sum_{j=1}^{L-1} \left(c_j^\dagger c_{j+1} + c_{j+1}^\dagger c_j + \gamma\, c_j^\dagger c_{j+1}^\dagger + \gamma\, c_{j+1} c_j \right) + Jh \sum_{j=1}^{L} \left(2 c_j^\dagger c_j - 1 \right) . \tag{1.88}$$

Here, there is not the need to separate the Hamiltonian in two sectors in order to diagonalize it, since there is not the problematic term (1.84).

Remark 1.4. The XY-chain with periodic boundary conditions is not considered a free fermionic system according to 1.1, while the two parity sectors are. On the other hand, the open chain is already free fermionic without the need to split it.

1.4.1 The Hamiltonian in Fourier Space

At this stage, both the PBC and OBC cases lead to a quadratic fermionic Hamiltonian, which can be diagonalized using a canonical transformation. We now want to determine this transformation and the corresponding energy eigenvalues by moving to Fourier space. For simplicity, we will focus on the PBC case, as it represents the standard example. See [45] for a treatment of the diagonalization of the OBC chain of the related Quantum Ising Chain.

We choose the following convention for the Fourier transform:

$$c_j^{(\pm)} = \frac{e^{i\pi/4}}{\sqrt{L}} \sum_{q\in\Gamma_\pm} e^{i\frac{2\pi}{L}qj} c_q \,, \qquad\qquad c_q \equiv \frac{e^{-i\pi/4}}{\sqrt{L}} \sum_{j=1}^{L} e^{-i\frac{2\pi}{L}qj} c_j^{(\pm)} \,. \tag{1.89}$$

The phase factors $e^{\pm i\pi/4}$ cancel out when applying the direct and inverse transformations one after the other, but they are included here for later convenience. With this choice of convention, the CAR (1.12) remain satisfied even in momentum space.

The allowed values of the momentum q depend on the parity sector. Indeed, the boundary conditions impose different quantization rules: in the odd-parity sector, where we have PBC, q takes integer values, while in the even-parity sector, where we have anti-PBC, q takes half-integer values. Let us denote the sets with $\Gamma_\pm$, where

$$\Gamma_+ = \{1/2, 3/2, ..., L-1/2\} \,, \qquad\qquad \Gamma_- = \{0, 1, ..., L-1\} \,. \tag{1.90}$$

It is more useful to choose q both positive and negative. However we have to differentiate the case of L even and L odd.

- *L even*: $\Gamma_+ = \{\pm 1/2, \pm 3/2, ..., \pm(L/2-1)\}$, $\Gamma_- = \{-L/2+1, ..., L/2\}$,
- *L odd*: $\Gamma_+ = \{-L/2+1, ..., L/2\}$, $\Gamma_- = \{-(L-1)/2, ..., (L-1)/2\}$.

Let us rewrite in Fourier space the terms of the Hamiltonian:

$$\begin{aligned}
\sum_{j=1}^{L} c_j^{(\pm)\dagger} c_{j+1}^{(\pm)} &= \sum_{q,q'\in\Gamma_\pm} \Big(\sum_{j=1}^{L} \frac{1}{L} e^{i\frac{2\pi}{L}(q'-q)\,j} \Big) e^{i\frac{2\pi}{L}q'} c_q^\dagger c_{q'} = \\
&= \sum_{q,q'\in\Gamma_\pm} \delta_{q,q'} e^{i\frac{2\pi}{L}q'} c_q^\dagger c_{q'} = \sum_{q\in\Gamma_\pm} e^{i\frac{2\pi}{L}q} c_q^\dagger c_q \,, \\
\sum_{j=1}^{L} c_{j+1}^{(\pm)\dagger} c_j^{(\pm)} &= \Big(\sum_{j=1}^{L} c_j^{(\pm)\dagger} c_{j+1}^{(\pm)} \Big)^\dagger = \Big(\sum_{q\in\Gamma_\pm} e^{i\frac{2\pi}{L}q} c_q^\dagger c_q \Big)^\dagger = \sum_{q\in\Gamma_\pm} e^{-i\frac{2\pi}{L}q} c_q^\dagger c_q \\
\sum_{j=1}^{L} (2 c_j^{(\pm)\dagger} c_j^{(\pm)} - 1) &= \sum_{q,q'\in\Gamma_\pm} \delta_{q,q'} (2 c_q^\dagger c_{q'} - 1) = \sum_{q\in\Gamma_\pm} (2 c_q^\dagger c_q - 1) \,,
\end{aligned} \tag{1.91}$$

and therefore

$$-J \sum_{j=1}^{L} \Big(c_j^{(\pm)\dagger} c_{j+1}^{(\pm)} + c_{j+1}^{(\pm)\dagger} c_j^{(\pm)} - h\,(2 c_j^{(\pm)\dagger} c_j^{(\pm)} - 1) \Big) = -2J \sum_{q\in\Gamma_\pm} \left\{ \left[\cos\left(\frac{2\pi}{L} q\right) - h \right] \left(c_q^\dagger c_q - \frac{1}{2} \right) \right\} \,, \tag{1.92}$$

where we used that $\sum_{q\in\Gamma_\pm} \cos(2\pi q/L) = 0$, which can be proven using the formula for the partial sum of the geometric series. The other terms of the Hamiltonian will look like, making use of the phase factor:

$$\begin{aligned}
\sum_{j=1}^{L} c_j^{(\pm)\dagger} c_{j+1}^{(\pm)\dagger} &= e^{-i\pi/2} \sum_{q,q'\in\Gamma_\pm} \delta_{q',-q} e^{-i\frac{2\pi}{L}q} c_{q'}^\dagger c_q^\dagger = -i \sum_{q\in\Gamma_\pm} e^{i\frac{2\pi}{L}q} c_{-q}^\dagger c_q^\dagger \,, \\
\sum_{j=1}^{L} c_{j+1}^{(\pm)} c_j^{(\pm)} &= \Big(\sum_{j=1}^{L} c_j^{(\pm)\dagger} c_{j+1}^{(\pm)\dagger} \Big)^\dagger = i \sum_{q\in\Gamma_\pm} e^{-i\frac{2\pi}{L}q} c_q c_{-q} \,.
\end{aligned} \tag{1.93}$$

To simplify these terms more, it is useful to separate the sum over positive and negative values of q. We have to consider separately the cases of L even or odd.

- *L even*: let us consider separately the two different parities.

  For $\mathcal{P}=+1$, we have:

$$\Gamma_+ = \{\pm 1/2, \pm 3/2, ..., \pm(L/2-1)\} = \Gamma_+^{>0} \cup \Gamma_+^{<0}\,, \tag{1.94}$$

  where clearly $\Gamma_+^{>0} = \{+1/2, ..., L/2-1\}$ and $\Gamma_+^{<0} = \{-1/2, ..., -(L/2-1)\}$. We then have

$$\begin{aligned}\sum_{j=1}^{L} c_j^{(+)\dagger} c_{j+1}^{(+)\dagger} &= -i\left(\sum_{q\in\Gamma_+^{>0}} e^{i\frac{2\pi}{L}q} c_{-q}^\dagger c_q^\dagger + \sum_{q\in\Gamma_+^{<0}} e^{i\frac{2\pi}{L}q} c_{-q}^\dagger c_q^\dagger\right) = \\ &= -i\sum_{q\in\Gamma_+^{>0}} (e^{i\frac{2\pi}{L}q} - e^{-i\frac{2\pi}{L}q}) c_{-q}^\dagger c_q^\dagger = 2\sum_{q\in\Gamma_+^{>0}} \sin\left(\frac{2\pi}{L}q\right) c_{-q}^\dagger c_q^\dagger\,, \\ \sum_{j=1}^{L} c_{j+1}^{(+)} c_j^{(+)} &= \left(\sum_{j=1}^{L} c_j^{(+)\dagger} c_{j+1}^{(+)\dagger}\right)^\dagger = 2\sum_{q\in\Gamma_+^{>0}} \sin\left(\frac{2\pi}{L}q\right) c_q c_{-q}\,,\end{aligned} \tag{1.95}$$

  where in the second line we changed the sum over $\Gamma_+^{<0}$ to a sum over $\Gamma_+^{>0}$ changing q with $-q$, used the fact that $c_q^\dagger$ and $c_{-q}^\dagger$ anticommute and noted that the sum over $\Gamma_+^{>0}$ is the same as half the sum over Γ_+. We can also split the term computed in (1.92) and proceed similarly with the computation to get:

$$\begin{aligned}-2J\sum_{q\in\Gamma_+}\left[\cos\left(\frac{2\pi}{L}q\right) - h\right]\left(c_q^\dagger c_q - \frac{1}{2}\right) &= -2J\sum_{q\in\Gamma_+^{>0}}\left[\cos\left(\frac{2\pi}{L}q\right) - h\right](c_q^\dagger c_q + c_{-q}^\dagger c_{-q} - 1) = \\ &= -2J\sum_{q\in\Gamma_+^{>0}}\left[\cos\left(\frac{2\pi}{L}q\right) - h\right](c_q^\dagger c_q - c_{-q} c_{-q}^\dagger)\,.\end{aligned} \tag{1.96}$$

  For $\mathcal{P}=-1$, we have:

$$\Gamma_- = \{-L/2+1, ..., L/2\} = \Gamma_-^{<0} \cup \Gamma_-^{>0} \cup \{0, L/2\}\,, \tag{1.97}$$

  where $\Gamma_-^{<0} = \{-L/2+1, ...\}$ and $\Gamma_-^{>0}\{1, ..., L/2-1\}$. The calculations for the terms which multiply γ are exactly the same since $\sin(0) = \sin(2\pi L/2L) = 0$, while for (1.92) we have

$$\begin{aligned}-2J\sum_{q\in\Gamma_-}\left[\cos\left(\frac{2\pi}{L}q\right) - h\right]\left(c_q^\dagger c_q - \frac{1}{2}\right) &= -2J\sum_{q\in\Gamma_-^{>0}}\left[\cos\left(\frac{2\pi}{L}q\right) - h\right](c_q^\dagger c_q - c_{-q} c_{-q}^\dagger) \\ &\quad + 4Jh\left(c_q^\dagger c_q - \frac{1}{2}\right)\,.\end{aligned} \tag{1.98}$$

  The last term comes up from the modes $q = 0, L/2$ and it is non zero, however we can neglect it since it will vanish in the thermodynamic limit.

- *L odd*: we now have an odd number of elements in $\Gamma_\pm$.

  For $\mathcal{P}=+1$, we have:

$$\Gamma_+ = \{-L/2+1, ..., L/2\} = \Gamma_+^{<0} \cup \Gamma_+^{>0} \cup \{L/2\}\,, \tag{1.99}$$

  where $\Gamma_+^{>0} = \{-L/2+1, ..., -1/2\}$ and $\Gamma_+^{<0} = \{1/2, ..., L/2-1\}$. We then obtain the same results in the thermodynamic limit.

  For $\mathcal{P}=-1$ we have:

$$\Gamma_- = \{-(L-1)/2, ..., (L-1)/2\} = \Gamma_-^{<0} \cup \Gamma_-^{>0} \cup \{0\}\,, \tag{1.100}$$

  where $\Gamma_-^{<0} = \{-(L-1)/2, ..., -1\}$ and $\Gamma_-^{>0} = \{1, ..., (L-1)/2\}$. In this case too the results are identical in the thermodynamic limit.

Finally, we can write the two Hamiltonians as:

$$H^{\pm} = 2J \sum_{q \in \Gamma_{\pm}^{>0}} \left\{ \left[h - \cos\left(\frac{2\pi}{L} q\right) \right] (c_q^\dagger c_q - c_{-q} c_{-q}^\dagger) + \gamma \sin\left(\frac{2\pi}{L} q\right) \left(c_q c_{-q} + c_{-q}^\dagger c_q^\dagger \right) \right\} . \tag{1.101}$$

1.4.2 The Bogoliubov Transformation

The Hamiltonians in Eq. (1.101) are sums of quadratic terms in the creation and annihilation operators, and can be rewritten using a matrix notation:

$$H^{\pm} = 2J \sum_{q \in \Gamma_{\pm}^{>0}} \begin{pmatrix} c_q^\dagger & c_{-q} \end{pmatrix} \begin{pmatrix} h - \cos\left(\frac{2\pi}{L} q\right) & -\gamma \sin\left(\frac{2\pi}{L} q\right) \\ -\gamma \sin\left(\frac{2\pi}{L} q\right) & \cos\left(\frac{2\pi}{L} q\right) - h \end{pmatrix} \begin{pmatrix} c_q \\ c_{-q}^\dagger \end{pmatrix} . \tag{1.102}$$

To diagonalize this type of Hamiltonian, we employ a **Bogoliubov transformation**. This transformation maps the original creation and annihilation operators to a new set of operators, chosen such that the Hamiltonian becomes diagonal. Conceptually, it plays the same role as the canonical transformation used for general quadratic fermionic Hamiltonians, but it is applied here in Fourier space. A key difference is that it couples only the modes with momenta q and $-q$.

To do this transformation, we can just diagonalize the matrices:

$$M_q = 2J \begin{pmatrix} h - \cos\left(\frac{2\pi}{L} q\right) & -\gamma \sin\left(\frac{2\pi}{L} q\right) \\ -\gamma \sin\left(\frac{2\pi}{L} q\right) & \cos\left(\frac{2\pi}{L} q\right) - h \end{pmatrix} . \tag{1.103}$$

This can be done via a $O(2)$ rotation in Fourier space, since the M_q are symmetric real matrices.

Let us define the new creation/annihilation operators as:

$$\begin{pmatrix} \tilde{c}_q \\ \tilde{c}_{-q}^\dagger \end{pmatrix} = R_q \begin{pmatrix} c_q \\ c_{-q}^\dagger \end{pmatrix} = \begin{pmatrix} \cos\theta_q & -\sin\theta_q \\ \sin\theta_q & \cos\theta_q \end{pmatrix} \begin{pmatrix} c_q \\ c_{-q}^\dagger \end{pmatrix} . \tag{1.104}$$

In this way we can write the Hamiltonian as:

$$H^{\pm} = \sum_{q \in \Gamma_{\pm}^{>0}} \begin{pmatrix} \tilde{c}_q^\dagger & \tilde{c}_{-q} \end{pmatrix} R_q^\dagger M_q R_q \begin{pmatrix} \tilde{c}_q \\ \tilde{c}_{-q}^\dagger \end{pmatrix} , \tag{1.105}$$

and to diagonalize it we have to impose $D_q = R_q^\dagger M_q R_q$ to be diagonal for each q and that the $\tilde{c}_q$ satisfy the canonical anticommutation relations (1.12).

The anticommutation relations will look like this

$$\begin{aligned} \{\tilde{c}_q, \tilde{c}_{q'}^\dagger\} &= (\cos^2\theta_q + \sin^2\theta_q)\delta_{q,q'} = \delta_{q,q'} \overset{!}{=} \delta_{q,q'} . \\ \{\tilde{c}_q, \tilde{c}_{q'}\} &= -\cos\theta_q \sin\theta_{q'} \{c_q, c_{-q'}^\dagger\} - \sin\theta_q \cos\theta_{q'} \{c_{-q}^\dagger, c_{q'}\} = \\ &= -(\cos\theta_q \sin\theta_{-q} + \sin\theta_q \cos\theta_{-q})\delta_{q,-q'} = -\sin(\theta_q + \theta_{-q})\delta_{q,-q'} \overset{!}{=} 0 , \\ \{\tilde{c}_q^\dagger, \tilde{c}_{q'}^\dagger\} &= \left(\{\tilde{c}_q, \tilde{c}_{q'}\}\right)^\dagger = \{\tilde{c}_q, \tilde{c}_{q'}\} = -\sin(\theta_q + \theta_{-q})\delta_{q,-q'} \overset{!}{=} 0 , \end{aligned} \tag{1.106}$$

The first condition is already satisfied, while the second one requires that $\theta_{-q} = -\theta_q$, considering $\theta_q \in (-\pi, \pi)$.

If we diagonalize the matrix, we obtain as eigenvalues:

$$\varepsilon(\pm q) = \pm\varepsilon(q) = \pm 2J \sqrt{\left[h - \cos\left(\frac{2\pi}{L} q\right) \right]^2 + \gamma^2 \sin^2\left(\frac{2\pi}{L} q\right)} , \tag{1.107}$$

and a rotation angle defined by

$$\tan\left(2\vartheta_q\right) = \frac{\gamma \sin\left(\frac{2\pi}{L}q\right)}{h - \cos\left(\frac{2\pi}{L}q\right)}\,, \tag{1.108}$$

which is such that $\tan(2\theta_{-q}) = -\tan(2\theta_q)$ and therefore $\theta_q = -\theta_q$ since $\tan(x)$ is an odd function in x.

The two Hamiltonians will look like:

$$H^{\pm} = \sum_{q\in\Gamma_{\pm}^{>0}} \varepsilon(q)\left(\tilde{c}_q^{\dagger}\tilde{c}_q - \tilde{c}_{-q}\tilde{c}_{-q}^{\dagger}\right)\,, \tag{1.109}$$

or, if we rewrite the sum over $\Gamma_{\pm}^{>0}$ as a sum over $\Gamma_{\pm}$, recalling that some terms can be discarded in the thermodynamic limit as discussed in the previous section

$$H^{\pm} = \sum_{q\in\Gamma_{\pm}} \varepsilon(q)\left(\tilde{c}_q^{\dagger}\tilde{c}_q - \tilde{c}_q\tilde{c}_q^{\dagger}\right) = \sum_{q\in\Gamma_{\pm}} 2\varepsilon(q)\left(\tilde{c}_q^{\dagger}\tilde{c}_q - 1/2\right)\,, \tag{1.110}$$

exactly as in (1.38). We therefore proved the free fermionicity of the model and we found its spectrum as (1.107).

Chapter 2

Quantum Circuits and Free Fermions

The concept of quantum computation was first introduced by Feynman [46], and since then, the field has been the subject of extensive research [47, 48]. Quantum computers have attracted considerable attention due to their potential to solve problems that are intractable for classical computers, offering exponential speedups. Of particular relevance to physicists is the possibility to simulate physical systems that cannot be efficiently modeled with classical computation.

In particular, simulating quantum many-body systems on classical computers is extremely challenging, as the size of the matrices involved grows exponentially with the system size. For instance, even in the case of a one-dimensional spin$-1/2$ chain – the simplest possible many-body system – the time evolution operator[1] $U(t) = e^{-iHt}$ act on a 2^L-dimensional space, where L is the lenght of the chain. In a computer, this is represented by a $2^L \times 2^L$ dimensional matrix. For a system with $L = 20$, this corresponds already to a matrix of size $1.048.576 \times 1.048.576$, which is practically intractable for a classical computer.

Quantum devices are built using quantum bits, or *qubits*, which represent the quantum analogue of classical bits. While classical bits can take only the values 0 and 1, qubits can also be in a superposition of these states. A general qubit state can be written as:

$$|\phi\rangle = \alpha\,|0\rangle + \beta\,|1\rangle\ , \tag{2.1}$$

where $\alpha, \beta \in \mathbb{C}$ and $\{|0\rangle, |1\rangle\}$ is the computational basis of the Hilbert space $\mathcal{H} = \mathbb{C}^2$. We shall also impose $|\alpha|^2 + |\beta|^2 = 1$ to have a normalized state.

Quantum features such as superposition and entanglement can provide an exponential speedup for certain computations compared to their classical counterparts. However, not all quantum systems cannot be simulated classically, and the same holds for some quantum circuit architectures. These systems can serve as valuable **benchmarks**, offering a controlled environment in which it is possible to verify that quantum devices operate as expected. Free fermionic systems are closely related to both benchmarking and classical simulability. In particular, free fermions can be used to construct **matchgate circuits** [21–24], a class of circuits which can shown to be classically simulable. Moreover, fermionic Gaussian states [15–17] are quantum states which arise in free fermionic systems and can be efficiently simulated on a classical computer using the *correlation matrix* formalism.

From this discussion, the relevance of free fermionic systems also in the context of quantum computation is clear.

We start with Section 2.1 by introducing the concept of quantum circuits and explaining how to construct them from spin$-1/2$ chain Hamiltonians. We will also discuss how and why these circuits can be used to

[1] Here, we assume a time-independent Hamiltonian and we consider natural units, for which $\hbar = 1$.

simulate the dynamics of many-body quantum systems. In Section 2.2, we introduce matchgate circuits and describe their connection to free fermions, classical simulability, and Gaussian operators. In Section 2.3, we then present fermionic Gaussian states and explain why they can be simulated classically, providing numerical simulations as examples. Finally, in Section 2.4, we define what it means for a circuit to be free fermionic and show that any circuit constructed from JW-diagonalizable models satisfies this property.

2.1 Quantum Circuits and Quantum Simulation

Quantum circuits are a model of quantum computation built upon the basic elements of classical circuits, such as bits and logic gates, by extending them to their quantum counterparts [47, 48].

We begin with a system of L qubits, described by the Hilbert space $\mathcal{H} = (\mathbb{C}^2)^{\otimes L}$. A sequence of *quantum gates* is then applied to this initial state. These gates are implemented by single- or multi-qubit unitary operators (typically two-qubit). Quantum gates can, in principle, be arbitrary unitaries, however, they are usually chosen from a finite gate set. Finally, the outcome of the computation is read off with a measurement. Figure 2.1 shows a simple example of a three-qubit quantum circuit.

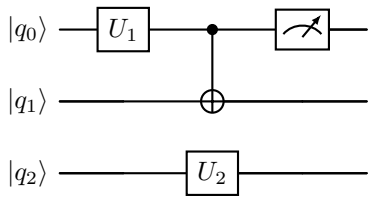

Figure 2.1: Example of a quantum circuit acting on three qubits. U_1 and U_2 are generic single-qubit gates, the one acting on the first two qubits is a CNOT gate, while the drawing on the top right represents a measurement.

The Hilbert space of a $L-$qubit system is identical to that of a spin$-1/2$ chain with L sites. It is therefore natural to explore how quantum circuits can be constructed from spin chain Hamiltonians. We now proceed to do so.

Let us now see how quantum circuits can be constructed from Hamiltonian systems. Consider a quantum system defined on a lattice, whose Hamiltonian can be expressed as a sum of local interaction terms:

$$H = \sum_{j=1}^{M} \alpha_j h_j \,. \tag{2.2}$$

Here, each h_j acts non-trivially on at most a constant number c of sites, and M denotes the number of "fundamental operators" in the Hamiltonian, which is typically related to the number of sites L. Spin$-1/2$ chain Hamiltonians are a perfect example of this, as they naturally act on an L-qubit system, as previously discussed. The assumption of locality is physically reasonable, since in most systems interactions decay with increasing distance. We can use these kinds of Hamiltonian to describe many-body quantum systems.

For each h_j, we can construct a local unitary gate with angle φ_j as:

$$u_j = e^{i\varphi_j h_j} = \cos\varphi_j + i h_j \sin\varphi_j \,. \tag{2.3}$$

We can then build quantum circuits as product of these local gates. Given a string of indices $\{s_1, s_2, ...s_N\}$, we can define a quantum circuit as:

$$\mathcal{V} = u_{s_N} ... u_{s_2} u_{s_1} \,. \tag{2.4}$$

The order of the operators in the product determines the *geometry of the circuit*, as illustrated in Figure 2.2: different sequences of indices lead to different graphical representations of the circuit. Another key concept is the *depth* of a circuit, defined as the number of layers it contains. For instance, the circuit on the left in Figure 2.2 has a depth of 3, whereas the one on the right has a depth of 6. Notice that the depth of the left circuit does not depend on the system size, while the depth of the right circuit increases linearly with it.

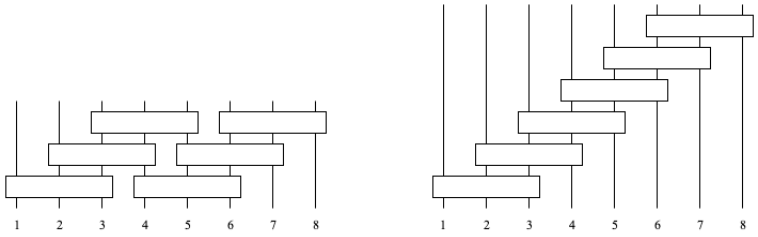

Figure 2.2: Example of two quantum circuits with different geometry. The system is composed by $L = 8$ qubits and the local unitaries act on three qubits. The expression of the circuit on the left is $\mathcal{V}_L = (u_3u_6)(u_2u_5)(u_1u_4)$, while the one on the right is $\mathcal{V}_R = u_6u_5u_4u_3u_2u_1$. Notice how we are using the same gates, but the left arrangement has a constant depth, while the right one has a depth growing linearly with the system size.

Well-known examples of quantum circuits are given by *brickwork circuits*. These circuits are characterized by a repeating pattern of n-qubit (typically two-qubit) gates arranged in a staggered or "bricklaying" formation. They are composed of a series of layers, with each layer applying gates to adjacent qubits. In the following layer, the gates are shifted so that they act on a different set of adjacent qubits (see the left circuit in Figure 2.2 and the circuit in Figure 2.3). The name "brickwork" arises from their visual resemblance to a brick wall.

Let us focus on the 2-brickwork circuit, the most commonly used. It consists of two layers of two-qubit gates acting on nearest-neighbor qubits, as shown in Figure 2.3. Circuits of this type can be generated by a nearest-neighbor Hamiltonian of the form:

$$H = \sum_{j=1}^{L} \alpha_j h_{j,j+1}\,, \tag{2.5}$$

such as the XY-chain, the XX-chain and the TFIM discussed in Section 1.4. To construct 2-brickwork circuits from an Hamitonian of the form (2.5), one can define local unitary gates $u_j = e^{-i\varphi_j h_{j,j+1}}$ and then apply first the gates with odd indices, followed by those with even indices:

$$\mathcal{V} = \left(\prod_{j \text{ even}} e^{-i\varphi_j h_{j,j+1}}\right)\left(\prod_{j \text{ odd}} e^{-i\varphi_j h_{j,j+1}}\right) = (u_2u_4...u_L)(u_1u_3...u_{L-1})\,, \tag{2.6}$$

where we assumed L even.

Since the local Hamiltonians act on different pairs of qubits, we have $[h_{j,j+1}, h_{j+2,j+3}] = 0$. This means that all the gates within the two parentheses of Eq. (2.6) act on distinct qubits and therefore commute, allowing them to be applied simultaneously. As a result, the circuit achieves a constant depth of 2, as illustrated in Figure 2.3.

Having seen how quantum circuits can be constructed from the Hamiltonians of many-body quantum systems, a natural question arises: can we use quantum circuits to simulate the dynamics of these systems? Ideally, one would like to express the time evolution entirely in terms of local unitary gates. While this is not exactly possible in general, it is always possible to approximate it, getting arbitrarily close.

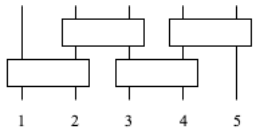

Figure 2.3: Graphical representation of the depth-2 brickwork circuit described by equation (2.6) acting on $L = 5$ spins.

If the local interactions of (2.2) are independent and/or all act on different qubits, and therefore $[h_j, h_{j'}] = 0$, we can always write the time evolution operator as a product of local unitaries as:

$$U(t) = e^{-itH} = e^{-it\sum_j \alpha_j h_j} = \prod_{j=1}^{M} e^{-it\alpha_j h_j} \,. \tag{2.7}$$

Unfortunately, in general $[h_j, h_{j'}] \neq 0$ and (2.7) does not hold. However, at the heart of quantum simulation lies the famous **Trotter formula** [49]: given two hermitian operators A and B, for any real t

$$\lim_{n\to\infty} \left(e^{iAt/n} e^{iBt/n}\right)^n = e^{i(A+B)t} \,. \tag{2.8}$$

This shows that, by considering sufficiently small timesteps, we can always simulate the dynamics of a system with a Hamiltonian of the form (2.2) using quantum gates constructed from the local Hamiltonians h_j. In particular, if we are interested in the state of the system at time t, we divide the evolution into n timesteps of size $dt = t/n$, construct the local unitaries $u_j = e^{-i\,dt\,\alpha_j\,h_j}$ and define a quantum circuit that contains all of these gates once. We then apply this circuit n times to the initial state, with each application moving the system by dt in time.

In principle, in the small-timestep limit, the choice of "trotterization", meaning the order in which the local unitaries are applied, does not matter. However, it is convenient to group together gates that commute, as they can be applied simultaneously, reducing the circuit depth, which corresponds here to the number of steps required to complete a single timestep. This is illustrated in Figure 2.2: the gates are the same in both circuits, but the ordering on the left allows for a smaller depth. Ideally, one aims to construct circuits whose depth is constant, meaning independent of the system size. In this way, the computational cost remains the same for both small and large systems. This is precisely the case for brickwork circuits, as can be seen in Figure 2.2 (left) and Figure 2.3.

2.2 Matchgate circuits

In this section, we introduce **matchgate circuits** and discuss their connection to free fermions and classical simulability. Matchgates were first introduced in [21] as a classically simulable computational model and were later shown to correspond to a free fermionic physical system in [22]. Subsequent works [23, 24] further extended the conditions under which these circuits remain classically simulable, in particular considering different input states and measurements on the output.

Let us start with the definition of a matchgate:

Definition 2.1 (**Matchgates**)**.** Let $G(A, B)$ be a two-qubit gate of the form:

$$G(A,B) = \begin{pmatrix} A_{11} & 0 & 0 & A_{12} \\ 0 & B_{11} & B_{12} & 0 \\ 0 & B_{21} & B_{22} & 0 \\ A_{21} & 0 & 0 & A_{22} \end{pmatrix} \tag{2.9}$$

where

$$A = \begin{pmatrix} A_{11} & A_{12} \\ A_{21} & A_{22} \end{pmatrix}, \qquad B = \begin{pmatrix} B_{11} & B_{12} \\ B_{21} & B_{22} \end{pmatrix}, \tag{2.10}$$

are one-qubit gates, i.e. $A, B \in U(2)$. Then, $G(A, B)$ is a *matchgate* if $\det A = \det B$.

This class of gates preserves the parity of the input bitstring: indeed the even parity sector, spanned by $\{|00\rangle, |11\rangle\}$, is decoupled from the odd parity sector spanned by $\{|01\rangle, |10\rangle\}$.

The set of all matchgates acting on qubits $\{i, j\}$ is generated by the set

$$\mathcal{A}_{i,j} = \{X_iX_j, X_iY_j, Y_iX_j, Y_iY_j, Z_i, Z_j\}. \tag{2.11}$$

This means that for any matchgate $G(A, B)$, there exists a Hamiltonian H, given by a linear combination of the elements of $\mathcal{A}_{i,j}$, such that $G(A, B) = e^{iH}$. See Appendix A for a proof.

From this point on, we will focus primarily on *nearest neighbors matchgates*. Circuits constructed using only nearest-neighbor matchgates are classically simulable and can be mapped to free fermionic systems, as we will show below. In contrast, allowing non–nearest-neighbor matchgates, or equivalently, introducing the possibility of swapping qubits, enables the resulting circuits to efficiently perform universal quantum computation [23]. Unless stated otherwise, all references to matchgates in the following will refer specifically to nearest-neighbor matchgates.

We now show that matchgates can be expressed in terms of non-interacting fermions. This connection can be established once again through the Jordan–Wigner transformation (1.71), which allows us to define fermionic operators in terms of Pauli strings. Using (1.70) and (1.72), it is straightforward to write all the generators in $\mathcal{A}_{i,i+1}$ in terms of fermionic operators as follows:

$$\begin{aligned}
Z_i &= 1 - 2c_i^\dagger c_i = c_ic_i^\dagger - c_i^\dagger c_i\,, \\
X_iX_{i+1} &= (c_i + c_i^\dagger)Z_i(c_{i+1} + c_{i+1}^\dagger) = -(c_i - c_i^\dagger)(c_{i+1} + c_{i+1}^\dagger)\,, \\
Y_iY_{i+1} &= -(c_i - c_i^\dagger)Z_i(c_{i+1} - c_{i+1}^\dagger) = (c_i + c_i^\dagger)(c_{i+1} - c_{i+1}^\dagger)\,, \\
X_iY_{i+1} &= i(c_i + c_i^\dagger)Z_i(c_{i+1} - c_{i+1}^\dagger) = i(c_i - c_i^\dagger)(c_{i+1} - c_{i+1}^\dagger)\,, \\
Y_iX_{i+1} &= i(c_i - c_i^\dagger)Z_i(c_{i+1} + c_{i+1}^\dagger) = i(c_i + c_i^\dagger)(c_{i+1} + c_{i+1}^\dagger)\,.
\end{aligned} \tag{2.12}$$

We can see that all the generators in Eq. (2.12) are quadratic in the fermionic operators and thus any Hamiltonian constructed as a linear combination of them is a fermionic quadratic Hamiltonian. It is important to note, however, that the Jordan–Wigner transformation does not preserve locality. As a result, the generators of non–nearest-neighbor matchgates are not mapped to quadratic fermionic operators. This explains why only nearest-neighbor matchgates are classically simulable, as they correspond to non-interacting fermions. On the other hand, operators that are quadratic in non–nearest-neighbor fermionic operators are still classically simulable, even though their get mapped to multi-qubit operators after an inverse JW transformation (1.72). This is because such operators can be expressed as products of matchgates [22, 23]. We will return to this point in Subsection 2.2.1.

We now give a more quantitative meaning to the notion of classical simulability, which we have mentioned several times so far. Following [24], we introduce the concept of *strong simulability*. For a more detailed discussion and alternative, weaker notions of simulability, see [24, 50, 51].

Let us consider a uniform family of quantum circuits $\{C_n\}$ acting on an arbitrary n-qubit input state $|\psi_n\rangle$. Suppose that the circuit is followed by some measurements performed on a subset of k out of the n qubits. The probability of obtaining the measurement outcome $|\tilde{y}\rangle$ on these k qubits is then given by:

$$P(\tilde{y}|\psi_n) = \mathrm{tr}\langle\tilde{y}|C_n|\psi_n\rangle\langle\psi_n|C_n|\tilde{y}\rangle\,. \tag{2.13}$$

We can now define a *strongly simulable* quantum circuit.

Definition 2.2. The uniform family of quantum circuits $\{C_n\}$ acting on the $n-$qubit input state $|\psi_n\rangle$, is *strongly simulable* if, given a measured $k-$qubit state $|\tilde{y}\rangle$, for any $k \leq n$, is possible to compute $P(\tilde{y}|\psi_n)$ to m digits precision in poly(n, m) time on a classical computer.

In a series of papers ([22–24]) various results on the classical simulability of matchgate circuits have been proven, considering different input states and measured observable. The most general result is the one proved in Ref. [24] and it is the following Theorem:

Theorem 2.1. *Let $\{M_n\}$ be a uniform family of quantum circuits composed of poly(n) nearest-neighbour matchgates acting on n qubits, and let the input be an arbitrary $n-$qubit product state $|\psi\rangle = |\psi_1\rangle \dots |\psi_n\rangle$. Then, there are polynomial-time classical algorithms to simulate the outcomes of measurements over arbitrary subsets of the output qubits.*

The proof of the theorem is divided into two parts. The first part demonstrates that any arbitrary product state can be obtained from the all-zero state by introducing an ancillary qubit in the state $|+\rangle = (|0\rangle+|1\rangle)/\sqrt{2}$. The second part (adapted from [22]) shows that any matchgate circuit initialized in a computational-basis state is strongly simulable, since all output probabilities can be expressed in terms of matrix determinants, which can be efficiently computed on a classical computer.

In [24], it was also shown that matchgate circuits remain classically simulable, even if in a weaker sense, also when considering arbitrary *non–computational-basis* measurements.

2.2.1 Gaussian Operators and Matchgate Circuits

We now introduce the definition of a *Gaussian operator* [16] and show that a matchgate circuit can be represented as such an operator [23].

Definition 2.3 (Gaussian Operator). Given a fermionic quadratic Hamiltonian H, written as (1.25) or (1.43), a *Gaussian operator* U is the unitary operator generated by H, i.e. $U = e^{iH}$.

It is clear that the time evolution operators defined starting from fermionic quadratic Hamiltonians are Gaussian operators.

Let us now state and prove an important result about Gaussian operators, mentioned in [16, 22, 23]. We will provide the proof given in [23].

Theorem 2.2. *Let H be any fermionic quadratic Hamiltonian (1.43) and $U = e^{iH}$ the corresponding Gaussian operator. Let $\{\gamma_\mu\}$ be a set of $2n$ Majorana operators (see Remark 1.1). Then for all μ:*

$$U\gamma_\mu U^\dagger = \sum_{\nu=1}^{2n} R_{\mu\nu}\gamma_\nu \,, \tag{2.14}$$

where the matrix R is in $SO(2n)$ and $R = e^{4h}$. Furthermore, we obtain all of $SO(2)$ in this way.

Proof. Let us move to the Heisenberg picture and write γ_μ as $\gamma_\mu(0)$. Then, the time evolved Majorana operators will be $\gamma_\mu(t) = U(t)^\dagger\gamma_\mu U(t)$, where $U(t) = e^{-iHt}$ is the time evolution operator. The time-dependent Majorana operators will follow the Heisenberg equation:

$$\frac{d\gamma_\mu(t)}{dt} = i[H, \gamma_\mu(t)] \,, \tag{2.15}$$

where $H = i\sum_{\nu,\sigma} h_{\nu\sigma}\gamma_\nu\gamma_\sigma$. Using linearity of the commutator, the fact that

$$[\gamma_\nu\gamma_\sigma, \gamma_\mu] = \gamma_\nu\{\gamma_\sigma, \gamma_\mu\} - \{\gamma_\nu, \gamma_\mu\}\gamma_\sigma = 2(\delta_{\sigma\mu}\gamma_\nu - \delta_{\nu\sigma}\gamma_\sigma) \tag{2.16}$$

due to the CAR (1.17) and the anti-symmetry of h ($h_{\nu\mu} = -h_{\mu\nu}$), we get:

$$\frac{d\gamma_\mu(t)}{dt} = \sum_{\nu=1}^{2n} 4h_{\mu\nu}\gamma_\nu(t)\,. \tag{2.17}$$

This is a simple system of linear differential equations which can be solved as:

$$\gamma_\mu(t) = \sum_{\nu=1}^{2n} (e^{4ht})_{\mu\nu}\gamma_\nu(0)\,. \tag{2.18}$$

We can finally set $t = 1$ to get (2.14). Moreover, we know that anti-symmetric matrices are infinitesimal generators of rotations, and therefore since h is an arbitrary anti-symmetric matrix, $R \in SO(2n)$ and we can generate the whole group. □

This theorem is saying that, even if e^{iH} generally involves all products of all generators $\{\gamma_\mu\}$ of the 2^{2n}-dimensional Clifford algebra $\mathcal{C}_{2n}$, $U\gamma_\mu U^\dagger$ is always in the $2n$-dimensional subspace spanned by the generators only.

We have already discussed that any matchgate can be generated by the set $\mathcal{A}_{i,j}$ of (2.11), and that for nearest-neighbor matchgates all elements of $\mathcal{A}_{i,i+1}$ are quadratic in fermionic operators. Therefore, it is clear that all nearest-neighbors matchgates must be Gaussian operators. However, the converse also holds: all nearest-neighbors Gaussian operators are matchgates. This can be seen by noticing that, since the Majorana fermions associated with nearest-neighbour spins after a Jordan–Wigner transformation are $\{\gamma_{2j-1}, \gamma_{2j}, \gamma_{2j+1}, \gamma_{2j+2}\}$, any nearest-neighbor Hamiltonian can be written as a linear combination of the following terms:

$$\begin{aligned} -i\gamma_{2i-1}\gamma_{2i} &= Z_i\mathbb{1}_{i+1}\,, & -i\gamma_{2i}\gamma_{2i+1} &= X_iX_{i+1}\,,\\ i\gamma_{2i-1}\gamma_{2i+1} &= Y_iX_{i+1}\,, & -i\gamma_{2i}\gamma_{2i+2} &= X_iY_{i+1}\,,\\ i\gamma_{2i-1}\gamma_{2i+2} &= Y_iY_{i+1}\,, & -i\gamma_{2i+1}\gamma_{2i+2} &= \mathbb{1}_iZ_{i+1}\,, \end{aligned} \tag{2.19}$$

which are exactly the generators of the matchgates circuits.

On the other hand, Gaussian gates generated by quadratic Hamiltonians involving non–nearest-neighbor fermions are not themselves matchgates. However, it can be shown that they can be expressed as a product of matchgates [23].

Theorem 2.3. *Let H be any quadratic Hamiltonian (1.43) with corresponding Gaussian operator $\mathcal{V} = e^{iH}$. Then $\mathcal{V}$ as an operator on n-qubits (after a Jordan-Wigner transformation) is expressible as a circuit of $O(n^3)$ n.n. $G(A, B)$ gates, i.e. $\mathcal{V} = u_N u_{N-1} \dots u_1$, where each $u_j = e^{ih_j}$ and h_j a linear combinations of the terms in (2.19).*

The proof makes use of (2.14), decomposing R into its generalized Euler angles and using the n.n. "modified swap" operations [52] defined as

$$S_{i,i+1} = \exp\left(-\frac{\pi}{4}(-\gamma_{2i-1}\gamma_{2i+2} + \gamma_{2i}\gamma_{2i+1} + \gamma_{2i-1}\gamma_{2i} + \gamma_{2i+1}\gamma_{2i+2})\right)\,. \tag{2.20}$$

See [23] for the complete proof.

We can conclude that any Gaussian operator, and thus the time evolution generated by any quadratic Hamiltonian, can be expressed in terms of matchgates. Consequently, such evolutions are classically simulable, given an appropriate choice of input states and measured observables.

Remark 2.1. Notice that the results we have discussed for matchgate circuits all rely on the correspondence between fermions and spins defined by the Jordan–Wigner transformation. This correspondence does not apply to spin chains that are mapped to free fermions in a different way, such as the Free Fermions in Disguise models [28, 34, 35]. We will examine this subtle issue in the following chapters.

2.3 Fermionic Gaussian States

In this section, we will explore *fermionic Gaussian states* (FGS). These quantum states have the remarkable property that they can be completely characterized by a $2n \times 2n$ *correlation matrix*, where n is the number of fermionic modes. Consequently, systems in an FGS can be fully analyzed using an object that scales linearly, rather than exponentially, with the system size, making them efficiently simulable on a classical computer.

Let us start by giving a definition of a Fermionic Gaussian State [17, 44].

Definition 2.4 (Fermionic Gaussian State). A state $\rho \in \mathcal{S}(\mathcal{H})$ is a *fermionic Gaussian state* (FGS) if it can be represented as

$$\rho = \frac{e^{-H}}{Z}\,, \tag{2.21}$$

where $Z = \mathrm{tr}\left[e^{-H}\right]$ is a normalization constant and H is a fermionic quadratic Hamiltonian called *parent Hamiltonian*.

These states have a natural interpretation as thermal Gibbs states of quadratic Hamiltonians. If we rescale the Hamiltonian as $H' = H/\beta$ with $\beta = 1/\|H\|$ so that $\|H'\| = 1$, we obtain a thermal state with $\beta \in [0, +\infty]$. Note that at infinite temperature ($\beta = 0$), the state becomes maximally mixed, while Fock states can be obtained by taking $\beta = \infty$ and choosing an appropriate parent Hamiltonian. This implies that the eigenstates of fermionic quadratic Hamiltonians are Gaussian, being Fock states.

To see this, consider a state with k particles in sites $\{i_l\}$, $l = 1, \ldots, k$:

$$c^\dagger_{i_1} c^\dagger_{i_2} \ldots c^\dagger_{i_k} |0\rangle\,. \tag{2.22}$$

In order to see it is a fermionic Gaussian state, we must choose the following parent Hamiltonian:

$$H = \beta \left[\sum_{i \notin \{i_l\}} c^\dagger_i c_i + \sum_{i \in \{i_l\}} (1 - c^\dagger_i c_i) \right] = \beta \left[\sum_{i \notin \{i_l\}} n_i + \sum_{i \in \{i_l\}} (1 - n_i) \right]\,. \tag{2.23}$$

Then, we can write the Gaussian state as, adding a resolution of the identity in the Fock basis on the right:

$$\rho = \frac{e^{-\beta\left[\sum_{i \notin \{i_l\}} n_i + \sum_{i \in \{i_l\}} (1 - n_i)\right]}}{Z} \sum_{n_m = 0,1} |n_1 n_2 \ldots n_n\rangle \langle n_1 n_2 \ldots n_n|\,. \tag{2.24}$$

We can now apply the exponential to each Fock state in the resolution of the identity. For all states except (2.22), the result includes a prefactor $e^{-\beta}$, since exactly one of the terms in the sum in (2.23) is 1, whereas all others are 0. On the other hand, for (2.22), all terms in (2.23) are 0 and therefore the prefactor is $e^0 = 1$. If we now take the limit $\beta \to \infty$, all terms vanish except the last one, and thus:

$$\rho = c^\dagger_{i_1} c^\dagger_{i_2} \ldots c^\dagger_{i_k} |0\rangle \langle 0| c_{i_k} \ldots c_{i_2} c_{i_1}\,. \tag{2.25}$$

Let us now consider as an example a single-mode parent Hamiltonian $H = \varepsilon(c^\dagger c - c c^\dagger)$. The related gaussian state can be represented in the $\{|0\rangle, c^\dagger |0\rangle = |1\rangle\}$ basis as

$$\rho = \begin{pmatrix} 1 - f & 0 \\ 0 & f \end{pmatrix}\,, \tag{2.26}$$

where $f := \langle 1|\rho|1\rangle = e^{\varepsilon}/(e^{-\varepsilon} + e^{\varepsilon})$. Notice that we can also write:

$$\langle c^\dagger c \rangle := \mathrm{tr}\left[\rho c^\dagger c\right] = \langle 0| \rho c^\dagger c |0\rangle + \langle 1| \rho c^\dagger c |1\rangle = \langle 1| \rho |1\rangle = f\,, \tag{2.27}$$

since $c^\dagger c\,|0\rangle = 0$. We therefore see that a single-mode fermionic gaussian state is characterized completely by the average of the occupation number $\langle c^\dagger c\rangle$ and it can be represented in matrix form as:

$$\rho = \begin{pmatrix} 1-\langle c^\dagger c\rangle & 0 \\ 0 & \langle c^\dagger c\rangle \end{pmatrix} . \tag{2.28}$$

Let us now go back to a generic parent Hamiltonian. We have seen that any fermionic quadratic Hamiltonian (1.25) can be diagonalized by a canonical transformation $\mathcal{C} = \mathcal{S}\tilde{\mathcal{C}}$ (with $\mathcal{C}$ and $\tilde{\mathcal{C}}$ defined as in (1.23) and (1.28), respectively) and written in the form (1.37). Therefore, any Gaussian state can be expressed as:

$$\rho = \frac{e^{-\sum_{j=1}^n \varepsilon_j(\tilde{c}_j^\dagger \tilde{c}_j - \tilde{c}_j\tilde{c}_j^\dagger)}}{Z} = \bigotimes_{j=1}^n \frac{e^{-\varepsilon_j(\tilde{c}_j^\dagger\tilde{c}_j-\tilde{c}_j\tilde{c}_j^\dagger)}}{Z_j} , \tag{2.29}$$

where $Z_j = \mathrm{tr}\left[e^{-\varepsilon_j(\tilde{c}_j^\dagger\tilde{c}-\tilde{c}_j\tilde{c}_j^\dagger)}\right]$. Therefore, any FGS can be decomposed into single-mode Gaussian states, which are fully characterized by their average occupation numbers $\langle \tilde{c}_j^\dagger \tilde{c}_j\rangle$. The set of average occupation numbers $\{\langle \tilde{c}_j^\dagger\tilde{c}_j\rangle\}_{j=1}^n$ thus provides a complete characterization of any FGS.

Using the inverse transformation $\tilde{\mathcal{C}} = \mathcal{S}^\dagger\mathcal{C}$, the occupation numbers are mapped to the correlators $\Gamma_{ij}^{c^\dagger c} = \langle c_i^\dagger c_j\rangle$, $\Gamma_{ij}^{cc} = \langle c_i c_j\rangle$ and their complex conjugates. These can then be collected into the **correlation matrix**, a $2n\times 2n$ matrix that fully characterizes the state of the system:

$$\Gamma := \langle \mathcal{C}\mathcal{C}^\dagger\rangle = \begin{pmatrix} \Gamma^{cc^\dagger} & \Gamma^{cc} \\ \Gamma^{c^\dagger c^\dagger} & \Gamma^{c^\dagger c}\end{pmatrix} . \tag{2.30}$$

From the canonical anticommutation relations (1.12), we obtain $\Gamma_{ij}^{cc} = -(\Gamma_{ij}^{c^\dagger c^\dagger})^*$ and $\Gamma_{ij}^{cc^\dagger} = (\mathbb{1} - \Gamma^{c^\dagger c})_{ij}^\dagger$. Furthermore, $\Gamma^{cc^\dagger}$ and $\Gamma^{c^\dagger c}$ are Hermitian, while Γ^{cc} and $\Gamma^{c^\dagger c^\dagger}$ are skew-symmetric. Γ is therefore Hermitian.

Let us now introduce the notion of a *number-conserving Hamiltonian* and study the structure of its correlation matrix. A Hamiltonian is number-conserving if it commutes with the number operator $N = \sum_{j=1}^N c_j^\dagger c_j$. Hence, it cannot contain terms of the form $c_i c_j$ or $c_i^\dagger c_j^\dagger$, as these violate number conservation. It must therefore be written as:

$$H = \sum_{i,j=1}^n \left(A_{ij}c_i^\dagger c_j + A_{ij}^* c_j^\dagger c_i\right) = \sum_{i,j=1}^n \left(A_{ij} + A_{ji}^*\right) c_i^\dagger c_j = \sum_{i,j=1}^n \tilde{H}_{ij} c_i^\dagger c_j , \tag{2.31}$$

where $\tilde{H}_{ij} = A_{ij} + A_{ji}^*$ is a Hermitian $n\times n$ matrix.

To diagonalize a number conserving Hamiltonian, we shall consider the eigenvectors $\phi_j(i)$ of $\tilde{H}$, each with eigenvalue ε_j, and introduce new creation and annihilation operators defined by $\tilde{c}_i = \sum_{k=1}^n \phi_k(i) c_i$. In this basis, the Hamiltonian takes the diagonal form:

$$H = \sum_{k=1}^n \varepsilon_k \tilde{c}_k^\dagger \tilde{c}_k \, . \tag{2.32}$$

From (2.32), it follows that for a number-conserving Hamiltonian the relevant correlators are fully captured by an $n\times n$ correlation matrix:

$$\Gamma = \begin{pmatrix} \langle c_1^\dagger c_1\rangle & \dots & \langle c_1^\dagger c_N\rangle \\ \vdots & \ddots & \vdots \\ \langle c_N^\dagger c_1\rangle & \dots & \langle c_N^\dagger c_1\rangle \end{pmatrix} , \tag{2.33}$$

since $\langle c_i c_j\rangle = \langle c_i^\dagger c_j^\dagger\rangle = 0$, and the quantities $\langle c_i c_j^\dagger\rangle$ can be obtained from this matrix.

2.3.1 Wick's Theorem and Fermionic Gaussian States

An equivalent definition of Fermionic Gaussian States says that a state ρ is Gaussian if the expectation value of any product of fermionic creation or annihilation operators can be computed utilizing **Wick's theorem** [15, 18–20]. In particular, any such n-point correlation function can be expressed as a sum of products of 2-point correlators, namely the entries of the correlation matrix (2.30).

Our goal is to show that the FGS defined in Definition 2.4 indeed satisfy Wick's theorem. Throughout this subsection, we denote by $c_j, c_j^\dagger$ the diagonalizing annihilation and creation operators, in terms of which the Hamiltonian is (1.38). Moreover, let C denote the vector introduced in Eq. (1.23). Hence, any individual creation or annihilation operator can be written as C_μ.

Let us first consider Wick's theorem in the context of pure states. In this setting, the theorem states that any arbitrary product of creation and annihilation operators can be written as

$$C_{\mu_1} C_{\mu_2} \dots C_{\mu_k} =: C_{\mu_1} C_{\mu_2} \dots C_{\mu_k} : + \text{sum of all possible contractions} : \tag{2.34}$$

where $: O :$ indicates the *normal ordering* of an operator, obtained by placing all creation operators to the left and all annihilation operators to the right. For example,

$$: c_1^\dagger c_3 c_5 c_2^\dagger := c_1^\dagger c_2^\dagger c_3 c_5 \,. \tag{2.35}$$

A *contraction* for many-body systems operators is essentially the anticommutator[2] (or the commutator in the bosonic case) of two operators, and is denoted by:

$$\overbrace{C_\mu C_\nu} = \{C_\mu, C_\nu\} \,. \tag{2.36}$$

A simple example illustrating Wick's theorem in practice is the following:

$$\begin{aligned} c_1^\dagger c_3 c_5 c_2^\dagger =: c_1^\dagger c_3 c_5 c_2^\dagger + \overbrace{c_1^\dagger c_3} c_5 c_2^\dagger + \overbrace{c_1^\dagger c_3 c_5} c_2^\dagger + \dots \\ + \overbrace{c_1^\dagger} c_3 \overbrace{c_5 c_2^\dagger} + \overbrace{c_1^\dagger \overbrace{c_3 c_5} c_2^\dagger} + \dots : \end{aligned} \tag{2.37}$$

It is clear from the definition of normal ordering that $\langle 0| : O : |0\rangle = 0$, since the annihilation operators on the right act on the vacuum. Hence,

$$\langle C_\mu C_\nu \rangle_0 := \langle 0| C_\mu C_\nu |0\rangle = \langle 0| \overbrace{C_\mu C_\nu} |0\rangle = \overbrace{C_\mu C_\nu}, \tag{2.38}$$

where $\langle O \rangle_0$ represents the vacuum expectation value of the operator O. From this it follows that the vacuum expectation value of any *odd* product of creation or annihilation operators is always zero, since there will necessarily be an unpaired operator, which annihilates the vacuum. Conversely, for an *even* product we obtain:

$$\langle 0| C_{\mu_1} C_{\mu_2} \dots C_{\mu_{2k}} |0\rangle = \text{sum of all possible contractions involving all operators} \,, \tag{2.39}$$

which is a sum of products of correlators $\langle C_\mu C_\nu \rangle_0$. Thus, any such expectation value is fully characterized by these two-point functions.

From this previous discussion, it is clear that computing the expectation value of any operator in a generic Fock state $|n_1 n_2 ... n_n\rangle$, with $n_i \in \{0, 1\}$, simply amounts to evaluating a vacuum expectation value of a product of creation and annihilation operators which considers also the one needed to create the Fock state itself. Therefore, the same conclusions apply. This is consistent with the fact that Fock states are themselves fermionic Gaussian states, as discussed above.

[2] In relativistic quantum field theory, one often considers *time ordered product* of operators, in which case contractions correspond to the Feynman propagator [53]. This will not be discussed further in this thesis.

We now turn to proving that Fermionic Gaussian States satisfy Wick's theorem. Our presentation follows the treatment for thermal states given in [20]. This proof applies only to FGS defined from a number conserving parent Hamiltonian as in Eq. (2.32). A proof for a generic FGS is provided in [15].

We aim to compute the expectation value:

$$\mathrm{tr}[C_{\mu_1} C_{\mu_2} \dots C_{\mu_k} \rho] \,, \tag{2.40}$$

where ρ is a fermionic Gaussian state with a number conserving parent Hamiltonian. We prove the result for even k by induction. Consider first the base case $k = 2$:

$$\mathrm{tr}[C_{\mu_1} C_{\mu_2}\, \rho] = \{C_{\mu_1}, C_{\mu_2}\} \,\mathrm{tr}\,\rho - \mathrm{tr}[C_{\mu_2} C_{\mu_1}\, \rho] \,, \tag{2.41}$$

where we used the fact that $\{C_{\mu_1}, C_{\mu_2}\}$ is a scalar. First, we note that $\mathrm{tr}\,\rho = 1$. We then make use of the identities:

$$\begin{aligned} e^{-\varepsilon_j c_j^\dagger c_j} c_j &= e^{\varepsilon_j} c_j e^{-\varepsilon_j c_j^\dagger c_j} \,, \\ e^{-\varepsilon_j c_j^\dagger c_j} c_j^\dagger &= e^{-\varepsilon_j} c_j^\dagger e^{-\varepsilon_j c_j^\dagger c_j} \,. \end{aligned} \tag{2.42}$$

These relations can be proven by acting with both sides of the equation on the single-site basis $\{|0\rangle_j, |1\rangle_j\}$. Consequently[3],

$$\begin{aligned} \rho\, c_j &= \bigotimes_{k=1}^{n} e^{-\varepsilon_k c_k^\dagger c_k} c_j = e^{\varepsilon_j} c_j\, \rho \,, \\ \rho\, c_j^\dagger &= \bigotimes_{k=1}^{n} e^{-\varepsilon_k c_k^\dagger c_k} c_j^\dagger = e^{-\varepsilon_j} c_j^\dagger\, \rho \,. \end{aligned} \tag{2.43}$$

From this relations, it follows that the second term in (2.41) can be written as:

$$\mathrm{tr}[C_{\mu_2} C_{\mu_1}\, \rho] = e^{\pm\varepsilon_{\mu_1}}\, \mathrm{tr}[C_{\mu_1} C_{\mu_2}\, \rho] \,, \tag{2.44}$$

where the sign in the exponent is plus if C_{μ_1} is an annihilation operator and minus otherwise. Moving this term to the left-hand side of Eq. (2.41) yields:

$$\mathrm{tr}[C_{\mu_1} C_{\mu_2}\ \rho] = \frac{\{C_{\mu_1}, C_{\mu_2}\}}{1 + e^{\pm\varepsilon_{\mu_1}}} := \overbracket{C_{\mu_1} C_{\mu_2}} \,, \tag{2.45}$$

which we define as a contraction. This contraction is non zero if and only if $\mu_1 = \pm k$ and $\mu_2 = \mp k$ for some $k = 1, 2, \dots, n$. The base case is therefore established.

We now assume, as the induction hypothesis, that the expectation value of any product of $2(l-1)$ operators can be expressed in terms of the contractions defined in (2.45). We then show that the expectation value of a product of $k = 2l$ operators can be written in the same form. To do so, we proceed as before and express the expectation value as follows:

$$\begin{aligned} \mathrm{tr}[C_{\mu_1} C_{\mu_2} \dots C_{\mu_k}\, \rho] =& \{C_{\mu_1}, C_{\mu_2}\}\, \mathrm{tr}[C_{\mu_3} C_{\mu_4} \dots C_{\mu_k}\, \rho] - \{C_{\mu_1}, C_{\mu_3}\}\, \mathrm{tr}[C_{\mu_2} C_{\mu_4} \dots C_{\mu_k}\, \rho] + \dots \\ &+ \{C_{\mu_1}, C_{\mu_k}\}\, \mathrm{tr}\big[C_{\mu_2} C_{\mu_3} \dots C_{\mu_{k-1}}\, \rho\big] - \mathrm{tr}[C_{\mu_2} C_{\mu_3} \dots C_{\mu_k} C_{\mu_1}\, \rho] \,. \end{aligned} \tag{2.46}$$

We can then apply (2.43) to the last term, move it to the left-hand side, and divide both sides accordingly, obtaining:

$$\begin{aligned} \mathrm{tr}[C_{\mu_1} C_{\mu_2} \dots C_{\mu_k}\, \rho] =& \overbracket{C_{\mu_1} C_{\mu_2}}\, \mathrm{tr}[C_{\mu_3} C_{\mu_4} \dots C_{\mu_k}\, \rho] - \overbracket{C_{\mu_1} C_{\mu_3}}\, \mathrm{tr}[C_{\mu_2} C_{\mu_4} \dots C_{\mu_k}\, \rho] + \dots \\ &+ \overbracket{C_{\mu_1} C_{\mu_k}}\, \mathrm{tr}\big[C_{\mu_2} C_{\mu_3} \dots C_{\mu_{k-1}}\, \rho\big] \,. \end{aligned} \tag{2.47}$$

[3] This is the step that does not hold for a non-number conserving Hamiltonian.

This completes the induction step, since all traces appearing on the right-hand side contain $2(l-1)$ operators.

After having determined that FGS satisfy Wick's theorem, it is clear that knowing the $2n \times 2n$ correlation matrix is enough to compute any correlation function.

Remark 2.2. Wick's theorem can be conveniently expressed for Gaussian states in terms of Majorana operators. To do so, we introduce the $2n \times 2n$ *covariance matrix* K [15–17], an alternative description of a Fermionic Gaussian State that complements the usual correlation matrix. Its elements are defined as:

$$K_{\mu\nu} := \frac{i}{2} \operatorname{tr}(\rho[\gamma_\mu, \gamma_\nu]) = \frac{i}{2}\langle[\gamma_\mu, \gamma_\nu]\rangle \,. \tag{2.48}$$

Wick's theorem can then be stated in the form

$$\operatorname{tr}[\rho\, \gamma_{\mu_1}\gamma_{\mu_2}\dots\gamma_{\mu_k}] = \operatorname{Pf}(K|_{\mu_1,\mu_2,\dots,\mu_k}) \,, \tag{2.49}$$

where Pf denotes the Pfaffian, defined as the square root of the determinant of an even-dimensional skew-symmetric matrix (and equal to zero for matrices of odd dimension). The submatrix $K|_{\mu_1,\mu_1,\dots,\mu_k}$ is the restriction of the covariance matrix to the two-point correlators involving only the Majorana operators $\{\gamma_{\mu_1}, \gamma_{\mu_2}, \dots, \gamma_{\mu_k}\}$.

As an example, consider a system with two fermionic modes. The corresponding Majorana operators are $\gamma_1, \gamma_2, \gamma_3, \gamma_4$. The covariance matrix then takes the form:

$$K = \frac{i}{2}\begin{pmatrix} 0 & \langle[\gamma_1,\gamma_2]\rangle & \langle[\gamma_1,\gamma_3]\rangle & \langle[\gamma_1,\gamma_4]\rangle \\ -\langle[\gamma_1,\gamma_2]\rangle & 0 & \langle[\gamma_2,\gamma_3]\rangle & \langle[\gamma_2,\gamma_4]\rangle \\ -\langle[\gamma_1,\gamma_3]\rangle & -\langle[\gamma_2,\gamma_3]\rangle & 0 & \langle[\gamma_3,\gamma_4]\rangle \\ -\langle[\gamma_1,\gamma_4]\rangle & -\langle[\gamma_2,\gamma_4]\rangle & -\langle[\gamma_3,\gamma_4]\rangle & 0 \end{pmatrix} . \tag{2.50}$$

Then, for instance:

$$\operatorname{tr}[\rho\gamma_1\gamma_2\gamma_3\gamma_4] = \operatorname{Pf} K = -\frac{1}{4}(\langle[\gamma_1,\gamma_2]\rangle\langle[\gamma_3,\gamma_4]\rangle - \langle[\gamma_1,\gamma_3]\rangle\langle[\gamma_2,\gamma_4]\rangle + \langle[\gamma_2,\gamma_3]\rangle\langle[\gamma_1,\gamma_4]\rangle) \,, \tag{2.51}$$

whereas

$$\operatorname{tr}[\rho\gamma_1\gamma_2\gamma_4] = \operatorname{Pf}\begin{pmatrix} 0 & \langle[\gamma_1,\gamma_2]\rangle & \langle[\gamma_1,\gamma_4]\rangle \\ -\langle[\gamma_1,\gamma_2]\rangle & 0 & \langle[\gamma_2,\gamma_4]\rangle \\ -\langle[\gamma_1,\gamma_4]\rangle & -\langle[\gamma_2,\gamma_4]\rangle & 0 \end{pmatrix} = 0 \,. \tag{2.52}$$

2.3.2 Time Evolution of Fermionic Gaussian States

We have discussed that the eigenstates of fermionic quadratic Hamiltonians are fermionic Gaussian states. Let us now consider a *quantum quench* [54, 55], one of the simplest protocols for studying nonequilibrium quantum statistical mechanics. In such a protocol, a many-body system is initially prepared in the ground state of some Hamiltonian and is then evolved under a different one. If both the initial and final Hamiltonians are free fermionic, the initial state is Gaussian, and the time-evolution operator is generated by a quadratic Hamiltonian as well.

A natural question is whether the time-evolved state remains Gaussian. If this were the case, one could efficiently simulate the dynamics of a free fermionic quench by tracking only the time-dependent correlation matrix, avoiding the exponential growth of computational cost with system size. Indeed, this is exactly what happens: the evolved state remains Gaussian, allowing an efficient numerical treatment of such quenches.

Let us show that Gaussian states are closed under the action of Gaussian operators [17]. In particular, consider the time evolution operator e^{-iHt} generated by an arbitrary free fermionic Hamiltonian H and a generic Gaussian state ρ with parent Hamiltonian H_ρ. The time-evolved Gaussian state is then given by:

$$\rho(t) = e^{iHt}\,\rho\, e^{-iHt} = \frac{e^{iHt}\, e^{-H_\rho}\, e^{-iHt}}{Z} \,. \tag{2.53}$$

This expression can be evaluated by applying the *Baker-Campbell-Hausdorff* (BCH) formula twice:

$$e^A e^B = e^Z \quad \text{where} \quad Z = A + B + \frac{1}{2}[A,B] + \frac{1}{12}\left([A,[A,B]] + [B,[A,B]]\right) + ... \tag{2.54}$$

Here, Z involves commutators of increasing order between A and B.

Both H and H_ρ are quadratic in Majorana operators, and it is straightforward to show that the commutator of two Majorana bilinears is still quadratic:

$$\begin{aligned}[\gamma_\mu\gamma_\nu, \gamma_\sigma\gamma_\rho] &= [\gamma_\mu\gamma_\nu, \gamma_\sigma]\gamma_\rho + \gamma_\sigma[\gamma_\mu\gamma_\nu, \gamma_\rho] = \\ &= \gamma_\mu\{\gamma_\nu,\gamma_\sigma\}\gamma_\rho - \{\gamma_\mu,\gamma_\sigma\}\gamma_\nu\gamma_\rho + \gamma_\sigma\gamma_\mu\{\gamma_\nu,\gamma_\rho\} - \gamma_\sigma\{\gamma_\mu,\gamma_\rho\}\gamma_\nu = \\ &= 2\left(\delta_{\nu\sigma}\gamma_\mu\gamma_\rho - \delta_{\mu\sigma}\gamma_\nu\gamma_\rho + \delta_{\nu\rho}\gamma_\sigma\gamma_\mu - \delta_{\mu\rho}\gamma_\sigma\gamma_\nu\right) .\end{aligned} \tag{2.55}$$

Therefore, the resulting exponent is also quadratic, and consequently, the state remains gaussian.

This result also allows us to establish a connection with the *Matchgate Circuits* discussed in Section 2.2. In fact, in Theorem 2.3, we stated that any Gaussian operator can be expressed as a product of matchgates. This implies that an appropriate circuit evolution also preserves the "Gaussianity" of a state.

Following the previous discussion, it is clear that the time evolution of a Gaussian state under a quadratic Hamiltonian can be studied simply by evolving the correlation matrix [17]. To this end, let us consider the creation and annihilation operators $\tilde{c}_j$ and $\tilde{c}_j^\dagger$ that diagonalize the Hamiltonian H, and compute their time evolution in the Heisenberg picture. The Heisenberg equation for $\tilde{c}_k$ is then given by:

$$\frac{d\tilde{c}_k(t)}{dt} = i[H, \tilde{c}_k(t)] = -2i\varepsilon_k\tilde{c}_k(t) , \tag{2.56}$$

where we used (1.39). Integrating this equation and taking the Hermitian conjugate for $\tilde{c}_k^\dagger$, we obtain:

$$\begin{aligned}\tilde{c}_k(t) &= e^{-2i\varepsilon_k t}\tilde{c}_k , \\ \tilde{c}_k^\dagger(t) &= e^{2i\varepsilon_k t}\tilde{c}_k^\dagger .\end{aligned} \tag{2.57}$$

In vector notation, this can be written more compactly as:

$$\tilde{\mathcal{C}}(t) = e^{-2iH_D t}\tilde{\mathcal{C}} , \tag{2.58}$$

where $\tilde{\mathcal{C}}$ is defined as (1.28), while H_D as (1.36).

The correlators composing the correlation matrix are now straightforward to compute:

$$\langle\tilde{\mathcal{C}}(t)\tilde{\mathcal{C}}^\dagger(t)\rangle = \langle e^{-2iH_D t}\tilde{\mathcal{C}}\tilde{\mathcal{C}}^\dagger e^{2iH_D t}\rangle . \tag{2.59}$$

By applying a unitary canonical transformation $\mathcal{S}$ to return to a generic basis, we obtain:

$$\begin{aligned}\langle\mathcal{C}(t)\mathcal{C}^\dagger(t)\rangle &= \langle\mathcal{S}\tilde{\mathcal{C}}(t)\tilde{\mathcal{C}}^\dagger(t)\mathcal{S}^\dagger\rangle = \langle\mathcal{S}e^{-2iH_D t}\tilde{\mathcal{C}}\tilde{\mathcal{C}}^\dagger e^{2iH_D t}\mathcal{S}^\dagger\rangle = \\ &= \langle\left(\mathcal{S}e^{-2iH_D t}\mathcal{S}^\dagger\right)\left(\mathcal{S}\tilde{\mathcal{C}}\right)\left(\tilde{\mathcal{C}}^\dagger\mathcal{S}^\dagger\right)\left(\mathcal{S}e^{2iH_D t}\mathcal{S}^\dagger\right)\rangle = e^{-2iHt}\langle\mathcal{C}\mathcal{C}^\dagger\rangle e^{2iHt} ,\end{aligned} \tag{2.60}$$

where we used the unitarity of $\mathcal{S}$ and the relation $\mathcal{S}e^{-2iH_D t}\mathcal{S}^\dagger = e^{-2iHt}$.

Recalling the definition of Γ in (2.30), we can finally express its time evolution under a quadratic Hamiltonian as:

$$\Gamma(t) = e^{-2iHt}\,\Gamma\,e^{2iHt} . \tag{2.61}$$

Let us now consider a number conserving Hamiltonian. In this case, the time evolution of the correlation matrix can be expressed in a simple form for a generic time evolution $U(t)$, even when the generating Hamiltonians are not free fermionic [44].

We start from $\Gamma_{ij}(t) = \langle c_i^\dagger(t) c_j(t)\rangle$, where $c_j(t), c_i^\dagger(t)$ are the annihilation and creation operators in the Heisenberg picture. The time-evolved fermionic operators can be written as

$$\begin{aligned} c_j(t) &= \sum_{l=1}^{n} U_{jl}(t) c_l \,, \\ c_i^\dagger(t) &= \sum_{k=1}^{N} U_{jk}^*(t) c_k^\dagger \,. \end{aligned} \tag{2.62}$$

Substituting these expressions into the definition of $\Gamma(t)$ gives:

$$\Gamma_{ij}(t) = \sum_{kl} \langle U_{ik}^* c_k^\dagger U_{jl} c_l\rangle = \sum_{kl} U_{ik}^* \langle c_k^\dagger c_l\rangle U_{lj}^T = \sum_{kl} U_{ik}^* \Gamma_{ij} U_{lj}^T = \left(U^*(t)\Gamma U^T(t)\right)_{ij} \,. \tag{2.63}$$

2.3.3 Numerical Simulations for the XX-chain

In this subsection, we present examples of numerical simulations to illustrate the power of the correlation matrix approach in practice. We focus on number conserving Hamiltonians, for which the correlation matrix is simply an $n \times n$ matrix, as in Eq. (2.33), and whose time evolution is given by Eq. (2.63).

In particular, let us consider the specific case of a *Hopping Hamiltonian*, a number conserving Hamiltonian with only nearest-neighbors interactions:

$$H = \sum_{j=1}^{n} \left(A_{j,j+1} c_j^\dagger c_{j+1} + A_{j+1,j} c_{j+1}^\dagger c_j \right) \,, \tag{2.64}$$

where $A_{j+1,j} = A_{j,j+1}^*$.

This Hamiltonian can be conveniently represented using the *circulant matrix* A:

$$A = \begin{pmatrix} 0 & A_{12} & 0 & \dots & A_{1n} \\ A_{21} & 0 & A_{23} & & \\ 0 & A_{32} & 0 & & \\ \vdots & & & \ddots & \\ A_{n1} & & & & \end{pmatrix} = \begin{pmatrix} 0 & A_{12} & 0 & \dots & A_{1n} \\ A_{12}^* & 0 & A_{23} & & \\ 0 & A_{23}^* & 0 & & \\ \vdots & & & \ddots & \\ A_{1n}^* & & & & \end{pmatrix} \,, \tag{2.65}$$

so that it can be written as $H = \boldsymbol{c}^\dagger A \boldsymbol{c}$. Note that for open boundary conditions, $A_{1n} = A_{n1} = 0$, while in general these elements are non-zero for periodic boundary conditions.

As the initial state, we choose, assuming even n without loss of generality, the *Néel state*:

$$|\Psi_0\rangle = |0101\dots01\rangle = \prod_{j=1}^{n/2} c_{2j}^\dagger |0\rangle \,, \tag{2.66}$$

for which the correlation matrix elements are simply:

$$\Gamma_{ij} = \langle\Psi_0| c_i^\dagger c_j |\Psi_0\rangle = \delta_{ij} \qquad \text{if} \qquad i,j \ \text{ even} \,, \tag{2.67}$$

or in matrix form,

$$\Gamma = \begin{pmatrix} 0 & & & & \\ & 1 & & & \\ & & 0 & & \\ & & & 1 & \\ & & & & \ddots \end{pmatrix} \,. \tag{2.68}$$

We want to verify numerically that the correlation matrix approach is equivalent to the standard time evolution. To this end, we consider an XX-chain of length[4] n. The Hamiltonian is given by Eq. (1.80) with $h = 0$ and $J = 1$, and it can be mapped to a Hopping Hamiltonian via the Jordan-Wigner transformation:

$$H = -\frac{1}{2}\sum_{j=1}^{n}(X_jX_{j+1} + Y_jY_{j+1}) = -\sum_{j=1}^{n}\left(c_j^\dagger c_{j+1} + c_{j+1}^\dagger c_j\right) . \tag{2.69}$$

This yields the following circulant matrix:

$$A = -\begin{pmatrix} 0 & 1 & 0 & \dots & k \\ 1 & 0 & 1 & & \\ 0 & 1 & 0 & & \\ \vdots & & & \ddots & \\ k & & & & \end{pmatrix} , \tag{2.70}$$

where k has different values for different boundary conditions. Specifically,

$$k = \begin{cases} 0 & \text{for OBC ,} \\ 1 & \text{for PBC if } n/2 \text{ odd ,} \\ -1 & \text{for PBC if } n/2 \text{ even .} \end{cases} \tag{2.71}$$

As discussed in Section 1.4, depending on the parity, we must impose either periodic or anti-periodic boundary conditions on the fermionic Hamiltonian when starting from periodic boundary conditions in the spin chain.

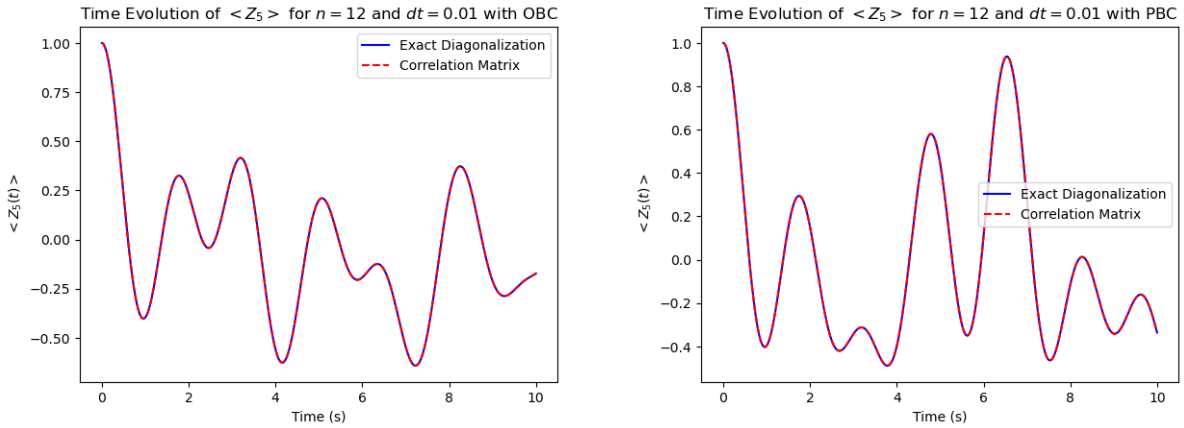

Figure 2.4: Time evolution of the expectation value of Z_5 in a $XX-$chain of $n = 12$ qubits, initialized in the Néel state and computed both with ED and using the correlation matrix. We used a timestep $dt = 0.01$ s and 1000 steps. On the left we chose open boundary conditions (OBC), while on the right periodic boundary conditions (PBC).

In Figure 2.4, we show the time evolution of the expectation value of the observable Z_j at site $j = 5$ for a system of size $n = 12$, computed using both exact diagonalization (ED) and the correlation matrix approach. Results are presented for both open and periodic boundary conditions.

Using ED, we evolve the initial state (2.66) via the standard discretized time evolution operator $e^{-i\,dt\,H}$ and compute the expectation value of Z_j at each time step. In the correlation matrix formalism, we instead use

$$\langle Z_j(t)\rangle = \langle\Psi_0|\,(1 - 2c_j^\dagger(t)c_j(t))\,|\Psi_0\rangle = 1 - 2\Gamma_{jj}(t) \tag{2.72}$$

[4]We denote the length by n rather than L since it coincides with the number of fermionic modes after the Jordan-Wigner transformation, which we usually denote by n.

and evolve the correlation matrix according to (2.63) with discretized time steps, using $U(dt) = e^{-i\,dt\,A}$:

$$\Gamma(t+dt) = U^*(dt)\Gamma(t)U^T(dt) = (e^{-i\,dt\,A})^*\,\Gamma(t)\,(e^{-i\,dt\,A})^T\,. \tag{2.73}$$

We observe that the two methods agree perfectly, for both periodic and open boundary conditions.

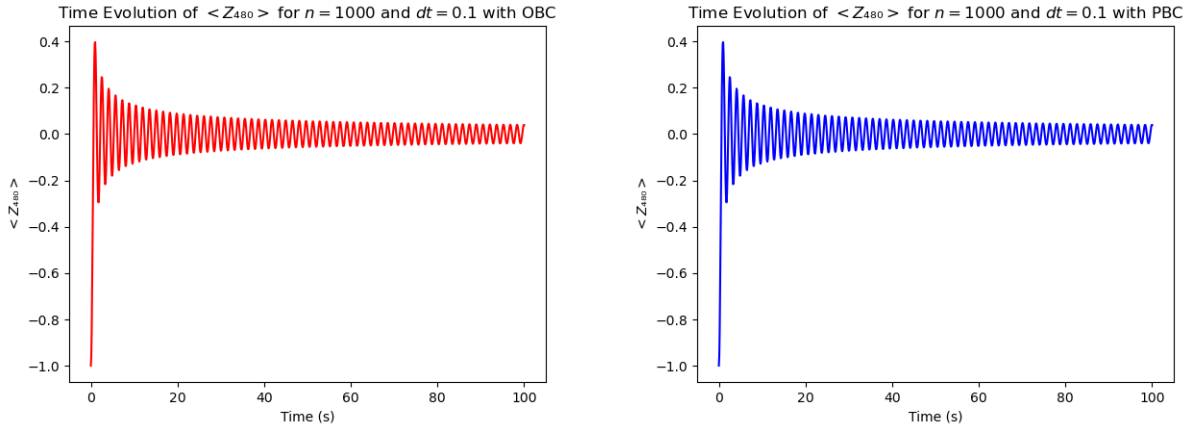

Figure 2.5: Time evolution of the expectation value of Z_{480} for a chain of $n = 1000$ qubits initialized in the Néel state computed using the correlation matrix. We used a timestep $dt = 0.1$ s and 1000 steps. On the left we chose open boundary conditions (OBC), while on the right periodic boundary conditions (PBC).

The difference between the two boundary conditions is apparent in Figure 2.4, but it is expected to vanish in the thermodynamic limit. Using ED, it is difficult to reach system sizes large enough to observe this behavior. In contrast, the correlation matrix approach allows us to explore much larger systems. In Figure 2.5, this is shown explicitly: we can easily reach $n = 1000$, and by considering a site in the bulk, such as Z_{480}, no differences are observed between the boundary conditions.

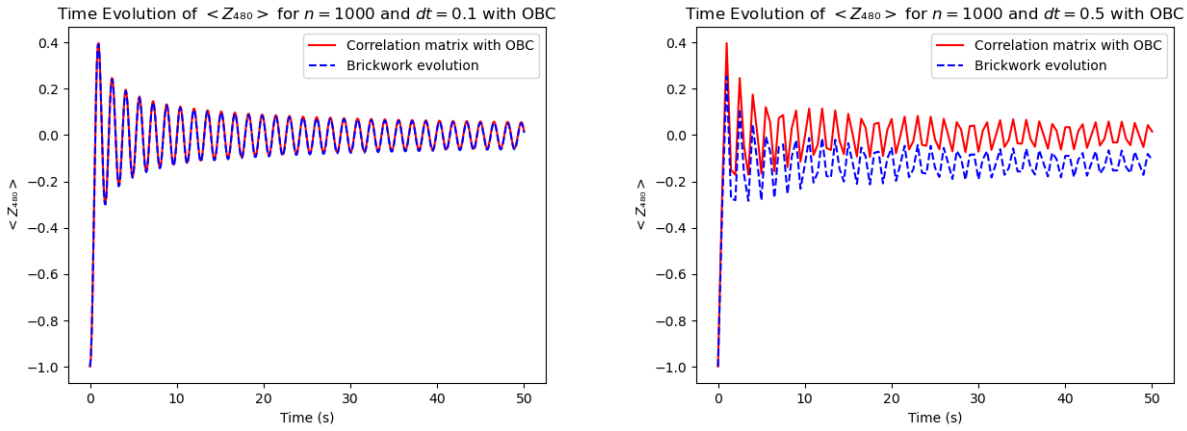

Figure 2.6: Time evolution of the expectation value of Z_{480} for a chain of $n = 1000$ qubits initialized in the Néel state computed using the correlation matrix and brickwork evolution. On the left we used a timestep $dt = 0.1$ s and 500 steps, while on the right $dt = 0.5$ s and 100 steps. We chose open boundary conditions (OBC).

As a final numerical check, we compare the discretized time evolution of (2.73) with a brickwork evolution. Indeed, we can construct a 2-brickwork circuit (2.6) starting from the Hamiltonian of Eq. (2.69). To implement this, we define the circulant matrices for the even and odd Hamiltonian densities, which take the following

form (assuming open boundary conditions, so that $k = 0$):

$$A_{even} = -\begin{pmatrix} 0 & 1 & 0 & 0 & \dots & 0 \\ 1 & 0 & 0 & 0 & & \\ 0 & 0 & 0 & 1 & & \\ 0 & 0 & 1 & 0 & & \\ \vdots & & & & \ddots & \\ 0 & & & & & 0 \end{pmatrix}, \qquad A_{odd} = -\begin{pmatrix} 0 & 0 & 0 & 0 & \dots & 0 \\ 0 & 0 & 1 & 0 & & \\ 0 & 1 & 0 & 0 & & \\ 0 & 0 & 0 & 0 & & \\ \vdots & & & & \ddots & \\ 0 & & & & & 0 \end{pmatrix}. \tag{2.74}$$

We can then implement the time evolution using (2.73), but with $U(dt) = \mathcal{V} = e^{-i\,dt\,A_{\text{even}}} e^{-i\,dt\,A_{\text{odd}}}$. As shown in Figure 2.6, the two evolutions coincide perfectly for $dt = 0.1$ (left), while noticeable deviations appear for the larger time step $dt = 0.5$ (right).

2.4 Free Fermionic Quantum Circuits

We now move away from the classical simulability of fermionic systems and introduce the concept of a **free fermionic quantum circuit**. This notion was first introduced in [32] and is related to the definition of a free fermionic system in terms of its spectrum discussed in Section 1.2.2.

This definition is necessary because, even when starting from a spin chain with a free fermionic spectrum, constructing a quantum circuit via a chosen trotterization does not automatically guarantee that the resulting circuit preserves this "free fermionicity". Preserving this property is crucial, as it defines the system as free fermionic. Therefore, having a precise definition allows us to determine whether this property is maintained in a given circuit.

To formalize this, we first define a free fermionic unitary operator in terms of its spectrum, since quantum circuits are composed of unitary gates.

For a generic Hamiltonian H, the unitary time evolution is given by $U(t) = e^{-iHt}$. Assuming H is free fermionic, we can use the properties of the spectrum of $U(t)$ at a fixed time t to provide a definition of a free fermionic unitary.

Definition 2.5 (Free Fermionic Unitary). A unitary operator U acting on Hilbert space $\mathcal{H}$ has a *free fermionic spectrum* if

1. There are n real numbers ϵ_k, $k = 1, ..., n$ such that the distinct eigenvalues λ are of the form

$$\lambda = \prod_{j=1}^{n} e^{\pm i\epsilon_k}\,. \tag{2.75}$$

2. If the ϵ_k are generic numbers, then every eigenvalue has the same degeneracy.

The quantities ϵ_k are called quasi-energies and are defined modulo 2π. In general, they are given by $t\varepsilon_k$, where ε_k are the energies of the single fermionic modes of the parent Hamiltonian. Note that this definition is equivalent to that of Gaussian operators (Definition 2.3), but it is expressed in terms of the spectrum rather than the operator structure.

Since our goal is to apply this framework to quantum circuits, we focus on local unitary operators. However, in general, $U(t)$ as defined above contains highly non-local terms, making it impossible to reproduce exactly with local quantum operations, as discussed in Section 2.1. For this reason, we discretize the time evolution using a quantum circuit.

Given a Hamiltonian $H = \sum_j \alpha_j h_j$, we can construct local unitaries u_j as in (2.3). For a string of indices $\mathcal{S} = s_1, s_2, \ldots, s_N$, we define a quantum circuit $\mathcal{V} = u_{s_N} ... u_{s_2} u_{s_1}$, exactly as in (2.4). The circuit $\mathcal{V}$ is called a free fermionic quantum circuit if it is a free fermionic unitary according to Definition 2.5.

Given this definition, a natural question arises: for a given free fermionic Hamiltonian, which choices of the indices $\mathcal{S}$ result in a circuit that is itself free fermionic?

Let us first answer this in the *limit of small angles*. As discussed in Section 2.1, we can write $\varphi_j \equiv -dt\,\alpha_j$, and interpret the circuit as an approximation of a small-timestep time evolution. In this regime, the local unitaries can be approximated as

$$u_j \approx 1 + i\varphi_j h_j = 1 - i\,dt\,\alpha_j\,h_j\,, \tag{2.76}$$

so that, to leading order in dt, the circuit becomes:

$$\mathcal{V} \approx 1 - iH dt\,. \tag{2.77}$$

This shows that, for sufficiently small angles, the circuit exhibits an approximately free fermionic spectrum, regardless of the choice of circuit geometry. However, this approximation is not exact in general.

Let us now consider *Jordan-Wigner diagonalizable model*. For these systems, the following theorem stated in Ref. [32] holds:

Theorem 2.4. *If every h_j in a Hamiltonian of the form (2.2) is bilinear in the Majorana operators $\{\gamma_\mu\}$, then every quantum circuit of the form (2.4) is free fermionic.*

Proof. This result can be proven by induction over the length of the operator product.

It is clear that a single local unitary u_j is bilinear in the Majorana operators, since, from (2.3), it consists of a term proportional to the identity and a term proportional to h_j, which is bilinear in γ_μ by definition. This establishes the base case of the induction.

Now, assume that for a product of length l, the circuit can be written as e^{iO_l}, where O_l is bilinear in the $\{\gamma_\mu\}$. By Definition 2.3, this means the circuit is a Gaussian operator and therefore a free fermionic unitary.

Consider now the product of length $l+1$. The operator at the exponent will be:

$$O_{l+1} = \log\big(u_{l+1} e^{iO_l}\big) = \log\big(e^{i\varphi_{l+1} h_{l+1}} e^{iO_l}\big),\,. \tag{2.78}$$

This logarithm can be evaluated using the BCH formula of (2.54).

Since both h_{l+1} and O_l are bilinear, all commutators that appear in the BCH expansion are also bilinear (see Subsection 2.3.2). Therefore, O_{l+1} is bilinear, and the circuit remains free fermionic. □

This theorem states that any quantum circuit constructed from Jordan-Wigner diagonalizable models is free fermionic. Unlike the case of the small-angle limit, this result holds without any approximation. However, this property does not necessarily extend to other free fermionic models, such as Free Fermions in Disguise. We will explore these cases in the following chapters.

Chapter 3

Free Fermions in Disguise: state of the art

Throughout this thesis, and in particular in Chapter 1, we repeatedly discussed the connection between spin$-1/2$ chains and fermionic systems established by the Jordan–Wigner transformation [1]. In several cases – such as the XY chain, the XX chain, and the transverse-field Ising model – this mapping transforms specific spin$-1/2$ Hamiltonians into free fermionic models, which are exactly solvable. This transformation has been generalized multiple times [6–12], but only recently a criterion to determine the free fermionicity of a given spin Hamiltonian has been introduced [13, 14].

We already mentioned that not all spin$-1/2$ chains with a free fermionic spectrum are JW-diagonalizable, as in [25–27] some models of this kind had appeared. Ultimately, in [28] *Free Fermions in Disguise* (FFD) models were introduced. These systems can be mapped onto free fermions, but only through a very complicated, non-linear, and non-local transformation. In addition, this mapping works only for systems with open boundary conditions. Some graph-theoretic criteria for FFD solvability have been introduced in [29–31].

As discussed earlier, particularly in Chapter 2, building quantum circuits from free fermionic models is natural. Fermionic Gaussian states [15–17] allow for efficient classical simulation of the dynamics, making these circuits useful as benchmarks. For JW-diagonalizable models, one can construct matchgate circuits [21–24], whose gates can be mapped to fermionic Gaussian operators, thus producing free fermionic quantum circuits. For FFD models, however, the situation is considerably more difficult: the mapping to free fermions is highly non-linear and non-local, and constructing a clear "dictionary" between operators on the spin chain and operators in the auxiliary fermionic system becomes extremely challenging. In particular, unlike in JW-diagonalizable models, the local Hamiltonians of FFD models do not appear to be quadratic in fermionic operators, and may not even admit a representation in terms of them at all.

A first attempt to construct quantum circuits based on FFD models appeared in [32]. On the other hand, the inverse problem, meaning the problem of expressing spin operators in terms of fermionic modes, was first addressed in [34], allowing the computation of certain spin correlation functions in FFD models. The Hilbert space structure of the FFD models was then studied in detail in [35], where the exponential degeneracy, another peculiar characteristic of FFD models, was fully resolved. This may have important implications in developing a more complete dictionary between spins and free fermions.

In this chapter, we present the state of the art on free fermions in disguise, beginning with an introduction to the model and its solution [28], and subsequently focusing on quantum circuits and the relation between spin and fermionic operators [32, 34, 35].

We begin in Section 3.1 by defining Free Fermions in Disguise, starting from the explicit model intro-

duced by Fendley in [28] and then focusing on the simple algebra that characterizes the model, examining alternative representations. In Section 3.2, we present the solution of the model as given in [28], showing that the Hamiltonian can be embedded into a transfer matrix structure that enables the definition of fermionic operators used to rewrite the Hamiltonian in free fermionic form. In Section 3.3, we address the inverse problem by first discussing spin operators that can be written in terms of fermionic modes, as shown in [34], and then examining the Hilbert-space structure analyzed in [35]. Finally, in Section 3.4, we attempt to construct free fermionic quantum circuits based on FFD models, beginning with a circuit proven to be free fermionic in [32] and then introducing additional conjectured free fermionic circuits also proposed in [32].

3.1 What are Free Fermions in Disguise

The Free Fermions in Disguise models were first introduced in [28] through two Hamiltonians expressed as sums of local interactions of the form:

$$h_m = Z_m Z_{m+1} X_{m+2} \qquad \text{and} \qquad \tilde{h}_m = X_m X_{m+1} Z_{m+2}\,. \tag{3.1}$$

These interactions define the Hamiltonians:

$$H = \sum_{m=1}^{L-2} b_m Z_m Z_{m+1} X_{m+2} \qquad \text{and} \qquad \tilde{H} = \sum_{m=1}^{L-2} \tilde{b}_m X_m X_{m+1} Z_{m+2}\ , \tag{3.2}$$

where L denotes the length of the spin chain. The Hamiltonian densities h_m and $\tilde{h}_m$ of (3.1) commute for all m and therefore the Hamiltonians in (3.2) commute as well. As a result, H and $\tilde{H}$ can be diagonalized independently.

Let us attempt a Jordan–Wigner transformation to this model. In this context, it is convenient to use a convention for the Majorana operators that differs from the one introduced in (1.77). We define Majorana operators as:

$$\gamma_{2m-1} = Z_m \prod_{k=1}^{m-1} X_k\,, \qquad \gamma_{2m} = -Y_m \prod_{k=1}^{m-1} X_k = i Z_m \prod_{k=1}^{m} X_k\,, \tag{3.3}$$

where the second expression for γ_{2m} follows from Eq. (1.64). This definition is unitarily related to the standard Jordan–Wigner transformation (1.77) via the *Hadamard operator* $\mathbb{H}$. This object is usually defined in matrix form as:

$$\mathbb{H} = \frac{1}{\sqrt{2}} \begin{pmatrix} 1 & 1 \\ 1 & -1 \end{pmatrix}\,, \tag{3.4}$$

and conjugation by $\mathbb{H}$ acts on the Pauli matrices (1.62) as:

$$\mathbb{H} X \mathbb{H} = Z\,, \qquad \mathbb{H} Y \mathbb{H} = -Y\,, \qquad \mathbb{H} Z \mathbb{H} = X\,. \tag{3.5}$$

In particular, we consider a Hamiltonian with uniform couplings that includes both types of local interactions in Eq. (3.1):

$$H_u = \sum_{m=1}^{L-2} (h_m + \tilde{h}_m) = \sum_{m=1}^{L-2} (Z_m Z_{m+1} X_{m+2} + X_m X_{m+1} Z_{m+2})\,. \tag{3.6}$$

Using the Majorana operators defined in (3.3), this Hamiltonian is mapped to a four-fermion Hamiltonian of the form:

$$H_u = -\sum_{\mu=1}^{2L-4} \gamma_\mu \gamma_{\mu+1} \gamma_{\mu+3} \gamma_{\mu+4}\,. \tag{3.7}$$

This mapping follows directly by separating the sum in Eq. (3.7) into contributions with $\mu = 2m-1$ and $\mu = 2m$. Substituting the expressions in (3.3) and simplifying the Pauli strings yields precisely the Hamiltonian densities in Eq. (3.1):

$$\begin{aligned}\gamma_{2m-1}\gamma_{2m}\gamma_{2m+2}\gamma_{2m+3} &= \left(Z_m \prod_{k=1}^{m-1} X_k\right)\left(iZ_m \prod_{k=1}^{m} X_k\right)\left(iZ_{m+1} \prod_{k=1}^{m+1} X_k\right)\left(Z_{m+2} \prod_{k=1}^{m+1} X_k\right) = -\tilde{h}_m\,,\\ \gamma_{2m}\gamma_{2m+1}\gamma_{2m+3}\gamma_{2m+4} &= \left(iZ_m \prod_{k=1}^{m} X_k\right)\left(Z_{m+1} \prod_{k=1}^{m} X_k\right)\left(Z_{m+2} \prod_{k=1}^{m+1} X_k\right)\left(iZ_{m+2} \prod_{k=1}^{m+2} X_k\right) = -h_m\,.\end{aligned} \tag{3.8}$$

From Eq. (3.7), we see explicitly that the FFD models are mapped to an interacting fermionic system when expressed in terms of Jordan–Wigner fermions. This four-fermion Hamiltonian has also been studied in the context of a simple lattice supersymmetry model [56], and was analyzed in [57] with a focus on the tricritical Ising point that it exhibits. However, we will not delve into these aspects in this thesis.

3.1.1 The FFD algebra

The defining property of this model is atually encoded in the algebra satisfied by the Hamiltonian densities (3.1), which we refer to as the **FFD algebra**:

$$\begin{aligned}&(h_m)^2 = 1\,,\\ &\{h_m, h_{m+1}\} = \{h_m, h_{m+2}\} = 0\,,\\ &[h_m, h_n] = 0 \qquad \text{if} \qquad |m-n| > 2\,.\end{aligned} \tag{3.9}$$

The local densities in Eq. (3.1) are not the only representation of the FFD algebra (3.9). A detailed analysis of the various representations of this algebra was indeed carried out in [32].

We can define a generic FFD Hamiltonian as:

$$H = \sum_{m=1}^{M} b_m h_m\,, \tag{3.10}$$

where the h_m satisfy the FFD algebra (3.9), and M is the number of local hamiltonians. In general, M is related to the number of sites L in a spin$-1/2$ chain, but it does not need to coincide with L. In the representations (3.1), $L = M+2$ for an open chain.

The FFD algebra is generated by the operators h_m, in the same way as the Clifford algebra mentioned in Remark 1.1 is generated by the Majorana operators $\{\gamma_\mu\}$. A generic element of the basis can be written as

$$\prod_{m=1}^{M} (h_m)^{n_m}\,, \qquad \text{where} \qquad n_m = 0, 1\,, \tag{3.11}$$

and the algebra is therefore 2^M-dimensional.

For $M = 6k+1$, $M = 6k+3$, $M = 6k+4$, $M = 6k+5$, one can define one or more *central elements* of the algebra [32]. These are elements which commute with all other elements of the algebra. Each central element squares to one, and therefore has eigenvalues ± 1. This allows us to study the eigenvalue problem of any operator separately within the sectors specified by the eigenvalues of the central elements. Note that central elements do not exist for $M = 6k$ and for $M = 6k+2$.

We now turn to possible representations of the algebra. For numerical implementations, it is useful to minimize the length L of the spin chain as much as possible. In particular, since the algebra of a spin$-1/2$

chain is 4^L-dimensional, the minimal length required for a faithful (i.e., injective) representation is $L = M/2$, for even M. Minimal representations for different values of M were provided in [32].

Fendley's representation (3.1) is defined on a chain of length $M + 2$. This can be reduced to a chain of length M, by modifying it as [32]:

$$h_m = Z_{m-2}Z_{m-1}X_m\,, \qquad m = 1, \ldots, M\,, \tag{3.12}$$

where, by convention, $Z_{-2} = Z_{-1} = 1$, and similarly for $\tilde{h}_m$. This implies that the first two elements are $h_1 = X_1$ and $h_2 = Z_1X_2$. When working with a specific representation later, we will typically use this one.

In general, since $[h_m, \tilde{h}_n] = 0$, this representation allows for the embedding of two independent copies of the algebra into the Hilbert space. Consequently, the full operator algebra of a spin chain of length $L = M$ is given by the product of two commuting copies of the FFD algebra, each with M generators.

3.2 The Solution of FFD Models

The solution of the FFD Hamiltonian was provided by Fendley in [28] and was inspired by the solution of a certain $\mathbb{Z}_n-$invariant Hamiltonian introduced in [58, 59], for which creation and annihilation operators can be defined using "free parafermions" [28, 45].

This solution relies solely on the algebra (3.9) and therefore does not depend on a specific representation. It is based on the construction of a tower of conserved charges, from which a *transfer matrix* depending on a spectral parameter can be defined. The existence of both these objects is a hallmark of *integrable models* [3, 60, 61]. Both the charges and the transfer matrix can be constructed for periodic as well as open boundary conditions, rendering both cases integrable. However, the transfer matrix can be used to define fermionic operators only in the case of open boundaries.

3.2.1 Conserved Charges and Transfer Matrix

Let us begin by defining $H_m = b_m h_m$, which satisfies the FFD algebra (3.9), with the only modification that $(H_m)^2 = (b_m)^2$. Using these operators, we can construct non-local conserved charges as sums of products of commuting H_m. For example, considering bilinears in H_m, we have:

$$Q^{(2)} = \sum_{|m-m'|>2} H_m H_{m'}\,. \tag{3.13}$$

The general formula for these conserved charges is

$$Q^{(s)} = \sum_{m_{r+1}>m_r+2} H_{m_1}H_{m_2}...H_{m_s}\,. \tag{3.14}$$

It is clear that $Q^{(1)} = H$, while $Q^{(2)}$ corresponds to the charge given in (3.13).

To prove this, let us start by commuting the Hamiltonian with a single term of $Q^{(s)}$.

$$[H, H_{m_1}H_{m_2}\ldots H_{m_s}] = \sum_{m=1}^{M}[H_m, H_{m_1}H_{m_2}\ldots H_{m_s}] = 2\sum_{\substack{|m-m_r|=1,2\\ |m-m_{r\pm1}|\neq 1,2}} H_m H_{m_1}H_{m_2}\ldots H_{m_s}\,. \tag{3.15}$$

The sum runs over all m such that H_m anticommutes with exactly one H_{m_r}. For example,

$$[H_{m+1}, H_m H_{m+3}] = H_{m+1}H_m H_{m+3} - H_m H_{m+3}H_{m+1} = H_{m+1}H_m H_{m+3} - H_{m+1}H_m H_{m+3} = 0\,, \tag{3.16}$$

because H_{m+1} anticommutes with both local Hamiltonians. Now, when considering the full conserved charge $Q^{(s)}$, there are additional terms where m and m_r are exchanged, with H_m coming from $Q^{(s)}$ while H_{m_r} from H. These terms cancel in the sum over m_r, since

$$H_m H_{m_1} ... H_{m_{r-1}} H_{m_r} H_{m_{r+1}} ... H_{m_s} + H_{m_r} H_{m_1} ... H_{m_{r-1}} H_m H_{m_{r+1}} ... H_{m_s} = 0 \,, \tag{3.17}$$

due to the fact that H_m and H_{m_r} anticommute with each other and commute with all other factors. This immediately gives $[H, Q^{(s)}] = 0$.

From our definition, it is clear that the system possesses an extensive number of conserved charges S. The exact number depends on the choice of boundary conditions: for periodic boundaries, $S = \lfloor M/3 \rfloor$, while for open boundaries, the case that yields a free fermionic spectrum, we have $S = \lfloor (M+2)/3 \rfloor$. Here, $\lfloor x \rfloor$ denotes the integer part of x.

Given this extensive hierarchy of conserved charges, it is natural, in the context of integrable models [60, 61], to define the following *transfer matrix*:

$$T_M(v) = \sum_{s=0}^{S} (-u)^s Q^{(s)} \,. \tag{3.18}$$

The parameter u is referred to as the *spectral parameter*. While the eigenvalues of the transfer matrix depend on u, its eigenvectors do not.

It is clear that the transfer matrix commutes with the Hamiltonian (3.10). However, it is not immediately obvious that transfer matrices corresponding to different values of the spectral parameter also commute with each other. In [28], a proof that the conserved charges are in involution is provided, which then implies

$$[T_M(u), T_M(v)] = 0 \,, \qquad \forall\, u, v \,. \tag{3.19}$$

From this point onward, we focus on the case of open boundary conditions. As mentioned previously, the model remains integrable under periodic boundary conditions [28], but in that case it does not admit a free fermionic spectrum.

For OBC, the transfer matrix satisfies the following fundamental recursive relation:

$$T_M(u) = T_{M-1}(u) - u H_M T_{M-3}(u) \,, \tag{3.20}$$

valid for $M \geq 1$, with the convention $T_M = 1$ for $M \leq 0$. This relation follows from the corresponding recursion for the conserved charges:

$$\begin{cases} Q_M^{(s)} = Q_{M-1}^{(s)} + H_M Q_{M-3}^{(s-1)} & \text{if } Q_{M-1}^{(s)} \text{ exists,} \\ Q_M^{(s)} = H_M Q_{M-3}^{(s-1)} & \text{otherwise,} \end{cases} \tag{3.21}$$

where $Q_M^{(s)}$ denotes the conserved charge of order s in a system with M Hamiltonian densities, and we adopt the convention $Q^{(s)} = 1$ for $s \leq 0$. Let us clarify this construction through an explicit example.

Example 3.1. Let us consider the cases $M = 8$ and $M = 7$. We have $S = 3$ for $M = 8$ and $M = 7$, but $S = 2$ for $M = 6$. This implies that for $Q_M^{(3)}$, we are in the first case of (3.21) for $M = 8$, while in the second case for $M = 7$. Explicitly, we have:

$$Q_8^{(3)} = H_1 H_4 H_7 + H_8 (H_1 H_4 + H_1 H_5 + H_2 H_5) = Q_7^{(3)} + H_8 Q_5^{(2)} \,, \tag{3.22}$$

while

$$Q_7^{(3)} = H_1 H_4 H_7 = H_7 Q_4^{(2)} \,. \tag{3.23}$$

The recursion relations for the transfer matrix can then be verified explicitly:

$$\begin{aligned} T_8(u) &= 1 - uQ_8^{(1)} + u^2Q_8^{(2)} - u^3Q_8^{(3)} = 1 - u(Q_7^{(1)} + H_8) + u^2(Q_7^{(2)} + H_8Q_5^{(1)}) - u^3(Q_7^{(3)} + H_8Q_5^{(2)}) \\ &= (1 - uQ_7^{(1)} + u^2Q_7^{(2)} - u^3Q_7^{(3)}) - uH_8(1 - uQ_5^{(1)} + u^2Q_5^{(2)}) = T_7(u) - uH_8T_5(u)\,, \end{aligned} \tag{3.24}$$

$$\begin{aligned} T_7(u) &= 1 - uQ_7^{(1)} + u^2Q_7^{(2)} - u^3Q_7^{(3)} = 1 - u(Q_6^{(1)} + H_7) + u^2(Q_6^{(2)} + H_7Q_4^{(1)}) - u^3(Q_6^{(3)} + H_7Q_4^{(2)}) \\ &= (1 - uQ_6^{(1)} + u^2Q_6^{(2)}) - uH_7(1 - uQ_4^{(1)} + u^2Q_4^{(2)}) = T_6(u) - uH_7T_4(u)\,. \end{aligned} \tag{3.25}$$

These examples illustrate how Eq. (3.20) naturally emerge from the recursion of the conserved charges.

The recursion relation (3.20) can be used to prove, by induction, the following product form for the transfer matrix:

$$T_M(u) = G_M(u)G_M(u)^T\,, \qquad G_M(u) = g_1g_2...g_M\,, \tag{3.26}$$

where the superscript T defines a linear operation with the property

$$(g_1g_2\dots g_M)^T = g_M\dots g_2g_1\,, \tag{3.27}$$

and coincides with the usual matrix transpose in most representations of the FFD algebra. The factors g_m are defined as

$$g_m = \cos\frac{\phi_m}{2} + h_m\sin\frac{\phi_m}{2} \tag{3.28}$$

with the angles ϕ_m determined recursively via

$$\sin\phi_{m+1} = \frac{-ub_{m+1}}{\cos\phi_{m-1}\cos\phi_m}\,, \tag{3.29}$$

and $\phi_0 = \phi_{-1} = 0$. Note that, in general, the sine in (3.29) is not automatically constrained to $[-1,1]$. Therefore, u must be chosen real and sufficiently small to ensure all ϕ_m are real, which in turn guarantees that the g_m are Hermitian.

The operators g_m defined in Eq. (3.28), have the following properties:

$$\begin{aligned} &g_m^2 = 1 + h_m\sin\phi_m = 1 - \frac{-ub_mh_m}{\cos\phi_{m-2}\cos\phi_{m-1}}\,, \\ &g_mh_{m\pm a}g_m = h_{m\pm a}\cos\phi_m \qquad a = 1,2\,. \end{aligned} \tag{3.30}$$

These can be used together with (3.20), to prove (3.26) by induction.

Let us first consider the base case $M = 1$: $G_1G_1^T = g_1^2 = 1 + h_1\sin\phi_1 = 1 - h_1u = T_1(u)$. Now, suppose that $T_{M-1} = G_{M-1}G_{M-1}^T$. Then, for $M \geq 2$, we have

$$\begin{aligned} G_MG_M^T &= G_{M-1}g_M^2G_{M-1}^T = G_{M-1}\left(1 + \frac{-ub_Mh_M}{\cos\phi_{M-2}\cos\phi_{M-1}}\right)G_{M-1}^T = \\ &= T_{M-1} - \frac{ub_M}{\cos\phi_{M-2}\cos\phi_{M-1}}G_{M-3}(g_{M-2}g_{M-1}h_Mg_{M-1}g_{M-2})G_{M-3}^T = \\ &= T_{M-1} - \frac{ub_M}{\cos\phi_{M-2}\cos\phi_{M-1}}G_{M-3}(h_M\cos\phi_{M-1}\cos\phi_{M-2})G_{M-3}^T = \\ &= T_{M-1} - ub_Mh_MG_{M-3}G_{M-3}^T = T_{M-1} - uH_MT_{M-3} = T_M\,. \end{aligned} \tag{3.31}$$

This product form allows us to determine the inverse of T_M. Noting that sending $u \to -u$ maps all angles ϕ_m to their opposite $-\phi_m$, we have

$$g_m(\pm u)g_m(\mp u) = \left(\cos\frac{\phi_m}{2} \pm h_m\sin\frac{\phi_m}{2}\right)\left(\cos\frac{\phi_m}{2} \mp h_m\sin\frac{\phi_m}{2}\right) = \cos^2\frac{\phi_m}{2} - \sin^2\frac{\phi_m}{2} = \cos\phi_m\,. \tag{3.32}$$

Consequently, we can write:

$$\begin{aligned} G_M(\pm u)G_M^T(\mp u) = G_M^T(\pm u)G_M(\mp u) &= \prod_{m=1}^{M} \cos\phi_m \ , \\ T_M(u)T_M(-u) = G_M(u)G_M^T(u)G_M(-u)G_M^T(-u) &= \prod_{m=1}^{M} \cos^2\phi_m \equiv P_M(u) \ . \end{aligned} \tag{3.33}$$

Hence, if $u \neq \pm u_k$, where $\pm u_k$ are roots of $P_M(u)$, the transfer matrix is invertible, and its inverse is proportional to $T_M(-u)$.

The function $P_M(u)$ is a polynomial in u^2, since the factors $\cos^2\phi_m$ must be themselves polynomials in u^2 from (3.29). A recursion relation can also be derived for $P_M(u)$. Indeed, we have

$$\frac{P_M}{P_{M-1}} = \cos^2\phi_M = 1 - \sin^2\phi_M = 1 - \frac{u^2 b_M^2}{\cos^2\phi_{M-2}\cos^2\phi_{M-1}} = 1 - u^2 b_M^2 \frac{P_{M-3}}{P_{M-1}} \ . \tag{3.34}$$

This leads to the recursion relation

$$P_M(u) = P_{M-1}(u) - u^2 b_M^2 P_{M-3}(u) \ , \tag{3.35}$$

with the convention $P_M = 1$ for $M \leq 0$. It is then clear that $P_M(u)$ is of order $S = \lfloor (M+2)/3 \rfloor$ in u^2 or of order $2S$ in u.

The similarity between the recursion (3.35) and the recursion for the transfer matrix (3.20) suggests that the polynomial has a structure analogous to the transfer matrix, but with $u^2 b_m^2$ replacing uH_m. In other words, it can be written as a sum of products of coefficients associated with commuting h_m.

Remark 3.1. A polynomial satisfying a recursion relation analogous to (3.35) also appears in the Ising chain with open boundary conditions [45].

3.2.2 Creation and Annihilation Operators

Let us now construct the fermionic creation and annihilation operators. To this end, we require one additional ingredient: the **edge operator** (or **edge mode**) χ. This is an operator that commutes with all h_m for $m \neq M$, anticommutes with h_M, and squares to the identity:

$$\begin{aligned} &\chi^2 = 1 \, , \\ &[h_m, \chi] = 0 \, , \qquad m = 1, 2, \dots M-1 \\ &\{h_M, \chi\} = 0 \, . \end{aligned} \tag{3.36}$$

The operator χ depends on the chosen representation, and even within a fixed representation there remains some freedom in selecting it. For instance, in the representation (3.12), one may choose $\chi = Z_M$ or $\chi = Y_M$. We will usually choose $\chi = Z_M$.

Given the edge operator, the fermionic operators are now defined as:

$$\Psi_{\pm k} \equiv \frac{1}{N_k} T(\mp u_k)\, \chi\, T(\pm u_k) \, , \tag{3.37}$$

where N_k is an appropriate normalization constant. Note that in this subsection we drop the subscript M on the transfer matrix for simplicity.

Firstly, let us compute the commutator with the Hamiltonian to verify that it satisfies Eq. (1.39). Using the $\Psi_{\pm k}$ notation, Eq. (1.39) reads:

$$[H, \Psi_{\pm k}] = \pm 2\varepsilon_k \Psi_{\pm k} \, . \tag{3.38}$$

To do so, we consider the following commutator, using the fact that the Hamiltonian commutes with the transfer matrix:

$$\begin{aligned}[H, T(u)\,\chi\,T(-u)] = T(u)[H,\chi]T(-u) = T(u)\sum_{m=1}^{M}[h_m,\chi]T(-u) = \\ = T(u)(h_M\chi - \chi h_M)T(-u) = 2T(u)h_M\chi\,T(-u)\,.\end{aligned} \tag{3.39}$$

We now exploit the following identity, proven in the appendix of [28]:

$$u\,T(u)h_M\chi\,T(-u) = -T(u)\,\chi\,T(-u) + P_M(u)(1-uh_M)\chi\,, \tag{3.40}$$

and evaluate it at $u = \mp u_k$. In this case, the second term vanishes, and we obtain:

$$[H, T(\mp u_k)\,\chi\,T(\pm u_k)] = \pm\frac{2}{u_k}T(\mp u_k)\,\chi\,T(\pm u_k)\,. \tag{3.41}$$

Thus, (3.38) is satisfied provided the single–mode energies are given by:

$$\varepsilon_k = \frac{1}{u_k}\,. \tag{3.42}$$

Since H is hermitian, the energies ε_k must be real, and therefore the parameters u_k. By convention, we choose $u_k > 0$ for $k > 0$.

Remark 3.2. If the polynomial $P_M(u)$ has zeros with multiplicity greater than one, the resulting creation and annihilation operators would not be distinct. Indeed, if $u_k = u_{k'}$, then $\Psi_{\pm k} = \Psi_{\pm k'}$. However, in [62] it was shown that the zeros of this polynomials are actually real and non-degenerate. Therefore, we can safely assume all the u_k to be distinct.

Let us now prove a number of identities needed to verify that the operators $\Psi_{\pm k}$ satisfy the canonical anti-commutation relations (1.50). For notational convenience, we denote the creation and annihilation operators collectively by Ψ_l, where $l = \pm k$, and $u_l = \pm u_k$ accordingly.

Let us start with the Pauli exclusion principle, and therefore with proving that $(\Psi_l)^2 = 0$:

$$(\Psi_l)^2 \propto T(u_l)T(-u_l) = P_M(u_l^2) = 0 \qquad \to \qquad \{\Psi_{\pm k}, \Psi_{\pm k}\} = 0\,. \tag{3.43}$$

We also note that $\Psi_{\pm k}$ are respectively left and right eigenvectors of the transfer matrix at $u = u_l$, since

$$\begin{aligned}T(u_l)\Psi_l \propto T(u_l)T(-u_l) = 0\,,\\ \Psi_l T(u_l) \propto T(-u_l)T(u_l) = 0\,.\end{aligned} \tag{3.44}$$

Moreover, from the definition (3.37), and using the fact that both $T(u)$ and χ are hermitian, it follows immediately that $\Psi_l^\dagger = \Psi_{-l}$, as expected for creation and annihilation operators.

Another useful relation connecting the transfer matrix and the creation/annihilation operators, proven in [28], is

$$(u_l + u)T(u)\Psi_l = (u_l - u)\Psi_l T(u)\,. \tag{3.45}$$

In the limit $u \to \pm u_k$, this reduces to (3.44).

Let us now prove the second identity in (1.50), namely $\{\Psi_l, \Psi_{-m}\} = \delta_{lm}$. We begin by expressing the anticommutator of two fermionic operators as

$$\{\Psi_l, \Psi_{-m}\} = \lim_{u\to u_m}\{\Psi_l, T(u)\,\chi\,T(-u)\}\,. \tag{3.46}$$

Then, using (3.45), we obtain:

$$\{\Psi_l, T(u)\,\chi\,T(-u)\} = \frac{u_l+u}{u_l-u}T(u)\{\Psi_l,\chi\}T(-u)\,, \tag{3.47}$$

and since, as shown in [28],

$$\{\Psi_l,\chi\} = \frac{4}{N_l}P_{M-1}(u_l)\,, \tag{3.48}$$

we can write

$$\{\Psi_l, T(u)\,\chi\,T(-u)\} = \frac{4}{N_l}P_{M-1}(u_l)P_M(u)\frac{u_l+u}{u_l-u}\,. \tag{3.49}$$

Taking the limit $u \to u_m$, the anticommutator vanishes for all $m \neq l$. For $m = l$, the expression is given by minus the derivative with respect to u of $P_M(u)$ (which we denote as $P'_M(u)$) computed in $u = u_l$. We therefore obtain:

$$\{\Psi_l, \Psi_{-m}\} = -\delta_{lm}\frac{8u_l}{N_l^2}P_{M-1}(u_l)P'_M(u_l) \stackrel{!}{=} \delta_{lm}\,. \tag{3.50}$$

This imposes the following expression for the normalization constant squared:

$$N_l^2 = -8u_lP_{M-1}(u_l)P'_M(u_l)\,. \tag{3.51}$$

We have therefore established the canonical anticommutation relations for the creation and annihilation operators.

Finally, in [28] it was shown that the Hamiltonian can be expressed in terms of the creation and annihilation operators as in (1.53), and therefore its spectrum is free fermionic, as in (1.41). Moreover, the transfer matrix can be written in the form:

$$T(u) = \prod_{k=1}^{S}(1 - u\varepsilon_k[\Psi_k, \Psi_{-k}]) \tag{3.52}$$

which implies that its eigenvalues are:

$$\Lambda(u) = \prod_{k=1}^{S}(1 \mp u\varepsilon_k)\,. \tag{3.53}$$

Remark 3.3 (Exponential Degeneracies). If we use the representation (3.12), we work with a 2^L-dimensional Hilbert space, with $L = M$. However, we have seen that the number of distinct single-particle energies is $S = \lfloor (M+2)/3 \rfloor$. Therefore, every eigenstate exhibits a degeneracy of 2^{L-S}, which grows exponentially with the system size. This exponential degeneracy persists for generic representations of the algebra and is a very peculiar characteristics of FFD models.

3.3 The Inverse Problem and the Hilbert Space Structure

In Section 3.2, we showed that the FFD model, defined by the algebra (3.9) and the Hamiltonian (3.10), can be mapped to a free fermionic system in the case of open boundaries. However, to compute physically relevant quantities in the original spin-chain model, such as correlation functions, one needs to express local spin operators in terms of fermionic eigenmodes. This constitutes the so-called **inverse problem**.

In Jordan-Wigner diagonalizable models, the inverse problem is relatively simple. For example, consider the XY-chain discussed in Section 1.4. The mapping to the diagonal form (1.110) proceeds in three steps: first, the Jordan-Wigner transformation (1.71) maps spins to fermions; next, a Fourier transformation (1.89) moves to momentum space; finally, a Bogoliubov transformation (1.104) diagonalizes the Hamiltonian through

a linear combination of fermionic operators. Each of these steps can be inverted, making it straightforward to express spin operators in terms of fermionic creation and annihilation operators.

In contrast, the mapping to the hidden free fermions in FFD models, given by (3.37), is much more involved than the JW and the Fourier transformations. Consequently, it is generally nontrivial to define a complete "dictionary" between spin operators and fermionic operators. Moreover, the exponential degeneracy of the model, as discussed in Remark 3.3, implies that the inverse problem cannot be fully solved, and one can expect solutions only for selected local operators.

Some findings in this direction were obtained in [34], while [35] analyzed the structure of the Hilbert space of FFD models and resolved the degeneracies, which provides a useful starting point for tackling the inverse problem.

We begin this section by focusing on the results of [34], introducing the family of local operators that can be mapped to free fermions identified there. Subsequently, we provide a brief review of the findings in [35] regarding the structure of the Hilbert space of the FFD model.

3.3.1 The Edge Operator

The first example of a local operator that can be expressed in terms of fermions, is the edge operator χ satisfying the algebra (3.36). It can be written as a linear combination of fermionic operators:

$$\chi = \sum_{l=-S}^{S} c_l \Psi_l \,. \tag{3.54}$$

The coefficients can be expressed as (using (3.51) to move from one expression to the other):

$$c_l = c_{-l} = \frac{N_l}{-2u_l P'_M(u_l)} = \frac{4P_{M-1}(u_l)}{N_l} = \sqrt{-\frac{2P_{M-1}(u_l)}{u_l P'_M(u_l)}} \,. \tag{3.55}$$

For $M = 3k$ and $M = 3k+2$, there also exists a *Majorana zero mode* Ψ_0. This is a Hermitian operator satisfying:

$$\begin{aligned} &(\Psi_0)^2 = \mathbb{1} \,, \\ &[H, \Psi_0] = 0 \,, \\ &\{\Psi_0, \Psi_{\pm k}\} = 0 \,, \end{aligned} \tag{3.56}$$

and its coefficient in the expansion is given by

$$c_0 = \sqrt{\lim_{u\to\infty} \frac{P_{M-1}(u)}{P_M(u)}} \,. \tag{3.57}$$

This expansion can be shown to be complete by introducing the operator-valued function:

$$\phi_M(u) = -\frac{1}{u}\left(\frac{P_M(u)\chi + T_M(-u)\chi T_M(u)}{2P_M(u)}\right) \,. \tag{3.58}$$

This function has a simple pole at $u = 0$ and additional poles at $u = u_l$, which in principle could be of higher order. However, as discussed in [62], the zeros of the polynomial are non-degenerate, so all poles can be treated as simple. We can now consider the integral over a left-handed contour enclosing only the pole at $u = 0$, as shown in Figure 3.1. From the residue theorem [63], we have:

$$-\operatorname{Res}_{u=0} \phi_M(u) = \frac{1}{2\pi i}\int_C \mathrm{d}u\, \phi_M(u) = \sum_{l=-S,\, l\neq 0}^{S} \operatorname{Res}_{u=u_l} \phi_M(u) + \operatorname{Res}_{u=\infty} \phi_M(u) \,, \tag{3.59}$$

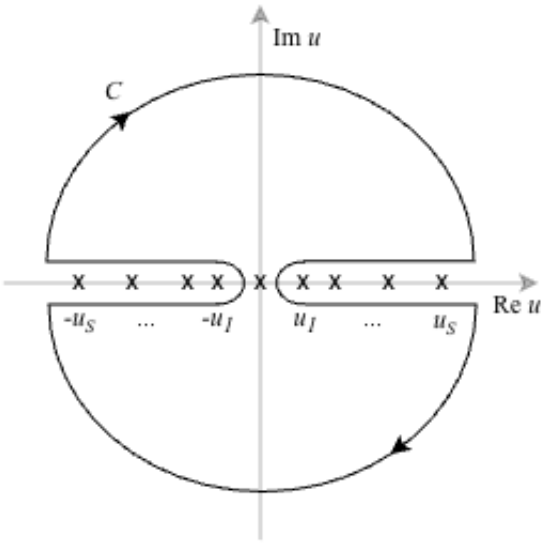

Figure 3.1: In this figure we draw the contour C, constructed to enclose the pole $u = 0$ of $\phi_M(u)$, whose residue is precisely the edge operator χ. On the other hand, outside this contour, one picks up the residues at the poles $u = \pm u_k$ as well as the residue at infinity. This image was realized following Figure 4 of [34].

where the residues are given by:

$$-\operatorname{Res}_{u=0}\phi_M(u) = -\lim_{u\to 0} u\,\phi_M(u) = \chi\,, \tag{3.60}$$

$$\operatorname{Res}_{u=u_l}\phi_M(u) = \frac{g(u_l)}{h'(u_l)} = \frac{N_l\Psi_l}{-2u_l P'_M(u_l)} = c_l\Psi_l \tag{3.61}$$

with $g(u)$ and $h(u)$ being the numerator and denominator of $\phi_M(u)$, respectively. The residue at infinity is

$$\mathcal{Q} := \operatorname{Res}_{u=\infty}\phi_M(u) \overset{v=1/u}{=} \operatorname{Res}_{v=0}\frac{-1}{v^2}\phi_M(v^{-1}) = \lim_{u\to\infty}\mathcal{Q}_u\,, \tag{3.62}$$

where $\mathcal{Q}_u = -u\phi_M(u)$, since $\lim_{u\to\infty}\phi_M(u) = 0$ [63]. Therefore, we can write:

$$\chi = \sum_{l=-S,\,l\neq 0}^{S} c_l\Psi_l + \mathcal{Q}\,. \tag{3.63}$$

We can use Eq. (3.48) and write χ as in Eq. (3.63) to see that $\mathcal{Q}$ must anticommute with each Ψ_l. Furthermore, it is easy to see that $[H, \mathcal{Q}] = 0$ by expressing H as in (1.53). We can then use the relation $\{T_M(u), \chi\} = 2T_{M-1}(u)\chi$, which can be easily proven using (3.36) and (3.20), to write:

$$\mathcal{Q}_u = \frac{T_M(-u)T_{M-1}(u)}{P_M(u)}\chi = \chi\frac{T_{M-1}(-u)T_M(u)}{P_M(u)}\,. \tag{3.64}$$

This quantity goes to zero in the limit $u \to \infty$ only if the order of the numerator is smaller than the order of the denominator. This happens only if the order S' of $T_{M-1}(u)$ is less than S:

$$S' = \left\lfloor\frac{(M-1)+2}{3}\right\rfloor < \left\lfloor\frac{M+2}{3}\right\rfloor = S\,, \tag{3.65}$$

which occurs only for $M \in 3\mathbb{N}+1$. We can now multiply the two forms of (3.64) to obtain

$$\mathcal{Q}^2 = \lim_{u\to\infty}\mathcal{Q}_u = \lim_{u\to\infty}\frac{P_{M-1}(u)}{P_M(u)}\mathbb{1} = c_0^2\mathbb{1}\,, \tag{3.66}$$

which allows us to define a Majorana zero mode as

$$\Psi_0 = \frac{\mathcal{Q}}{c_0}\,, \tag{3.67}$$

which satisfies the properties (3.56).

3.3.2 Other Local Operators in Terms of Fermions

Having now expressed χ linearly in the creation and annihilation operators, we can construct a series of operators linear in the fermions recursively. These are defined as:

$$\begin{aligned} o_j &= \frac{1}{2}[H, o_{j-1}]\,, \\ o_0 &= \chi\,. \end{aligned} \tag{3.68}$$

The operators o_j must be given by a linear combination of the Ψ_l. This is because H is bilinear while χ is linear in the fermions, and the commutator of a bilinear and a linear operator in the fermions will also be linear. In particular, using the expressions (1.53) and (3.54) for H and χ respectively, we can write:

$$o_j = \sum_{l=-S}^{S} (\varepsilon_l)^j c_l \Psi_l\,, \tag{3.69}$$

where $\varepsilon_{-k} = -\varepsilon_k$. If we want to construct bilinear, trilinear, or higher-order operators in the fermionic operators, we can simply multiply two, three, or more o_j respectively.

Let us now construct the first elements of this sequence. Clearly, using the properties of χ given in Eq. (3.36), we get

$$o_1 = b_M h_M \chi\,, \tag{3.70}$$

therefore by multiplying on the right by χ and dividing by b_M, we can express h_M as bilinear in the fermions:

$$h_M = \frac{o_1 \chi}{b_M} = \frac{1}{b_M} \sum_{j,k=-S}^{S} \varepsilon_j c_j c_k \Psi_j \Psi_k\,. \tag{3.71}$$

The next element is

$$o_2 = [(b_{M-2} h_{M-2} + b_{M-1} h_{M-1}) b_M h_M + b_M^2]\,\chi\,, \tag{3.72}$$

from which we can express the linear combination $b_{M-2}h_{M-2} + b_{M-1}h_{M-1}$ as a fermion bilinear. However, unlike in JW-diagonalizable models, the Hamiltonian densities h_m in general cannot be expressed purely in terms of fermionic operators.

Expressing some local operators in terms of fermions allows one to study their exact real-time dynamics, or the dynamics of certain correlation functions. In particular, in [34], the self-correlator of the boundary energy h_M, defined as:

$$D(t) := \langle h_M(t) h_M(0) \rangle = \frac{\operatorname{tr}\left[h_M e^{-iHt} h_M e^{iHt}\right]}{\operatorname{tr} \mathbb{1}}\,, \tag{3.73}$$

was computed using (3.71).

3.3.3 Hilbert Space Structure

Let us finally present the findings of [35] about the Hilbert space structure of FFD models, which allows us to resolve the degeneracies of the spectrum..

The first important result states that the Hilbert space $\mathcal{H}$ can be decomposed as:

$$\mathcal{H} = \mathcal{H}_F \otimes \mathcal{H}_D \,. \tag{3.74}$$

Here $\mathcal{H}_F$ is the 2^S-dimensional space where the fermionic operators are supported, while $\mathcal{H}_D$ accounts for the exponential degeneracies and has dimension 2^{M-S}. To prove this, let us begin by introducing the subspace annihilated by all annihilation operators:

$$\mathcal{K} = \{|v\rangle \in \mathcal{H} \;:\; \Psi_{-k}\,|v\rangle = 0\,,\, \forall k = 1,\dots,S\}\,, \tag{3.75}$$

which clearly coincides with the eigenspace of the ground-state energy and has dimension 2^{M-S}. Let $\{|w_j\rangle\}$ be an orthonormal basis of $\mathcal{K}$ and define:

$$|f_{j,\alpha}\rangle = (\Psi_1)^{\alpha_1}(\Psi_2)^{\alpha_2}\dots(\Psi_S)^{\alpha_S}\,|w_j\rangle\ , \tag{3.76}$$

where $\alpha_j = 0,1$ and $\alpha_1\alpha_2\dots\alpha_S$ is the binary representation of the integer $\alpha = 0,\dots,2^S-1$. From the CAR (1.50), it is clear that the $|f_{j,\alpha}\rangle$ are mutually orthogonal:

$$\langle f_{j,\alpha}|f_{k,\beta}\rangle = \delta_{j,k}\delta_{\alpha\beta}\,, \tag{3.77}$$

and therefore form a basis of the full Hilbert space $\mathcal{H}$. We can now define the following isomorphism to make the factorization apparent:

$$\begin{aligned} \varphi \;:\; \mathcal{H} \quad &\to \mathcal{H}_F \otimes \mathcal{H}_D \\ |f_{j,\alpha}\rangle &\to |\alpha\rangle \otimes |j\rangle\ , \end{aligned} \tag{3.78}$$

where $|\alpha\rangle = (c_1^\dagger)^{\alpha_1}(c_2^\dagger)^{\alpha_2}\dots(c_S^\dagger)^{\alpha_S}\,|\Omega\rangle$ generates $\mathcal{H}_F$ ($c_k^\dagger$ are fermionic creation operators and $|\Omega\rangle$ is the fermionic vacuum), and $\{|j\rangle\}$ generates $\mathcal{H}_D$. It is then clear that $\Psi_k = c_k^\dagger \otimes \mathbb{1}_D$ and all operators which can be written in terms of fermionic operators, can be decomposed as

$$O = O_F \otimes \mathbb{1}_D\,. \tag{3.79}$$

The structure of $\mathcal{H}_D$ can be further refined. In particular, it can be factorized as:

$$\mathcal{H}_D = \mathcal{H}_{\tilde{D}} \otimes \mathcal{H}_{F'}\,. \tag{3.80}$$

Here, $\mathcal{H}_{\tilde{D}}$ supports the action of all operators that commute with all the generators h_m and the edge operator χ, and therefore with all fermionic operators as well. The algebra of such operators will depend on the representation. On the other hand, $\mathcal{H}_{F'}$ supports the action of all operators written *in terms of the generators* h_m that commute with the creation/annihilation operators. These operators form another fermionic algebra, which we call *ancillary*. This ancillary algebra does not depend on the representation, but it depends on the Hamiltonian couplings. For further details, we refer to [35]

This characterization of the Hilbert space structure could be very useful in the computation of dynamical quantities such as correlation functions. Indeed, having a clear understanding of the symmetry algebra allows one to study the dynamics of spin operators which admit a simple representation not only in terms of fermionic operators, but also in terms of the elements of the symmetry algebra.

3.4 Free Fermionic Quantum Circuits from FFD

In Section 2.4, we introduced the concept of a *free fermionic quantum circuit*, a circuit $\mathcal{V}$ which can be interpreted as a fermionic Gaussian operator. We also demonstrated that any quantum circuit constructed

from Jordan-Wigner diagonalizable models is free fermionic. The natural question that now arises is what occurs for quantum circuits built from FFD models. This question was first posed in [32], where several exact and conjectured free fermionic circuits were presented. In this section, we summarize the results and conjectures reported in [32]. In Chapter 4, we will examine the resolution of some of these conjectures following [36], which is closely related to the work presented in this thesis.

3.4.1 A Circuit from Fendley's Transfer Matrix

The first quantum circuit we consider [32] can be directly obtained from the transfer matrix factorization of Eq. (3.26). As shown in Section 3.2, the transfer matrix of the model can be written as $T_M(u) = GG^T$, where $G = g_1 g_2 \dots g_M$ and the local operators g_m are given by (3.28). For reference, we rewrite them here:

$$g_m = \cos\frac{\phi_m}{2} + h_m \sin\frac{\phi_m}{2}\,. \tag{3.81}$$

The angles are defined by the recursion (3.29). These operators closely resemble the local unitaries of Eq. (2.3), which we also rewrite here:

$$u_m = \cos\varphi_m + i h_m \sin\varphi_m\,. \tag{3.82}$$

These were used to define quantum circuits from Hamiltonians composed of sums of local interactions.

The only crucial problem in using the g_m to construct a quantum circuit is that they are Hermitian for real u, whereas a circuit requires unitary operators. However, this issue can be resolved by choosing a purely imaginary spectral parameter, $u = iv$ with $v \in \mathbb{R}$. In fact, using the fact that:

$$\cos(ix) = \cosh(x)\,, \qquad\qquad \sin(ix) = i\sinh(x)\,, \tag{3.83}$$

tt is clear from (3.29) that ϕ_m becomes purely imaginary. We can therefore define real variables θ_m such that $\phi_m = i\theta_m$, and rewrite the recursion as

$$\sinh\theta_{m+1} = -\frac{v b_{m+1}}{\cosh\theta_m \cosh\theta_{m-1}}\,, \tag{3.84}$$

which has the same form as (3.29), but with hyperbolic functions replacing the trigonometric ones. Moreover, the g_m are now given by:

$$g_m = \cosh\frac{\theta_m}{2} + i h_m \sinh\frac{\theta_m}{2}\,. \tag{3.85}$$

These operators are still not unitary, since, using the fact that h_m is Hermitian, we have

$$g_m g_m^\dagger = g_m^\dagger g_m = \cosh^2\frac{\theta_m}{2} + \sinh^2\frac{\theta_m}{2} = \cosh\theta_m\,. \tag{3.86}$$

However, the required local unitaries can easily be obtained as:

$$u_m = \frac{g_m}{\sqrt{\cosh\theta_m}} = e^{i\varphi_m h_m}\,, \tag{3.87}$$

where

$$\tan\varphi_m = \tanh\frac{\theta_m}{2}\,. \tag{3.88}$$

We can therefore express a quantum circuit as a quantity proportional to the transfer matrix evaluated at a complex spectral parameter:

$$\mathcal{V} = \mathcal{G}\mathcal{G}^T = \frac{1}{\mathcal{F}} T(iv)\,, \tag{3.89}$$

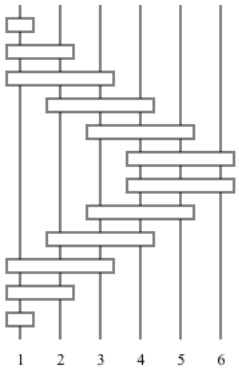

Figure 3.2: A diagram of circuit (3.89) using representation (3.12) with $M = L = 6$. Notice it has depth linear in the system size.

where $\mathcal{G} = u_1 u_2 \dots u_M$, with u_m defined as in (3.87), and

$$\mathcal{F} = \prod_{m=1}^{M} \cosh \theta_m \,. \tag{3.90}$$

In Figure 3.2, we provide a graphical representation of the circuit (3.89). This circuit is free fermionic by construction, since it is built from the transfer matrix of the FFD model (3.18). This property is also evident from the explicit expression of the transfer matrix eigenvalues (3.53), which can be used to write the eigenvalues of the quantum circuit as in (2.75). Specifically, we have:

$$\Lambda(iv) = \prod_{k=1}^{S} (1 \mp iv\varepsilon_k) = \mathcal{F} \prod_{k=1}^{S} \left(\frac{1}{\sqrt[S]{\mathcal{F}}} \pm i \frac{-v\varepsilon_k}{\sqrt[S]{\mathcal{F}}} \right) , \tag{3.91}$$

where the product on the right-hand side gives the eigenvalues of $\mathcal{V}$, since $T(iv)$ and $\mathcal{V}$ are proportional with factor $\mathcal{F}$. We can then impose:

$$\frac{1}{\sqrt[S]{\mathcal{F}}} = \cos \tilde{\epsilon}_k \,, \qquad\qquad -\frac{v\varepsilon_k}{\sqrt[S]{\mathcal{F}}} = \sin \tilde{\epsilon}_k \,, \tag{3.92}$$

which is equivalent to choosing $\tilde{\epsilon}_k$ such that $\tan \tilde{\epsilon}_k = -v\varepsilon_k$. This allows us to write the eigenvalues of $\mathcal{V}$ as

$$\prod_{k=1}^{S} e^{\pm i\tilde{\epsilon}_k} \,, \tag{3.93}$$

thereby proving that the circuit is free fermionic according to Definition (2.5).

3.4.2 Conjectured Free Fermionic Circuits

In [32], numerical methods were used to conjecture the free fermionicity of several other quantum circuits at different system sizes. The main focus was on circuits with a structure similar to Fendley's circuit (3.89), namely

$$\mathcal{V} = GG^T \,, \tag{3.94}$$

where G is a finite product of local unitaries of the form $e^{i\varphi_m h_m}$.

Circuits of the form (3.94) can be proven to be free fermionic for $M = 4$ [32]. Numerical results also indicate that they seem to be all free fermionic for system sizes $4 < M < 8$. However, for $M = 8$, it was found that the circuit with $G = u_1 u_4 u_3 u_5 u_6 u_8$ is not free fermionic.

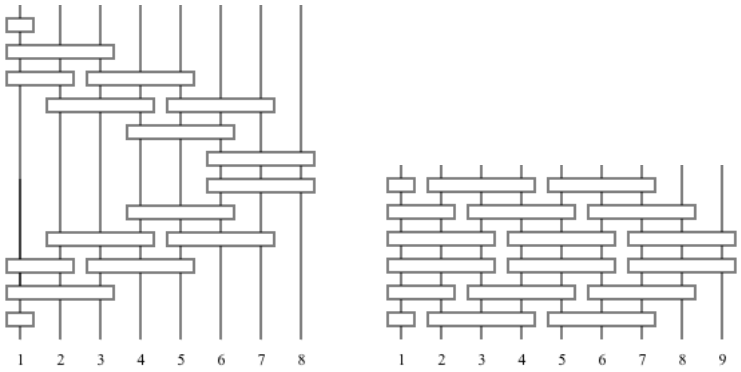

Figure 3.3: Diagrams of the circuits conjectured to be free fermionic in [32], using representation (3.12). On the left we have the circuit with G as in (3.95) with $M = L = 8$. On the right we have the circuit with G as in (3.96) with $M = L = 9$. Notice that the first one has depth linear in the system size, while the second has a constant depth of 6.

The most interesting conjectures in [32], concern two particular choices of G. First, for even M, we choose G as:

$$G = (u_1 u_3 \dots u_{M-1})(u_2 u_4 \dots u_M)\,, \tag{3.95}$$

whereas for M divisible by 3, we choose:

$$G = (u_1 u_4 \dots u_{M-2})(u_2 u_5 \dots u_{M-1})(u_3 u_6 \dots u_M)\,. \tag{3.96}$$

A graphical representation of these circuits is shown in Figure 3.3.

Both circuits were observed to be free fermionic for system sizes up to $M = 12$. Based on this numerical evidence, [32] conjectured that they remain free fermionic for arbitrary M.

The 2-periodic circuit in Eq. (3.95) was later proven to be free fermionic in [33]. However, the 3-periodic circuit in Eq. (3.96) is more interesting, as it appears to have constant depth. In the representation (3.12), its depth is 6, as shown in Figure 3.3. In [36], we provided a proof valid for both circuits, as well as for the circuit (3.89), which relies on an MPO structure. We will discuss this in Chapter 4.

Chapter 4

New results on Free Fermion in Disguise

In Chapter 3, we provided an overview of previously known results on the Free Fermions in Disguise models first introduced in [28]. In this Chapter, we focus on the new results obtained in [36], together with some preliminary work carried out for this thesis.

In [36], we introduced a method to analytically prove the free fermionicity of slightly modified versions of the circuits conjectured to be free fermionic in [32], reported in Eqs. (3.89), (3.95), and (3.96), and shown in Figures 3.2 and 3.3. This method relies on rewriting the quantum circuits as matrix product operators (MPOs) [64] and embedding them into a family of mutually commuting transfer matrices. Furthermore, we also studied the simulability of these quantum circuits, showing that the discrete dynamics of certain local observables that can be written in terms of fermionic operators can be efficiently simulated on a classical computer.

In Section 4.1, we present the proof of the free fermionicity (or FFD solvability) of the quantum circuits introduced in [32]. We then continue in Section 4.2 with a study of the dynamics of local observables expressible in terms of fermions. In particular, we perform numerical simulations for small system sizes of the edge operator, comparing its evolution in the spin representation with that in the fermionic one. This constitutes the original contribution of this thesis. Finally, in Subsection 4.2.1, we report results of [36] concerning the classical simulability of these quantum circuits.

4.1 Proof of Free Fermionicity of conjectured quantum circuits

In this section, we prove analytically the free fermionicity of some circuits similar to the one introduced in Eqs. (3.89), (3.95), and (3.96). In this Chapter, however, we fully depart from the Hamiltonian formulation discussed in Chapter 3 and instead begin directly from quantum gates defined as follows:

$$g_m = \cos\frac{\phi_m}{2} + i \sin\frac{\phi_m}{2} h_m \,, \tag{4.1}$$

where the operators h_m satisfy the FFD algebra (3.9). In this setting, the angles ϕ_m are no longer defined through the recursion relation (3.29): they are real parameters that control the spatial inhomogeneity of the circuit as the coefficients b_m were doing for the Hamiltonian model of (3.10). For (3.89), these angles can be explicitely related to the b_m of (3.10).

The g_m defined as in Eq. (4.1), satisfy some slightly different properties than the one given in Eq. (3.30), due to the presence of the factor i in the second term. We have the following:

$$\begin{aligned} (g_m)^2 &= x_m + i y_m h_m \,, \\ g_m h_{m\pm a} g_m &= h_{m\pm a} \qquad a = 1, 2 \,, \end{aligned} \tag{4.2}$$

where $x_m = \cos\phi_m$ and $y_m = \sin\phi_m$. These can be derived straightforwardly from the FFD algebra (3.9).

Let us now introduce the family of circuits that we will prove to be free fermionic. The first family is defined as:

$$\mathcal{V}_M^{(\mathrm{I})} = G_M G_M^T \,, \qquad G_M = g_1 g_2 \dots g_M \,. \tag{4.3}$$

This corresponds exactly to the circuit introduced in Eq. (3.89), which we have already shown to be free fermionic in Section 3.4, following [32].

The second family of circuits is defined for even values of M as:

$$\mathcal{V}_M^{(\mathrm{II})} = G_M G_M^T \,, \qquad G_M = (g_2 g_4 \dots g_M)(g_1 g_3 \dots g_{M-1}) \,. \tag{4.4}$$

These circuits correspond to the one of Eq. (3.95) after applying a mirror symmetry, or equivalently, relabelling the sites $1, 2, \dots, M \to M, M-1, \dots, 1$. This circuit was shown to be free fermionic also in [33] using an alternative method, which we will not explore here.

The third family of circuits is defined for M divisible by 3, and is obtained from (3.96) after applying, once again, a mirror symmetry:

$$\mathcal{V}_M^{(\mathrm{III})} = G_M G_M^T \,, \qquad G_M = (g_3 g_6 \dots g_M)(g_2 g_5 \dots g_{M-1})(g_1 g_4 \dots g_{M-2}) \,. \tag{4.5}$$

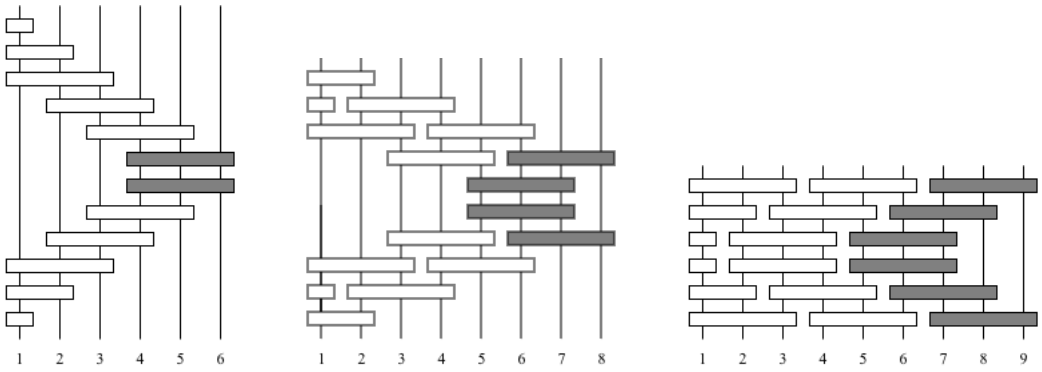

Figure 4.1: Diagrams of circuits (from left to right) I, II, and III corresponding to Eqs. (4.3), (4.4), and (4.5), respectively, using the representation of Eq. (3.12). Each rectangle represents a gate g_m as defined in Eq. (4.1). Note that, according to the representation (3.12), the gates g_1 and g_2 act only on one and two qubits, respectively. The rightmost gates are highlighted in gray as a guide for the reader through the solution of the circuits: these are the gates that must be evaluated to determine the recursion relations. This picture was inspired by Figure 1 of [36].

We provide a graphical representation of the circuits in Figure 4.1. We emphasize once again that the circuit in Eq. (4.5) is the only one with finite depth (depth 6), and therefore its application requires a time that does not depend on the system size, since gates acting on disjoint sets of qubits can be applied simultaneously.

We now proceed with the solution of these circuits. To prove their free fermionicity, we embed the corresponding evolution operators into a family of commuting transfer matrices, from which we will define fermionic creation and annihilation operators. We first illustrate the method in the simpler and already well-understood case of Circuit I (4.3), and then apply the same approach to the remaining two circuits.

4.1.1 Solution of Circuit I

For all three circuits the method is the same: we start by evaluating the rightmost pairs of gates, highlighted in gray in Figure 4.1. This produces terms proportional to the identity and terms proportional to some of the operators h_m, specifically $m = M$ for circuit I, $m = M-1, M$ for circuit II and $m = M-2, M-1, M$ for circuit III. When we proceed to evaluate the next product of gates, it follows directly from the FFD algebra (3.9) and the properties (4.2) that the product of two g_m depends only on whether h_{m+1} and/or h_{m+2} are present. It is therefore convenient to introduce the following four families of operators:

$$A_m = G_m G_m^T \,, \tag{4.6}$$
$$B_m = i\, G_m h_{m+1} G_m^T \,, \tag{4.7}$$
$$C_m = i\, G_m h_{m+2} G_m^T \,, \tag{4.8}$$
$$D_m = G_m h_{m+1} h_{m+2} G_m^T \,. \tag{4.9}$$

Evaluating the product of the rightmost gray gates in Figure 4.1 then yields recursion relations among these operators, with each family coupling to the others.

Let us illustrate this more explicitly with the first circuit. We begin by evaluating the product $(g_M)^2$ using (4.2), which is expressed as a sum of a term proportional to the identity and a term proportional to h_M. From the first term, we can similarly evaluate $(g_{M-1})^2$, while the second term, $g_{M-1} h_M g_{M-1}$, can be evaluated using the second line of (4.2). In general, performing this procedure for each of the operators defined in Eqs. (4.6)-(4.9) yields the following recursion relations:

$$A_m = x_m A_{m-1} + y_m B_{m-1} \,, \tag{4.10}$$
$$B_m = C_{m-1} \,, \tag{4.11}$$
$$C_m = i\, A_{m-1} h_{m+2} \,, \tag{4.12}$$
$$D_m = (x_m + i y_m h_{m+2}) D_{m-1} \,, \tag{4.13}$$

with initial conditions $A_0 = 1$, $B_0 = i h_1$, $C_0 = i h_2$, $D_0 = h_1 h_2$. Notice that the recursion for D_m is completely independent of the others, and can therefore be ignored when analyzing the first circuit.

The next step is to use the recursion relations (4.10)–(4.12) to express the circuit $\mathcal{V}_M^{(I)}$ as a *matrix product operator* (MPO). This means writing the operator as a product of matrices acting on an auxiliary space[1]. Here, the auxiliary space is three-dimensional, with basis states denoted as $|a\rangle, |b\rangle, |c\rangle$ corresponding to the operators defined above. We can then write

$$\mathcal{V}_M^{(\mathrm{I})} = (1\ 1\ 1)\ \Omega_1 \Omega_2 \dots \Omega_M\ |a\rangle \,, \tag{4.14}$$

where the matrices Ω_m, which encode the recursion relations, are given by

$$\Omega_m = \begin{pmatrix} x_m & 0 & 1 \\ i y_m h_m & 0 & 0 \\ 0 & 1 & 0 \end{pmatrix} . \tag{4.15}$$

Finally, we need to construct a family of commuting transfer matrices. To this end, we introduce a spectral parameter u and we attach a factor u to each h_m appearing in the MPO. The goal is to recover a transfer matrix analogous to the one defined in [28] and given in Eq. (3.18), where the k-th charge, which involves the product of k Hamiltonian densities h_m, is multiplied by u^k. With this prescription, we obtain

[1] See [64] for more details on MPO.

the same structure. In particular, the matrices Ω_m are promoted to:

$$\Omega_m(u) = \begin{pmatrix} x_m & 0 & 1 \\ iuy_m h_m & 0 & 0 \\ 0 & 1 & 0 \end{pmatrix}, \tag{4.16}$$

and the operators A, B, C to:

$$A_m(u) = (1\ 1\ 1)\ \Omega_1(u)\Omega_2(u)\dots\Omega_m(u)\,|a\rangle\,, \tag{4.17}$$
$$B_m(u) = (1\ 1\ 1)\ \Omega_1(u)\Omega_2(u)\dots\Omega_m(u)\,|b\rangle\,iuh_{m+1}\,, \tag{4.18}$$
$$C_m(u) = (1\ 1\ 1)\ \Omega_1(u)\Omega_2(u)\dots\Omega_m(u)\,|c\rangle\,iuh_{m+2}\,, \tag{4.19}$$

Finally, the recursion relations get the following form, with initial conditions $A_0(u) = 1$, $B_0(u) = iuh_1$, $C_0(u) = iuh_2$:

$$A_m(u) = x_m A_{m-1}(u) + y_m B_{m-1}(u)\,, \tag{4.20}$$
$$B_m(u) = C_{m-1}(u)\,, \tag{4.21}$$
$$C_m(u) = iuA_{m-1}(u)h_{m+2}\,. \tag{4.22}$$

We can use this new recursion relations (4.20), (4.21) and (4.22) to prove the following commutation relations for the operators A, B, C:

$$\begin{aligned} &[A_m(u), A_m(v)] = [B_m(u), B_m(v)] = [C_m(u), C_m(v)] = 0\,,\\ &[A_m(u), B_m(v)] + [B_m(u), A_m(v)] = 0\,,\\ &[A_m(u), C_m(v)] + [C_m(u), A_m(v)] = 0\,,\\ &[B_m(u), C_m(v)] + [C_m(u), B_m(v)] = 0\,,\\ &u\{A_m(u), B_m(v)\} = v\{B_m(u), A_m(v)\}\,,\\ &u\{A_m(u), C_m(v)\} = v\{C_m(u), A_m(v)\}\,. \end{aligned} \tag{4.23}$$

From this construction, it is evident that we obtain the desired family of commuting transfer matrices, denoted $A_M(u)$, from which Circuit I can be recovered as $\mathcal{V}_M^{(I)} = A_M(1)$.

Remark 4.1. Note that $A_M(u)$ is not exactly the same as Fendley's transfer matrix (3.18). This difference arises from the normalization factor[2] $\mathcal{F}_M$ of Eq. (3.90), which we should try to express in terms of our new parameters. The angles ϕ_m in the gates g_m of Eq (4.1) can be related to the angles θ_m in Eq. (3.87) via $\tanh(\theta_m/2) = \tan(\phi_m/2)$. Using the parametric formulas for the hyperbolic and standard cosines, we then obtain:

$$\cosh\theta_m = \frac{1+\tanh^2(\theta_m/2)}{1-\tanh^2(\theta_m/2)} = \frac{1+\tan^2(\phi_m/2)}{1-\tan^2(\phi_m/2)} = \frac{1}{\cos\phi_m} = x_m^{-1}\,. \tag{4.24}$$

Thus, the normalization factor can be expressed as

$$\mathcal{F}_M = \prod_{m=1}^{M} x_m^{-1}\,. \tag{4.25}$$

To recover a Hermitian transfer matrix, as in Eq. (3.18), we must choose a purely imaginary spectral parameter. This leads to

$$T_M(u) = \mathcal{F}_M A_M(iu)\,. \tag{4.26}$$

[2]We add a subscript M to emphasize the dependence of $\mathcal{F}$ from the system size.

Furthermore, the recursions (4.20)–(4.22) can be combined to yield

$$A_m(u) = x_m A_{m-1}(u) + iuy_m h_m A_{m-3}(u)\,, \tag{4.27}$$

which, by setting $m = M$, substituting $u \to iu$ and multiplying by the normalization factor $\mathcal{F}_M$, becomes

$$T_M(u) = T_{M-1}(u) - u\frac{y_M}{x_{M-2}x_{M-1}x_M} h_M T_{M-3}(u)\,. \tag{4.28}$$

This exactly reproduces the recursion relation in Eq. (3.20), with the identification

$$b_m = \frac{y_m}{x_{m-2}x_{m-1}x_m}\,. \tag{4.29}$$

Let us now construct the fermionic operators. To do so, we first define a polynomial analogous to that in Eq. (3.35) and determine its zeros. To this end, we introduce the operators

$$\mathcal{A}_m(u) = A_m(u)A_m(-u)\,, \tag{4.30}$$

and similarly for $\mathcal{B}(u)$, $\mathcal{C}(u)$, $\mathcal{D}(u)$. These operators can be shown to be proportional to the identity and can therefore be treated as scalar polynomials. They satisfy the following recursion relations:

$$\mathcal{A}_m(u) = x_m^2 \mathcal{A}_{m-1}(u) + y_m^2 \mathcal{B}_{m-1}(u)\,, \tag{4.31}$$
$$\mathcal{B}_m(u) = \mathcal{C}_{m-1}(u)\,, \tag{4.32}$$
$$\mathcal{C}_m(u) = u^2 \mathcal{A}_{m-1}(u)\,, \tag{4.33}$$

which can be derived from the recursion relations for the operators (4.20)-(4.22) and the algebra (4.23). With the initial conditions

$$\mathcal{A}_0(u) = 1\,, \qquad \mathcal{B}_0(u) = \mathcal{C}_0(u) = u^2\,, \tag{4.34}$$

it is clear that all these operators are proportional to the identity. Note also that the recursions above can be rewritten as $\mathcal{A}_m(u) = x_m^2 \mathcal{A}_{m-1}(u) + u^2 y_m^2 \mathcal{A}_{m-3}(u)$, which can be cast into the form of Eq. (3.35) in the same way as (4.27) led to Eq. (4.28).

The polynomial $\mathcal{A}_M(u)$, is a polynomial in u^2 of degree $S = \lfloor (M+2)/3 \rfloor$. It has purely imaginary roots, which we label as $\{\pm iu_k\}$, with $k = 1, 2, \ldots, S$.

We can define fermionic creation and annihilation operators by adapting Eq. (3.37) to this setting:

$$\Psi_{\pm k} = \frac{1}{N_k} A_M(\mp iu_k)\chi A_M(\pm iu_k)\,, \qquad k = 1, 2, \ldots, S\,, \tag{4.35}$$

where χ is the edge operator defined by the properties Eq. (3.36). The normalization must also be adapted from Eq. (3.51) to

$$N_k^2 = -8iu_k x_M^2 \mathcal{A}_{M-1}(iu_k)\mathcal{A}'_M(iu_k)\,. \tag{4.36}$$

These operators can be shown to satisfy the canonical anticommutation relations (1.50), in a way analogous to the proof presented for the original FFD models in Section 3.2.

We can also adapt Eq. (3.52) to the circuit case, writing

$$A_M(u) = \prod_{k=1}^{S} \frac{iu_k + u[\Psi_k, \Psi_{-k}]}{\sqrt{1+u_k^2}}\,. \tag{4.37}$$

From this expression, the evolution operator can be recovered by setting $u = 1$. Then, defining the pseudoenergies as

$$\epsilon_k = \arctan\frac{1}{u_k}\,, \tag{4.38}$$

the circuit can be rewritten in the free fermionic form

$$\mathcal{V}_M^{(\mathrm{I})} = \exp\left(-i\sum_{k=1}^{S}\epsilon_k[\Psi_k,\Psi_{-k}]\right), \tag{4.39}$$

thereby proving its free fermionicity.

4.1.2 Solution of Circuits II and III

We now turn to the solution of circuits II and III, following exactly the same method as for circuit I.

The first step consists of evaluating the rightmost gray gates in Figure 4.1 to determine the recursion relations for the operators (4.6)–(4.9). For circuit II, we obtain

$$A_m = x_{m-1}x_mA_{m-2} + y_{m-1}B_{m-2} + x_{m-1}y_mC_{m-2}\,, \tag{4.40}$$
$$B_m = iA_{m-2}h_{m+1}\,, \tag{4.41}$$
$$C_m = i(x_{m-1}A_{m-2} + y_{m-1}x_mB_{m-2} + y_{m-1}y_mD_{m-2})h_{m+2}\,, \tag{4.42}$$
$$D_m = (x_mA_{m-2} + y_mC_{m-2})h_{m+1}h_{m+2}\,, \tag{4.43}$$

whereas for circuit III we have

$$A_m = x_{m-2}x_{m-1}A_{m-3}\kappa_m^+ + y_{m-2}B_{m-3} + x_{m-2}y_{m-1}C_{m-3}\,, \tag{4.44}$$
$$B_m = i[x_{m-2}A_{m-3} + y_{m-2}x_{m-1}B_{m-3}\kappa_m^- + y_{m-2}y_{m-1}D_{m-3}]h_{m+1}\,, \tag{4.45}$$
$$C_m = i[x_{m-1}x_{m-2}A_{m-3}+(y_{m-2}B_{m-3} + x_{m-2}y_{m-1}C_{m-3})\kappa_m^-]h_{m+2}\,, \tag{4.46}$$
$$D_m = [(x_{m-2}A_{m-3}+y_{m-2}y_{m-1}D_{m-3})\kappa_m^+ + y_{m-2}x_{m-1}B_{m-3}]h_{m+1}h_{m+2}. \tag{4.47}$$

where we defined $\kappa_m^\pm = x_m \pm iy_mh_m$.

We see that for these two circuits the operator D_m enters the recursion and cannot be ignored as in circuit I. Consequently, the MPO representation now requires a four-dimensional auxiliary space, with basis states denoted as $\{|a\rangle, |b\rangle, |c\rangle, |d\rangle\}$. The circuits can then be written as

$$\mathcal{V}_M^{(\mathrm{II})} = (1\ 1\ 1\ 1)\ \Omega_1^{(\mathrm{II})}\Omega_3^{(\mathrm{II})}\ldots\Omega_{M-1}^{(\mathrm{II})}\,|a\rangle\,, \tag{4.48}$$
$$\mathcal{V}_M^{(\mathrm{III})} = (1\ 1\ 1\ 1)\ \Omega_1^{(\mathrm{III})}\Omega_4^{(\mathrm{III})}\ldots\Omega_{M-2}^{(\mathrm{III})}\,|a\rangle\,, \tag{4.49}$$

where the local matrices Ω_m are given by

$$\Omega_m^{(\mathrm{II})} = \Theta_m\cdot\begin{pmatrix} x_mx_{m+1} & 1 & x_m & x_{m+1} \\ 1 & 0 & x_{m+1} & 0 \\ x_m & 0 & 0 & 1 \\ 0 & 0 & 1 & 0 \end{pmatrix}, \tag{4.50}$$

$$\Omega_m^{(\mathrm{III})} = \Theta_m\cdot\begin{pmatrix} \kappa_{m+2}^+x_mx_{m+1} & x_m & x_mx_{m+1} & x_m\kappa_{m+2}^+ \\ 1 & \kappa_{m+2}^-x_{m+1} & \kappa_{m+2}^- & x_{m+1} \\ x_m & 0 & \kappa_{m+2}^-x_m & 0 \\ 0 & 1 & 0 & \kappa_{m+2}^+ \end{pmatrix}, \tag{4.51}$$

with $\Theta_m = \mathrm{diag}(1, iy_mh_m, iy_{m+1}h_{m+1}, y_my_{m+1}h_mh_{m+1})$.

As for circuit I, we now attempt to lift the MPOs (4.48) and (4.49) to families of commuting transfer matrices. In this case, however, it is not sufficient to simply multiply a spectral parameter u in front of each of the Hamiltonian densities $\{h_m\}$ in the matrices (4.50) and (4.51). Doing so leads to an incorrect result.

Instead, one must multiply a factor of u only to the linear and trilinear terms in h_m inside the Ω_m, while leaving the bilinear terms unchanged. This yields the following u-dependent matrices

$$\Omega_m^{(\mathrm{II})}(u) = \Theta_m \cdot \begin{pmatrix} x_m x_{m+1} & 1 & x_m & x_{m+1} \\ u & 0 & u x_{m+1} & 0 \\ u x_m & 0 & 0 & u \\ 0 & 0 & 1 & 0 \end{pmatrix}, \tag{4.52}$$

$$\Omega_m^{(\mathrm{III})}(u) = \Theta_m \cdot \begin{pmatrix} \kappa_{m+2}^+(u) x_m x_{m+1} & x_m & x_m x_{m+1} & x_m \kappa_{m+2}^+(u) \\ u & \kappa_{m+2}^-(u) x_{m+1} & \kappa_{m+2}^-(u) & u x_{m+1} \\ u x_m & 0 & \kappa_{m+2}^-(u) x_m & 0 \\ 0 & 1 & 0 & \kappa_{m+2}^+(u) \end{pmatrix}, \tag{4.53}$$

where for circuit III we defined:

$$\kappa_m^+(u) = x_m + iu y_m h_m \,, \tag{4.54}$$

$$\kappa_m^-(u) = u x_m - i y_m h_m \,. \tag{4.55}$$

We can now construct the operators A, B, C, D of Eqs (4.6)-(4.9) in terms of the MPOs as follows. For circuit II:

$$A_m(u) = (1\ 1\ 1\ 1)\ \Omega_1^{(\mathrm{II})}(u)\Omega_3^{(\mathrm{II})}(u)\dots\Omega_m^{(\mathrm{II})}(u)\,|a\rangle \,, \tag{4.56}$$

$$B_m(u) = (1\ 1\ 1\ 1)\ \Omega_1^{(\mathrm{II})}(u)\Omega_3^{(\mathrm{II})}(u)\dots\Omega_m^{(\mathrm{II})}(u)\,|b\rangle\, iuh_{m+1} \,, \tag{4.57}$$

$$C_m(u) = (1\ 1\ 1\ 1)\ \Omega_1^{(\mathrm{II})}(u)\Omega_3^{(\mathrm{II})}(u)\dots\Omega_m^{(\mathrm{II})}(u)\,|c\rangle\, iuh_{m+2} \,, \tag{4.58}$$

$$D_m(u) = (1\ 1\ 1\ 1)\ \Omega_1^{(\mathrm{II})}(u)\Omega_3^{(\mathrm{II})}(u)\dots\Omega_m^{(\mathrm{II})}(u)\,|d\rangle\, h_{m+1}h_{m+2} \,, \tag{4.59}$$

while for circuit III, we have:

$$A_m(u) = (1\ 1\ 1\ 1)\ \Omega_1^{(\mathrm{III})}(u)\Omega_4^{(\mathrm{III})}(u)\dots\Omega_m^{(\mathrm{III})}(u)\,|a\rangle \,, \tag{4.60}$$

$$B_m(u) = (1\ 1\ 1\ 1)\ \Omega_1^{(\mathrm{III})}(u)\Omega_4^{(\mathrm{III})}(u)\dots\Omega_m^{(\mathrm{III})}(u)\,|b\rangle\, iuh_{m+1} \,, \tag{4.61}$$

$$C_m(u) = (1\ 1\ 1\ 1)\ \Omega_1^{(\mathrm{III})}(u)\Omega_4^{(\mathrm{III})}(u)\dots\Omega_m^{(\mathrm{III})}(u)\,|c\rangle\, iuh_{m+2} \,, \tag{4.62}$$

$$D_m(u) = (1\ 1\ 1\ 1)\ \Omega_1^{(\mathrm{III})}(u)\Omega_4^{(\mathrm{III})}(u)\dots\Omega_m^{(\mathrm{III})}(u)\,|d\rangle\, h_{m+1}h_{m+2} \,. \tag{4.63}$$

From these MPO expressions, the recursion relations follow directly. For circuit II:

$$A_m(u) = x_m x_{m-1} A_{m-2}(u) + y_{m-1} B_{m-2}(u) + x_{m-1} y_m C_{m-2}(u) \,, \tag{4.64}$$

$$B_m(u) = iu A_{m-2}(u) h_{m+1} \,, \tag{4.65}$$

$$C_m(u) = iu(x_{m-1} A_{m-2}(u) + x_m y_{m-1} B_{m-2}(u) + y_{m-1} y_m D_{m-2}(u)) h_{m+2} \,, \tag{4.66}$$

$$D_m(u) = (x_m A_{m-2}(u) + y_m C_{m-2}(u)) h_{m+1} h_{m+2} \,, \tag{4.67}$$

whereas for circuit III.

$$A_m(u) = x_{m-1} x_{m-2} A_{m-3}(u) \kappa_m^+(u) + y_{m-2} B_{m-3}(u) + x_{m-2} y_{m-1} C_{m-3}(u) \,, \tag{4.68}$$

$$B_m(u) = i[u x_{m-2} A_{m-3}(u) + x_{m-1} y_{m-2} B_{m-3}(u) \kappa_m^-(u) + u y_{m-2} y_{m-1} D_{m-3}(u)] h_{m+1} \,, \tag{4.69}$$

$$C_m(u) = i[u x_{m-1} x_{m-2} A_{m-3}(u) + (y_{m-2} B_{m-3}(u) + x_{m-2} y_{m-1} C_{m-3}(u)) \kappa_m^-(u)] h_{m+2} \,, \tag{4.70}$$

$$D_m(u) = [(x_{m-2} A_{m-3}(u) + y_{m-1} y_{m-2} D_{m-3}(u)) \kappa_m^+(u) + y_{m-2} x_{m-1} B_{m-3}(u)] h_{m+1} h_{m+2} \,, \tag{4.71}$$

The algebra (4.23) continues to hold. Additionally, there are relations involving the D operators given by:

$$\begin{aligned}&[D_m(u), D_m(v)] = 0\,,\\ &\{A_m(u), D_m(v)\} = \{D_m(u), A_m(v)\}\,,\end{aligned} \tag{4.72}$$

which can again be proven using the recursion relations above.

Once the embedding into a family of transfer matrices is established, we can proceed in the same way as for circuit I by defining the polynomials $\mathcal{A}$, $\mathcal{B}$, $\mathcal{C}$, $\mathcal{D}$ and deriving their recursion relations from those of the operators A, B, C, D. For circuit II, the recursions read:

$$\mathcal{A}_m(u) = x_{m-1}^2 x_m^2 \mathcal{A}_{m-2}(u) + y_{m-1}^2 \mathcal{B}_{m-2}(u) + x_{m-1}^2 y_m^2 \mathcal{C}_{m-2}(u)\,, \tag{4.73}$$

$$\mathcal{B}_m(u) = u^2 \mathcal{A}_{m-2}(u)\,, \tag{4.74}$$

$$\mathcal{C}_m(u) = u^2 \left(x_{m-1}^2 \mathcal{A}_{m-2}(u) + x_m^2 y_{m-1}^2 \mathcal{B}_{m-2}(u) - y_m^2 y_{m-1}^2 \mathcal{D}_{m-2}(u)\right)\,, \tag{4.75}$$

$$\mathcal{D}_m(u) = -x_m^2 \mathcal{A}_{m-2}(u) - y_m^2 \mathcal{C}_{m-2}(u)\,, \tag{4.76}$$

whereas for circuit III:

$$\mathcal{A}_m(u) = x_{m-2}^2 x_{m-1}^2 (x_m^2 + u^2 y_m^2) \mathcal{A}_{m-3}(u) + y_{m-2}^2 \mathcal{B}_{m-3}(u) + x_{m-2}^2 y_{m-1}^2 \mathcal{C}_{m-3}(u)\,, \tag{4.77}$$

$$\mathcal{B}_m(u) = u^2 x_{m-2}^2 \mathcal{A}_{m-3}(u) + y_{m-2}^2 x_{m-1}^2 (u^2 x_m^2 + y_m^2) \mathcal{B}_{m-3}(u) - u^2 y_{m-1}^2 y_{m-2}^2 \mathcal{D}_{m-3}(u)\,, \tag{4.78}$$

$$\mathcal{C}_m(u) = u^2 x_{m-2}^2 x_{m-1}^2 \mathcal{A}_{m-3}(u) + \left(y_{m-2}^2 \mathcal{B}_{m-3}(u) + x_{m-2}^2 y_{m-1}^2 \mathcal{C}_{m-3}(u)\right)(u^2 x_m^2 + y_m^2)\,, \tag{4.79}$$

$$\mathcal{D}_m(u) = (-x_{m-2}^2 \mathcal{A}_{m-3}(u) + y_{m-2}^2 y_{m-1}^2 \mathcal{D}_{m-3}(u))(x_m^2 + u^2 y_m^2) - y_{m-2}^2 x_{m-1}^2 \mathcal{B}_{m-3}(u)\,. \tag{4.80}$$

Here, $\mathcal{A}_m(u)$ remains a polynomial of degree $S = \lfloor (M+2)/3 \rfloor$ in u^2 and possesses purely imaginary roots, which we denote as $\{\pm i u_k\}_{k=1}^S$. These roots can once again be used to define the fermionic operators satisfying canonical anticommutation relations as in Eq. (4.35). The corresponding normalization constants are given by (see [36]):

$$(N_k^{(\mathrm{II})})^2 = -8 i u_k (x_M x_{M-1})^2 \mathcal{A}_{M-2}(i u_k) \mathcal{A}'_M(i u_k)\,, \tag{4.81}$$

$$(N_k^{(\mathrm{III})})^2 = 8 i u_k (i u_k x_{M-2} x_{M-1} y_M)^2 \mathcal{A}_{M-3}(i u_k) \mathcal{A}'_M(i u_k)\,. \tag{4.82}$$

For circuit II, however, it is necessary to slightly modify the defining properties of the edge operator as follows:

$$\begin{aligned}&\chi^2 = 1\,,\\ &[h_m, \chi] = 0\,, \qquad m = 1, 2, \dots M-2\\ &\{h_{M-1}, \chi\} = \{h_M, \chi\} = 0\,.\end{aligned} \tag{4.83}$$

In the representation of Eq. (3.12), one possible choice is $\chi = Z_{M-1} Z_M$.

We observe that it is possible to define free fermionic operators starting from the transfer matrices for all three circuits. Furthermore, Eq. (4.37) could, in principle, be proven for circuits II and III as well. However, such a proof would require the explicit construction of conserved charges from the transfer matrix, which can become cumbersome. Therefore, the formula has been instead verified numerically for many values of u and for system sizes up to $M = 12$.

Once Eq. (4.37) is established, one can follow the same procedure as for circuit I to express the circuits in the form of Eq. (4.39), thereby demonstrating their free fermionic nature.

4.2 Circuit Dynamics of Fermionic Local Observables

In the previous section, we showed that all three circuits in Eqs. (4.3), (4.4), and (4.5) have a free fermionic spectrum, as defined in Definition 2.5. We now turn to the study of the time evolution generated by these quantum circuits. In particular, as discussed in detail in Chapter 2, free fermionic systems are often classically simulable, especially JW-diagonalizable models. For FFD models, however, the situation is less clear.

To investigate this, we consider a simple protocol in which the system is initialized in a product state and we focus on the dynamics of local observables. This setup is analogous to a quantum-quench problem in the Hamiltonian framework [54], where one studies the out-of-equilibrium evolution of a many-body system under a Hamiltonian, starting from the ground state of a different Hamiltonian. The protocol is also experimentally motivated, as current quantum-simulator platforms are typically initialized in unentangled states and evolved through the application of local gates [65].

In JW-diagonalizable models, spin product states can be straightforwardly mapped to fermionic Gaussian states, making the dynamics analytically tractable and classically simulable. In FFD models, however, the situation is more involved. As discussed in Section 3.3, the correspondence between spin and fermionic states is considerably more complicated, and no clear strategy exists for selecting "simple" initial spin states. Similarly, the choice of observables is nontrivial, since the inverse problem remains unsolved for generic local operators. Nevertheless, we focus on the edge operator, which, as shown in Section 3.3, can be expressed as a linear combination of fermionic modes as in Eq. (3.54), at least in the Hamiltonian setting.

In this section, we present original results that are preliminary to [36]. We first analytically determine the time-evolved fermionic operators under the action of the circuits. We then adapt the expression of the edge operator in terms of fermions, originally derived in the Hamiltonian framework, to the circuit setting. Finally, we compare the resulting dynamics of the edge operator with those obtained from a direct application of the quantum circuit. This procedure serves as a verification analogous to an exact-diagonalization check, confirming the validity of the fermionic description. Our analysis is carried out for all three circuits, with the corresponding plots shown in Figures 4.2, 4.3, and 4.4 for circuits I, II, and III, respectively.

Let us first provide the expression for the time-evolved fermionic operators. To this end, we use an adaptation of Eq. (3.45) to the case of the circuits, which reads:

$$(iu_k - u)A_M(u)\Psi_k = (iu_k + u)\Psi_k A_M(u)\,. \tag{4.84}$$

This relation holds for all the three circuits and can be proven using the recursion relations and the algebra (4.23) (see Appendix A of [36]). By choosing $u = 1$, we get the quantum circuit from the A operator, obtaining:

$$(iu_k - 1)\mathcal{V}_M\Psi_k = (iu_k + 1)\Psi_k\mathcal{V}_M\,. \tag{4.85}$$

Multiplying on the left by $\mathcal{V}_M^\dagger$ and dividing both sides by $(iu_k + 1)$, yields an analytical expression for the fermionic operator after a single application of the circuit:

$$\mathcal{V}_M^\dagger\Psi_k\mathcal{V}_M = \frac{iu_k - 1}{iu_k + 1}\,\Psi_k\,. \tag{4.86}$$

Therefore, at a generic time $t \in \mathbb{N}$, the time evolved operator is given by:

$$\Psi_k(t) := (\mathcal{V}_M^\dagger)^t\Psi_k\mathcal{V}_M^t = \left(\frac{iu_k - 1}{iu_k + 1}\right)^t\Psi_k\,. \tag{4.87}$$

We now adapt the derivation of Section 3.3 for the expression of the edge operator in terms of fermionic operators to all three circuits. To this end, we start from the operator-valued function of Eq. (3.58), but

replacing T_M with A_M and P_M with $\mathcal{A}_M$. For the circuits, however, the zeros of the polynomials are purely imaginary, and in order to still utilize the contour of Figure 3.1, we consider the variable $v = iu$. This yields:

$$\phi_M(v) = -\frac{1}{v}\left(\frac{\mathcal{A}_M(v)\chi + A_M(-v)\chi A_M(v)}{2\mathcal{A}_M(v)}\right) \equiv -\frac{1}{iu}\left(\frac{\mathcal{A}_M(iu)\chi + A_M(-iu)\chi A_M(iu)}{2\mathcal{A}_M(iu)}\right). \tag{4.88}$$

The remaining steps of the calculation proceed as before. The only difference is that the final expressions now involve iu rather than u. For instance, the coefficients of the expansion are given by:

$$c_l = c_{-l} = \frac{N_l}{-2iu_l\mathcal{A}'_M(iu_l)}, \tag{4.89}$$

while the residue at infinity reads:

$$\mathcal{Q} = \lim_{u\to\infty}\frac{1}{2}\left(\chi + \frac{A_M(-iu)\chi A_M(iu)}{\mathcal{A}_M(iu)}\right) \equiv \lim_{u\to\infty}\mathcal{Q}_u\,. \tag{4.90}$$

This construction applies to all three circuits, and thus for all of them the edge mode can be written as

$$\chi = \sum_{l=-S,\,l\neq 0}^{S} c_l\Psi_l + \mathcal{Q}\,. \tag{4.91}$$

The completeness of this decomposition has also been numerically verified for system sizes up to $M = 12$ for all three circuits.

Let us now analyze $\mathcal{Q}$ for the various circuit to determine whether it is proportional to a Majorana zero mode, which should satisfy the following properties:

$$\begin{aligned}&(\Psi_0)^2 = \mathbb{1}\,,\\ &[\mathcal{V}_M, \Psi_0] = 0\,,\\ &\{\Psi_0, \Psi_{\pm k}\} = 0\,,\end{aligned} \tag{4.92}$$

where we have replaced $[H, \Psi_0] = 0$ from (3.56) with $[\mathcal{V}_M, \Psi_0] = 0$, since now we have a circuit evolution and not a continuous one generated by the Hamiltonian.

To prove the first property, we begin by computing $\mathcal{Q}_u^2$. If this operator is proportional to the identity, we can then easily define an operator that squares to the identity. For all three circuits, we have:

$$\mathcal{Q}_u^2 = \frac{1}{4}\left(2 + \frac{1}{\mathcal{A}_M(iu)}\{\chi, A_M(-iu)\chi A_M(iu)\}\right). \tag{4.93}$$

If the anticommutator $\{\chi, A_M(-v)\chi A_M(v)\}$ is known, we can clearly determine the above expression by setting $v = iu$ and then taking the limit $u \to \infty$. We show in Appendix B that for circuit I we have:

$$\{\chi, A_M(-v)\chi A_M(v)\} = -2\mathcal{A}_M(v) + 4x_M^2\mathcal{A}_{M-1}(v)\,, \tag{4.94}$$

for circuit II

$$\{\chi, A_M(-v)\chi A_M(v)\} = -2\mathcal{A}_M(v) + 4(x_M x_{M-1})^2\mathcal{A}_{M-2}(v)\,, \tag{4.95}$$

and for circuit III

$$\{\chi, A_M(-v)\chi A_M(v)\} = 2\mathcal{A}_M(v) - 4(vx_{M-2}x_{M-1}y_M)^2\mathcal{A}_{M-3}(v)\,. \tag{4.96}$$

All of these expressions are proportional to the identity, as they depend only on the characteristic polynomials $\mathcal{A}_m(v)$. Therefore, we can always define an operator that squares to the identity as $\Psi_0 = \mathcal{Q}/c_0$, where, for circuit I:

$$c_0^2 = \lim_{u\to\infty} x_M^2\frac{\mathcal{A}_{M-1}(iu)}{\mathcal{A}_M(iu)}\,, \tag{4.97}$$

for circuit II

$$c_0^2 = \lim_{u\to\infty} (x_{M-1}x_M)^2 \frac{\mathcal{A}_{M-2}(iu)}{\mathcal{A}_M(iu)}\,, \tag{4.98}$$

and for circuit III

$$c_0^2 = 1 + \lim_{u\to\infty} \frac{(ux_{M-2}x_{M-1}y_M)^2 \mathcal{A}_{M-3}(iu)}{\mathcal{A}_M(u)}\,. \tag{4.99}$$

We can also use the anticommutator $\{\chi, A_M(-v)\chi A_M(v)\}$ to prove the third property in (4.92). Indeed, by setting $v = iu_l$ and dividing by the normalization constants, we obtain the anticommutator between χ and Ψ_l, which reads:

$$\{\chi, \Psi_l\} = \frac{1}{N_l} \begin{cases} 4x_M^2 \mathcal{A}_{M-1}(iu_l) & \text{for circuit I,} \\ 4(x_M x_{M-1})^2 \mathcal{A}_{M-2}(iu_l) & \text{for circuit II,} \\ -(2iu_l x_{M-2}x_{M-1}y_M)^2 \mathcal{A}_{M-3}(iu_l) & \text{for circuit III}\,. \end{cases} \tag{4.100}$$

Next, expressing the terms $\mathcal{A}_m(iu_l)$ in terms of the normalization constants (4.36),(4.81) and (4.82) for circuit I, II and III, respectively, we find that, for all three circuits:

$$\{\chi, \Psi_l\} = \frac{N_l}{-2iu_l \mathcal{A}'_M(iu_l)} = c_l\,. \tag{4.101}$$

Finally, using the decomposition in Eq. (4.91), we have:

$$c_l = \{\chi, \Psi_l\} = \sum_{l'=-S,\, l'\neq 0}^{S} c_{l'}\{\Psi_{l'}, \Psi_l\} + \{\mathcal{Q}, \Psi_l\} = c_l + \{\mathcal{Q}, \Psi_l\}\,. \tag{4.102}$$

It then follows immediately that $\{\mathcal{Q}, \Psi_l\} = 0$ confirming that the third property in (4.92) is satisfied.

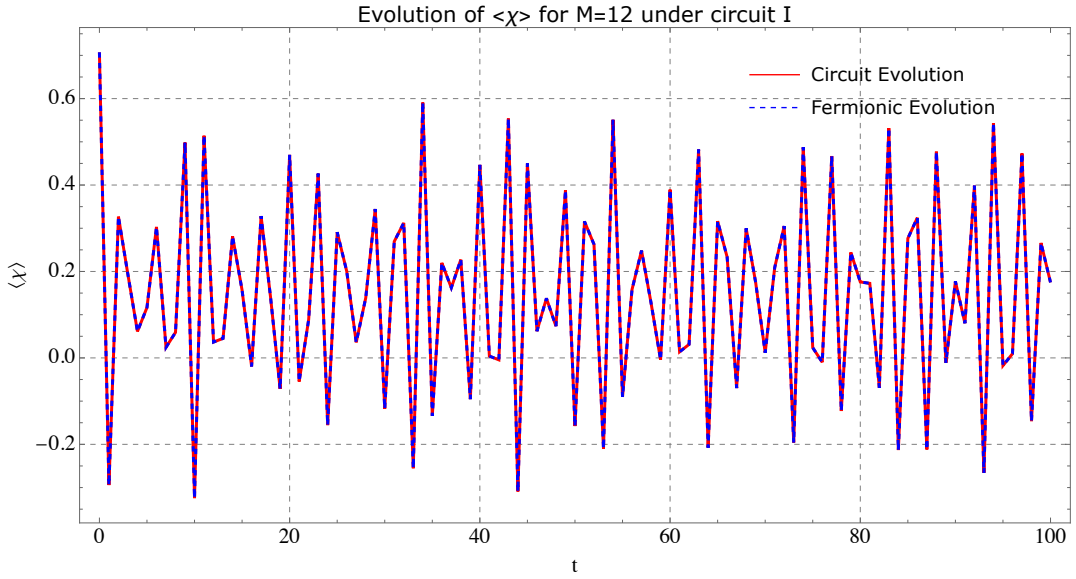

Figure 4.2: Time evolution under circuit I of the expectation value of the edge operator $\chi = Z_M$ starting from the initial spin state $|\psi_0\rangle = \otimes_{m=1}^{M}(\cos\theta\,|0\rangle + \sin\theta\,|1\rangle)$, with $\theta = \pi/8$. We chose the angles as $\phi_m = 1$.

We did not provide an analytical proof of the second property for circuits I and II. However, we have verified numerically, for system sizes up to $M = 12$ that

$$[A_M(v), \mathcal{Q}] = 0 \tag{4.103}$$

which reduces to the second property for $v = 1$. For circuit III, an analytical proof is given in the appendix of [36].

With these results established, we can now compare the time evolution for all three circuits. Our goal is to compute the time evolution of the expectation value of χ for a generic initial spin product state. In particular, we consider a state of the form

$$|\psi_0\rangle = \bigotimes_{m=1}^{M} (\cos\theta\,|0\rangle_m + \sin\theta\,|1\rangle_m)\,, \tag{4.104}$$

with $\theta = \pi/8$. Furthermore, we set all angles $\phi_m = 1$, corresponding to a homogeneous circuit. However, we tested the code also for random angles and other simple initial product states.

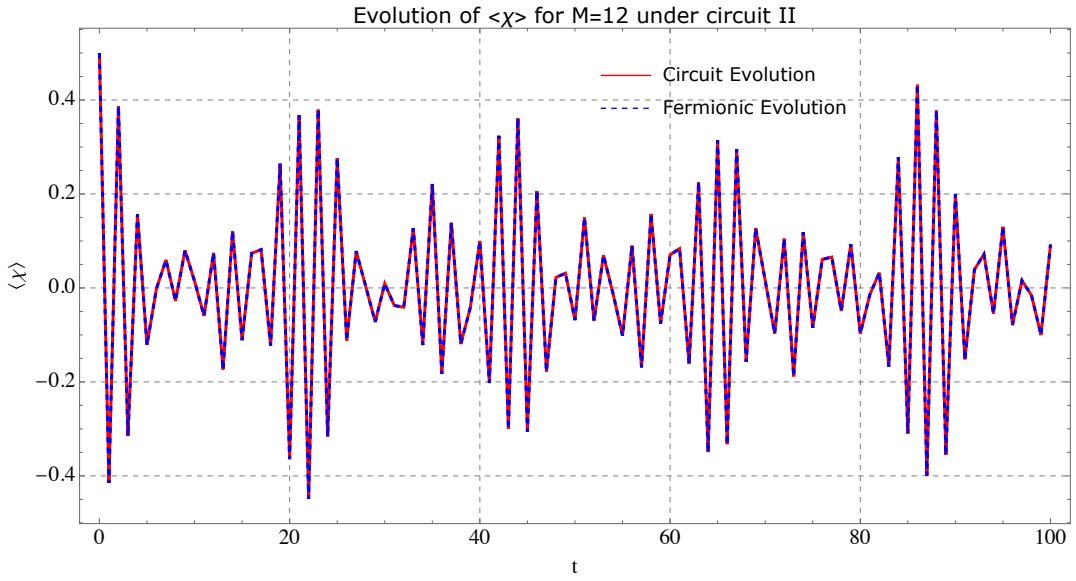

Figure 4.3: Time evolution under circuit II of the expectation value of the edge operator $\chi = Z_{M-1}Z_M$ starting from the initial spin state $|\psi_0\rangle = \otimes_{m=1}^{M}(\cos\theta\,|0\rangle + \sin\theta\,|1\rangle)$, with $\theta = \pi/8$. We chose the angles as $\phi_m = 1$.

Let us now consider the two types of time evolution we are comparing. On one hand, we have the "fermionic evolution", where the time-evolved edge operator is represented as

$$\chi(t) = \sum_{l=-S, l\neq 0}^{S} c_l \left(\frac{iu_l - 1}{iu_l + 1}\right)^t \Psi_l + c_0 \Psi_0\,, \tag{4.105}$$

with $t \in \mathbb{N}$, and therefore the corresponding expectation value is

$$\langle\chi(t)\rangle = \langle\psi_0|\,\chi(t)\,|\psi_0\rangle = \sum_{l=-S, l\neq 0}^{S} c_l \left(\frac{iu_l - 1}{iu_l + 1}\right)^t \langle\psi_0|\,\Psi_l\,|\psi_0\rangle + c_0\,\langle\psi_0|\,\Psi_0\,|\psi_0\rangle\,, \tag{4.106}$$

On the other hand, we have the standard circuit evolution, given by

$$\langle\chi(t)\rangle = \langle\psi_0|\,(\mathcal{V}_M^\dagger)^t \chi (\mathcal{V}_M)^t\,|\psi_0\rangle\,. \tag{4.107}$$

The circuit evolution of Eq. (4.107), is applied to the edge operator in its spin representation. In the representation (3.12), this corresponds to $\chi = Z_M$ for circuit I and III, whereas $\chi = Z_{M-1}Z_M$ for circuit II.

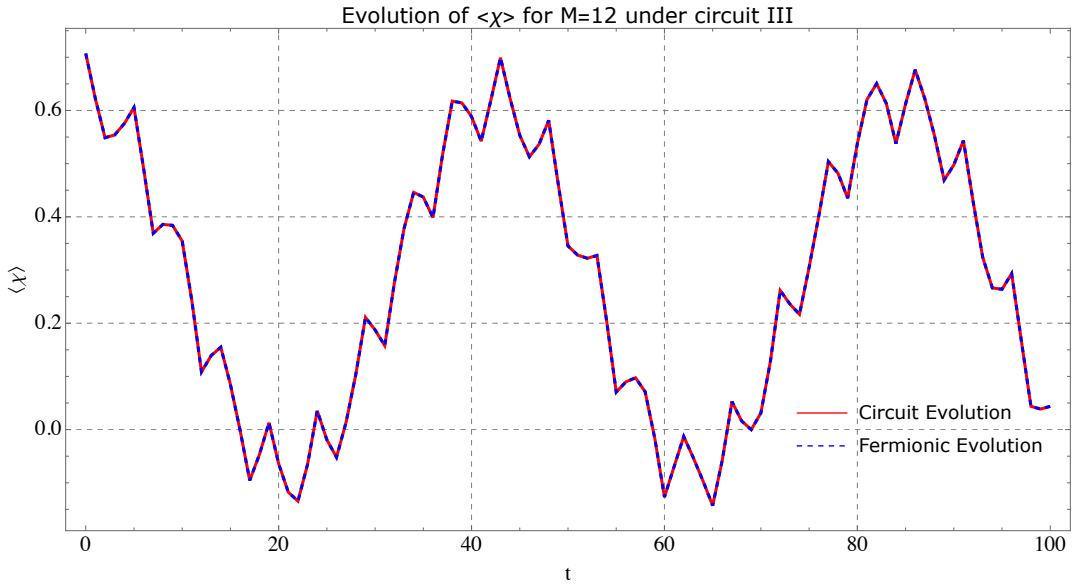

Figure 4.4: Time evolution under circuit III of the expectation value of the edge operator $\chi = Z_M$ starting from the initial spin state $|\psi_0\rangle = \otimes_{m=1}^{M}(\cos\theta\,|0\rangle + \sin\theta\,|1\rangle)$, with $\theta = \pi/8$. We chose the angles as $\phi_m = 1$.

In contrast, the so-called fermionic evolution does not treat χ as a spin operator, and rather it describes the evolution entirely within the fermionic space.

In Figures 4.2, 4.3, and 4.4, we show the time evolution of $\langle\chi(t)\rangle$ computed using both Eq. (4.106) and Eq. (4.107) for circuits I, II, and III, respectively. We consider a system size of $M = 12$, although we also tested the code for smaller system sizes, with time t ranging from 0 to 100. In all three circuits, the results from the two methods agree perfectly.

4.2.1 Simulability of FFD Circuits

We now turn to the question of the simulability of FFD circuits. Specifically, we ask whether it is possible to simulate the time evolution of the edge operator in a time that scales polynomially with the system size. For this analysis, we focus on circuit III, following [36], since its finite depth makes it particularly suitable for implementation on current noisy quantum devices [37].

From Eq. (4.106), we see that determining the time evolution of $\langle\chi(t)\rangle$ requires only the computation of the initial expectation values $\langle\psi_0|\,\Psi_l\,|\psi_0\rangle$. This can be done in two steps.

The first step is to compute the roots of the polynomial $\mathcal{A}_M(u)$ in order to define the fermionic operators Ψ_l. This step can be carried out efficiently, as the computational cost of finding the complex roots of a polynomial of degree n scales as $O(n^3)$ [66].

Next, we actually compute the expectation values $\langle\psi_0|\,\Psi_l\,|\psi_0\rangle$. This can also be done efficiently thanks to the matrix product operator (MPO) form of the transfer matrix in Eq. (4.60). The expectation values can be expressed as a tensor network [64] constructed from the $\Omega_m^{(\mathrm{III})}(\pm iu_l)$ and the edge operator χ, which can then be contracted with a computational cost that scales polynomially with system size. While we will not discuss tensor networks further in this thesis, we refer the reader to [36] for more details. In that work, this method was used to compute $\langle\chi(t)\rangle$ for system sizes up to $M = 150$ and times $t = 70$, going far beyond the reach of exact-diagonalization approaches.

Conclusions and Outlook

Free fermionic models have played a central role in theoretical physics for decades. Their connection to qubit systems through the Jordan–Wigner transformation has been crucial for analytically solving paradigmatic spin$-1/2$ chain models. Moreover, due to their classical simulability, these models also became valuable benchmarks for numerical simulations in quantum computers. It appeared that free fermionic systems were well understood, serving mainly as tools for exploring new phenomena within simple and familiar settings.

However, Free Fermions in Disguise (FFD) shifted this view by introducing new types of free fermionic models connected to spin chains in significantly more elaborate ways. These models raised numerous doubts about what had been assumed regarding qubit systems associated with free fermions. Their intricate structure led to new questions about how observables and states in the qubit representation relate to those in the auxiliary fermionic description, and about whether one can design free fermionic quantum circuits that are classically simulable starting from these models.

In this thesis, we have addressed these questions. Specifically, in Chapter 4, we present the findings of our work [36], where we analytically demonstrated the free fermionic nature of certain quantum circuits constructed from FFD models, which were previously introduced in the literature. Furthermore, in Section 4.2, we examined the time evolution of the edge mode under the action of these circuits. This operator had already been shown to admit an expansion as a linear combination of the FFD creation and annihilation operators in the Hamiltonian context. Here, we generalized this decomposition in the circuit context, and we compared the dynamics in the qubit representation with those in the fermionic one, demonstrating their complete equivalence for all three circuits, as illustrated in Figures 4.2, 4.3, and 4.4. This provided a type of exact-diagonalization check for these circuit evolutions. Finally, in [36] we also examined more closely the simulability of one particular circuit, the only one with finite depth. Particularly, we showed that local observables written in terms of fermionic operators can be computed efficiently, with computational cost growing polynomially rather than exponentially with system size. However, we did not examine this aspect in detail within this thesis.

From these results, there are still several open questions and directions worth exploring about Free Fermions in Disguise. To begin with, the classical simulability of these circuits motivates the development of a systematic method for expressing spin operators in terms of fermionic ones. Progress beyond what was discussed in Section 3.3 might be possible by using the full description of the Hilbert-space structure presented in Subsection 3.3.3. Since it has been established that local observables expressible in terms of fermionic operators can be computed efficiently, being able to rewrite physically relevant local quantities, such as the magnetization, in that language would allow us to study their dynamics in FFD models, a question that remains entirely open.

It would also be interesting to investigate the computation of expectation values of local observables starting from low-entangled states rather than simple product states. The proof of simulability for these circuits essentially reduces to contracting certain tensor networks, a procedure that could in principle be carried out for any Matrix Product State (MPS), not only for product states. This would make it possible

to explore how initial entanglement affects the time evolution of local quantities.

Finally, it would be valuable to identify spin states that can be mapped to fermionic Gaussian states through the FFD mapping. Such a characterization would allow the study of arbitrary observables on this particular class of states, which, as discussed in Section 2.3, remain classically simulable, since are fully described by a matrix whose size grows only polynomially with the system size. This would also make it possible to investigate global observables such as the entanglement entropy, which does not appear to be accessible with the methods developed in [36].

Many additional questions could certainly be posed, as Free Fermions in Disguise remain a relatively new and largely unexplored class of models, and several of their potential applications may still be entirely unknown.

Appendix A

Proof of Matchgates Generators

In this Appendix, we provide a proof that the generators of the matchgates defined in Definition 2.1 are the one given in (2.11).

To prove this, one can use the following parametrization for the unitaries A and B:

$$A = e^{i\varphi_A/2}\begin{pmatrix} e^{i\alpha_A}\cos\theta_A & e^{i\beta_A}\sin\theta_A \\ -e^{-i\beta_A}\sin\theta_A & e^{-i\alpha_A}\cos\theta_A \end{pmatrix}, \qquad B = e^{i\varphi_B/2}\begin{pmatrix} e^{i\alpha_B}\cos\theta_B & e^{i\beta_B}\sin\theta_B \\ -e^{-i\beta_B}\sin\theta_B & e^{-i\alpha_B}\cos\theta_B \end{pmatrix}, \tag{A.1}$$

then notice that $\det A = e^{i\varphi_A/2}$ and the same for B. The matchgate condition $\det A = \det B$ then implies $\varphi_A = \varphi_B$. We therefore obtain:

$$G(A,B) = e^{i\varphi/2}\begin{pmatrix} e^{i\alpha_A}\cos\theta_A & 0 & 0 & e^{i\beta_A}\sin\theta_A \\ 0 & e^{i\alpha_B}\cos\theta_B & e^{i\beta_B}\sin\theta_B & 0 \\ 0 & -e^{-i\beta_B}\sin\theta_B & e^{-i\alpha_B}\cos\theta_B & 0 \\ -e^{-i\beta_A}\sin\theta_A & 0 & 0 & e^{-i\alpha_A}\cos\theta_A \end{pmatrix}. \tag{A.2}$$

To compute the generators, we can then simply evaluate the derivatives of (A.2) with respect to each of the parameters divided by i at the identity, by posing all parameters equal to zero. This is related to Lie Group and Lie Algebra theory [67, 68].

For the generators, we get the following matrices:

$$\begin{aligned}
&\frac{1}{i}\frac{dG(A,B)}{d\alpha_A}\bigg|_{\mathbb{1}} = \mathrm{diag}(0,1,-1,0), \qquad \frac{1}{i}\frac{dG(A,B)}{d\alpha_B}\bigg|_{\mathbb{1}} = \mathrm{diag}(1,0,0,-1), \\
&\frac{1}{i}\frac{dG(A,B)}{d\beta_A}\bigg|_{\mathbb{1}} = \begin{pmatrix} 0&0&0&0\\0&0&1&0\\0&1&0&0\\0&0&0&0 \end{pmatrix}, \qquad \frac{1}{i}\frac{dG(A,B)}{d\beta_B}\bigg|_{\mathbb{1}} = \begin{pmatrix} 0&0&0&1\\0&0&0&0\\0&0&0&0\\1&0&0&0 \end{pmatrix}, \\
&\frac{1}{i}\frac{dG(A,B)}{d\theta_A}\bigg|_{\mathbb{1}} = \begin{pmatrix} 0&0&0&0\\0&0&-i&0\\0&i&0&0\\0&0&0&0 \end{pmatrix}, \qquad \frac{1}{i}\frac{dG(A,B)}{d\theta_B}\bigg|_{\mathbb{1}} = \begin{pmatrix} 0&0&0&-i\\0&0&0&0\\0&0&0&0\\i&0&0&0 \end{pmatrix}.
\end{aligned} \tag{A.3}$$

The derivative with respect to φ is zero and we can therefore ignore it.

The generators of (A.3) are still not the one in the set (2.11). To obtain those, we must linearly combine

some of the generators above, as:

$$
\begin{aligned}
Z \otimes \mathbb{1} &= \mathrm{diag}(1,1,-1,-1) = \frac{1}{i}\frac{dG(A,B)}{d\alpha_A}\bigg|_{\mathbb{1}} + \frac{1}{i}\frac{dG(A,B)}{d\alpha_B}\bigg|_{\mathbb{1}}, \\
\mathbb{1} \otimes Z &= \mathrm{diag}(1,-1,1,-1) = -\frac{1}{i}\frac{dG(A,B)}{d\alpha_A}\bigg|_{\mathbb{1}} + \frac{1}{i}\frac{dG(A,B)}{d\alpha_B}\bigg|_{\mathbb{1}}, \\
X \otimes X &= \begin{pmatrix} 0 & 0 & 0 & 1 \\ 0 & 0 & 1 & 0 \\ 0 & 1 & 0 & 0 \\ 1 & 0 & 0 & 0 \end{pmatrix} = \frac{1}{i}\frac{dG(A,B)}{d\beta_A}\bigg|_{\mathbb{1}} + \frac{1}{i}\frac{dG(A,B)}{d\beta_B}\bigg|_{\mathbb{1}}, \\
Y \otimes Y &= \begin{pmatrix} 0 & 0 & 0 & -1 \\ 0 & 0 & 1 & 0 \\ 0 & 1 & 0 & 0 \\ -1 & 0 & 0 & 0 \end{pmatrix} = \frac{1}{i}\frac{dG(A,B)}{d\beta_A}\bigg|_{\mathbb{1}} - \frac{1}{i}\frac{dG(A,B)}{d\beta_B}\bigg|_{\mathbb{1}}, \\
X \otimes Y &= \begin{pmatrix} 0 & 0 & 0 & -i \\ 0 & 0 & i & 0 \\ 0 & -i & 0 & 0 \\ i & 0 & 0 & 0 \end{pmatrix} = -\frac{1}{i}\frac{dG(A,B)}{d\theta_A}\bigg|_{\mathbb{1}} + \frac{1}{i}\frac{dG(A,B)}{d\theta_B}\bigg|_{\mathbb{1}}, \\
Y \otimes X &= \begin{pmatrix} 0 & 0 & 0 & -i \\ 0 & 0 & -i & 0 \\ 0 & i & 0 & 0 \\ i & 0 & 0 & 0 \end{pmatrix} = \frac{1}{i}\frac{dG(A,B)}{d\theta_A}\bigg|_{\mathbb{1}} + \frac{1}{i}\frac{dG(A,B)}{d\theta_B}\bigg|_{\mathbb{1}}.
\end{aligned}
\tag{A.4}
$$

Then, the set $\mathcal{A}_{i,j}$ of Eq. (2.11) is recovered.

Appendix B

Proof of Useful Results for FFD Circuits

In this appendix we show explicitely some useful calculations which we did not include in the main text of Chapter 4.

In particular, we compute the commutators $\{\chi, A_M(-v)\chi A_M(v)\}$ for circuit I, II and III of Eqs. (4.3)-(4.5). Here, χ is the edge operator, satisfying (3.36) for circuit I and III, while (4.83) for circuit II. On the other hand, the $A_M(v)$ are the transfer matrices defined from the operator A of (4.6) for the three circuits.

Let us start with circuit I. We use the recursion (4.20) for $A_M(u)$, the one of Eq. (4.31) for $\mathcal{A}_M(u) = A_M(u)A_M(-u)$ and that χ must commute with $A_{M-1}(u)$, while it anticommutes with $B_{M-1}(u)$, as one can easily see from their definitions. This yields to Eq. (4.94):

$$\begin{aligned}\{\chi, A_M(-v)\chi A_M(v)\} &= \chi A_M(-v)\chi A_M(v) + A_M(-v)\chi A_M(v)\chi = \\ &= (x_M A_{M-1}(-v) - y_M B_{M-1}(-v))A_M(v) + A_M(-v)(x_M A_{M-1}(v) - y_M B_{M-1}(v)) = \\ &= 2x_M^2 \mathcal{A}_{M-1}(v) - 2y_M^2 \mathcal{B}_{M-1}(v) = -2\mathcal{A}_M(v) + 4x_M^2 \mathcal{A}_{M-1}(v)\,.\end{aligned} \tag{B.1}$$

Next, we consider circuit II. Using (4.64) for $A_M(u)$ and that χ commute with $A_{M-2}(u)$, while it anti-commutes with $B_{M-2}(u)$ and $C_{M-2}(u)$, we get two following two terms:

$$X \equiv (x_M x_{M-1} A_{M-2}(-v) - y_{M-1} B_{M-2}(-v) - x_{M-1} y_M C_{M-2}(-v))A_M(v)\,, \tag{B.2}$$

$$Y \equiv A_M(-v)(x_M x_{M-1} A_{M-2}(v) - y_{M-1} B_{M-2}(v) - x_{M-1} y_M C_{M-2}(v))\,. \tag{B.3}$$

We use (4.64) once again to express the two terms as:

$$\begin{aligned}X =&(x_M x_{M-1})^2 \mathcal{A}_{M-2}(v) - y_{M-1}^2 \mathcal{B}_{M-2}(v) - (x_{M-1} y_M)^2 \mathcal{C}_{M-2}(v) \\ &+ x_M x_{M-1} y_{M-1}[A_{M-2}(-v)B_{M-2}(v) - B_{M-2}(-v)A_{M-2}(v)] \\ &+ x_M x_{M-1}^2 y_M[A_{M-2}(-v)C_{M-2}(v) - C_{M-2}(-v)A_{M-2}(v)] \\ &- x_M y_{M-1} y_M[B_{M-2}(-v)C_{M-2}(v) + C_{M-2}(-v)B_{M-2}(v)]\,,\end{aligned} \tag{B.4}$$

$$\begin{aligned}Y =&(x_M x_{M-1})^2 \mathcal{A}_{M-2}(v) - y_{M-1}^2 \mathcal{B}_{M-2}(v) - (x_{M-1} y_M)^2 \mathcal{C}_{M-2}(v) \\ &+ x_M x_{M-1} y_{M-1}[-A_{M-2}(-v)B_{M-2}(v) + B_{M-2}(-v)A_{M-2}(v)] \\ &+ x_M x_{M-1}^2 y_M[-A_{M-2}(-v)C_{M-2}(v) + C_{M-2}(-v)A_{M-2}(v)] \\ &- x_M y_{M-1} y_M[B_{M-2}(-v)C_{M-2}(v) + C_{M-2}(-v)B_{M-2}(v)]\,.\end{aligned} \tag{B.5}$$

We see that the terms in the second and third line of (B.4) and (B.5) are one the opposite of another and therefore cancel. On the other hand, one can use (4.23) to show that $B_{M-2}(-v)C_{M-2}(v)+C_{M-2}(-v)B_{M-2}(v)=0$. We therefore obtain Eq. (4.95), using (4.73):

$$\begin{aligned}\{\chi, A_M(-v)\chi A_M(v)\} &= 2(x_M x_{M-1})^2\mathcal{A}_{M-2}(v) - 2y_{M-1}^2\mathcal{B}_{M-2}(v) - 2(x_{M-1}y_M)^2\mathcal{C}_{M-2}(v) = \\ &= -2\mathcal{A}_M(v) + 4(x_M x_{M-1})^2\mathcal{A}_{M-2}(v)\,.\end{aligned} \tag{B.6}$$

Finally, let us consider circuit III. In (4.68), we have $A_{M-3}(u)$, $B_{M-3}(u)$, $C_{M-3}(u)$ and $\kappa_M^+(u)$ as terms that interact with χ. Here, we get that χ commutes with $A_{M-3}(u)$, $B_{M-3}(u)$ and $C_{M-3}(u)$, but it anticommutes with the h_M in $\kappa_M^+(u)$, sending $\kappa_M^+(u)\to\kappa_M^+(-u)$ and viceversa. Hence, we obtain:

$$X \equiv (x_{M-1}x_{M-2}A_{M-3}(-v)\kappa_M^+(v) + y_{M-2}B_{M-3}(-v) + x_{M-2}y_{M-1}C_{M-3}(-v))A_M(v)\,, \tag{B.7}$$

$$Y \equiv A_M(-v)(x_{M-1}x_{M-2}A_{M-3}(v)\kappa_M^+(-v) + y_{M-2}B_{M-3}(v) + x_{M-2}y_{M-1}C_{M-3}(v))\,. \tag{B.8}$$

Expanding the prodcuts, this time we get the following, using that inverting the order of $\kappa_M^+(u)$ with $B_M(u)$ and $C_M(u)$ sends once again $\kappa_M^+(u)\to\kappa_M^+(-u)$ and viceversa:

$$\begin{aligned}X =&(x_{M-1}x_{M-2})^2\mathcal{A}_{M-3}(v)(\kappa_M^+(v))^2 + y_{M-2}^2\mathcal{B}_{M-3}(v) + (x_{M-2}y_{M-1})^2\mathcal{C}_{M-3}(v)\\ &+ x_{M-1}x_{M-2}y_{M-2}[\kappa_M^+(v)A_{M-3}(-v)B_{M-3}(v) + \kappa_M^+(-v)B_{M-3}(-v)A_{M-3}(v)]\\ &+ x_{M-1}x_{M-2}^2y_{M-1}[\kappa_M^+(v)A_{M-3}(-v)C_{M-3}(v) + \kappa_M^+(-v)C_{M-3}(-v)A_{M-3}(v)]\\ &+ y_{M-2}x_{M-2}y_{M-1}[B_{M-3}(-v)C_{M-3}(v) + C_{M-3}(-v)B_{M-3}(v)]\,,\end{aligned} \tag{B.9}$$

$$\begin{aligned}Y =&(x_{M-1}x_{M-2})^2\mathcal{A}_{M-3}(-v)(\kappa_M^+(v))^2 + y_{M-2}^2\mathcal{B}_{M-3}(v) + (x_{M-2}y_{M-1})^2\mathcal{C}_{M-3}(v)\\ &+ x_{M-1}x_{M-2}y_{M-2}[\kappa_M^+(-v)A_{M-3}(-v)B_{M-3}(v) + \kappa_M^+(v)B_{M-3}(-v)A_{M-3}(v)]\\ &+ x_{M-1}x_{M-2}^2y_{M-1}[\kappa_M^+(-v)A_{M-3}(-v)C_{M-3}(v) + \kappa_M^+(v)C_{M-3}(-v)A_{M-3}(v)]\\ &+ y_{M-2}x_{M-2}y_{M-1}[B_{M-3}(-v)C_{M-3}(v) + C_{M-3}(-v)B_{M-3}(v)]\,.\end{aligned} \tag{B.10}$$

Now, we can notice that in the second and third lines of Eqs. (B.9) and (B.10), $\kappa_M^+(v)$ and $\kappa_M^+(-v)$ are exchanged: the terms proportional to h_M will be opposite to each other and therefore cancel. On ther other hand, we can also use that $A_{M-3}(-v)B_{M-3}(v) + B_{M-3}(-v)A_{M-3}(v) = A_{M-3}(-v)C_{M-3}(v) + C_{M-3}(-v)A_{M-3}(v) = B_{M-3}(-v)C_{M-3}(v) + C_{M-3}(-v)B_{M-3}(v) = 0$ from (4.23) to cancel the second, third and fourth lines. Then, using that $(\kappa_M^+(\pm v))^2 = x_M^2 - v^2y_M^2 \pm 2ivx_My_Mh_M$, we see that once again in the sum $X+Y$ the terms proportional to h_M cancel and we remain with:

$$\begin{aligned}\{\chi, A_M(-v)\chi A_M(v)\} &= 2(x_{M-1}x_{M-2})^2\mathcal{A}_{M-3}(v)(x_M^2 - v^2y_M^2) + 2y_{M-2}^2\mathcal{B}_{M-3}(v) + 2(x_{M-2}y_{M-1})^2\mathcal{C}_{M-3}(v) = \\ &= 2\mathcal{A}_M(v) - 4(vx_{M-2}x_{M-1}y_M)^2\mathcal{A}_{M-3}(v)\,,\end{aligned} \tag{B.11}$$

where we used (4.77). Hence, we proved also (4.96).

Bibliography

[1] P. Jordan and E. Wigner, "Über das Paulische äquivalenzverbot", Zeitschrift für Physik **47**, 631–651 (1928).

[2] E. Lieb, T. Schultz, and D. Mattis, "Two soluble models of an antiferromagnetic chain", Ann. Phys. **16**, 407–466 (1961).

[3] F. Franchini, *An introduction to integrable techniques for one-dimensional quantum systems*, Vol. 940 (Springer, 2017).

[4] G. B. Mbeng, A. Russomanno, and G. E. Santoro, "The quantum ising chain for beginners", SciPost Phys. Lect. Notes, 82 (2024).

[5] T. D. Schultz, D. C. Mattis, and E. H. Lieb, "Two-dimensional ising model as a soluble problem of many fermions", Rev. Mod. Phys. **36**, 856–871 (1964).

[6] E. Fradkin, "Jordan-wigner transformation for quantum-spin systems in two dimensions and fractional statistics", Phys. Rev. Lett. **63**, 322–325 (1989).

[7] Y. R. Wang, "Ground state of the two-dimensional antiferromagnetic heisenberg model studied using an extended wigner-jordon transformation", Phys. Rev. B **43**, 3786–3789 (1991).

[8] L. Huerta and J. Zanelli, "Bose-fermi transformation in three-dimensional space", Phys. Rev. Lett. **71**, 3622–3624 (1993).

[9] F. Verstraete and J. I. Cirac, "Mapping local hamiltonians of fermions to local hamiltonians of spins", J. Stat. Mech: Theory Exp. **2005**, P09012 (2005).

[10] C. D. Batista and G. Ortiz, "Generalized jordan-wigner transformations", Phys. Rev. Lett. **86**, 1082–1085 (2001).

[11] K. Minami, "Solvable hamiltonians and fermionization transformations obtained from operators satisfying specific commutation relations", J. Phys. Soc. Jpn. **85**, 024003 (2016).

[12] K. Minami, "Infinite number of solvable generalizations of xy-chain, with cluster state, and with central charge c=m/2", Nucl. Phys. B **925**, 144–160 (2017).

[13] A. Chapman and S. T. Flammia, "Characterization of solvable spin models via graph invariants", Quantum **4**, 278 (2020).

[14] M. Ogura, Y. Imamura, N. Kameyama, K. Minami, and M. Sato, "Geometric criterion for solvability of lattice spin systems", Phys. Rev. B **102**, 245118 (2020).

[15] V. Bach, E. H. Lieb, and J. P. Solovej, "Generalized hartree-fock theory and the hubbard model", J. Stat. Phys. **76**, 3–89 (1994).

[16] S. Bravyi, "Lagrangian representation for fermionic linear optics", arXiv quant-ph/0404180 (2004).

[17] J. Surace and L. Tagliacozzo, "Fermionic Gaussian states: an introduction to numerical approaches", SciPost Phys. Lect. Notes, 54 (2022).

[18] G. C. Wick, "The evaluation of the collision matrix", Phys. Rev. **80**, 268–272 (1950).

[19] L. G. Molinari, "Notes on wick's theorem in many-body theory", arXiv:1710.09248 (2023).

[20] M. Gaudin, "Une démonstration simplifiée du théorème de wick en mécanique statistique", Nuclear Physics **15**, 89–91 (1960).

[21] L. G. Valiant, "Quantum computers that can be simulated classically in polynomial time", in Proceedings of the thirty-third annual acm symposium on theory of computing, STOC '01 (2001), pp. 114–123.

[22] B. M. Terhal and D. P. DiVincenzo, "Classical simulation of noninteracting-fermion quantum circuits", Phys. Rev. A **65**, 032325 (2002).

[23] R. Jozsa and A. Miyake, "Matchgates and classical simulation of quantum circuits", Proc. R. Soc. A **464**, 3089–3106 (2008).

[24] D. J. Brod, "Efficient classical simulation of matchgate circuits with generalized inputs and measurements", Phys. Rev. A **93**, 062332 (2016).

[25] P. Fendley and K. Schoutens, "Cooper pairs and exclusion statistics from coupled free-fermion chains", J. Stat. Mech: Theory Exp. **2007**, P02017 (2007).

[26] J. de Gier, G. Z. Feher, B. Nienhuis, and M. Rusaczonek, "Integrable supersymmetric chain without particle conservation", J. Stat. Mech: Theory Exp. **2016**, 023104 (2016).

[27] G. Z. Feher, A. Garbali, J. d. Gier, and K. Schoutens, "A curious mapping between supersymmetric quantum chains", in *2017 matrix annals*, edited by J. de Gier, C. E. Praeger, and T. Tao (Springer International Publishing, Cham, 2019), pp. 167–184.

[28] P. Fendley, "Free fermions in disguise", J. Phys. A: Math. Theor. **52**, 335002 (2019).

[29] S. J. Elman, A. Chapman, and S. T. Flammia, "Free fermions behind the disguise", Commun. Math. Phys. **388**, 969–1003 (2021).

[30] A. Chapman, S. J. Elman, and R. L. Mann, "A unified graph-theoretic framework for free-fermion solvability", arXiv:2305.15625 (2023).

[31] P. Fendley and B. Pozsgay, "Free fermions beyond Jordan and Wigner", SciPost Phys. **16**, 102 (2024).

[32] K. Fukai and B. Pozsgay, "Quantum circuits with free fermions in disguise", J. Phys. A: Math. Theor. **58**, 175202 (2025).

[33] K. Fukai, I. Vona, and B. Pozsgay, "A free fermions in disguise model with claws", arXiv:2508.05789 (2025).

[34] I. Vona, M. Mestyán, and B. Pozsgay, "Exact real-time dynamics with free fermions in disguise", Phys. Rev. B **111**, 144306 (2025).

[35] E. Vernier and L. Piroli, "The hilbert-space structure of free fermions in disguise", arXiv:2507.15959 (2025).

[36] D. Szász-Schagrin, D. Cristani, L. Piroli, and E. Vernier, "Construction and simulability of quantum circuits with free fermions in disguise", arXiv:2509.22585 (2025).

[37] J. Preskill, "Quantum Computing in the NISQ era and beyond", Quantum **2**, 79 (2018).

[38] L. D. Landau, E. M. Lifshitz, and L. Pitaevskii, *Statistical physics: theory of the condensed state*, Vol. 9 (Butterworth-Heinemann, 1980).

[39] L. D. Landau, "The theory of a fermi liquid", Soviet Physics Jetp-Ussr **3**, 920–925 (1957).

[40] D. J. Griffiths and D. F. Schroeter, *Introduction to quantum mechanics* (Cambridge University Press, 2018).

[41] M. Kardar, *Statistical physics of particles* (Cambridge University Press, 2007).

[42] J. W. Negele, *Quantum many-particle systems* (CRC Press, 2018).

[43] J. van Hemmen, "A note on the diagonalization of quadratic boson and fermion hamiltonians", Z. Physik B - Condensed Matter **38**, 271–277 (1980).

[44] M. Barbieri, "Measurement induced phase transitions in free-fermionic quantum circuits", MA thesis (University of Bologna, 2024).

[45] P. Fendley, "Free parafermions", J. Phys. A: Math. Theor. **47**, 075001 (2014).

[46] R. P. Feynman, "Simulating physics with computers", Int. J. Theor. Phys. **21**, 467–488 (1982).

[47] M. A. Nielsen and I. L. Chuang, *Quantum computation and quantum information* (Cambridge University Press, 2010).

[48] M. M. Wilde, *Quantum information theory* (Cambridge University Press, 2013).

[49] H. F. Trotter, "On the product of semi-groups of operators", Proc. Am. Math. Soc. **10**, 545–551 (1959).

[50] M. Van Den Nes, "Classical simulation of quantum computation, the gottesman-knill theorem, and slightly beyond", Quantum Info. Comput. **10**, 258–271 (2010).

[51] M. J. Bremner, R. Jozsa, and D. J. Shepherd, "Classical simulation of commuting quantum computations implies collapse of the polynomial hierarchy", Proc. R. Soc. A **467**, 459–472 (2011).

[52] S. B. Bravyi and A. Y. Kitaev, "Fermionic quantum computation", Ann. Phys. **298**, 210–226 (2002).

[53] M. E. Peskin, *An introduction to quantum field theory* (CRC press, 2018).

[54] F. H. L. Essler and M. Fagotti, "Quench dynamics and relaxation in isolated integrable quantum spin chains", J. Stat. Mech: Theory Exp. **2016**, 064002 (2016).

[55] T. Kinoshita, T. Wenger, and D. S. Weiss, "A quantum Newton's cradle", Nature **440**, 900–903 (2006).

[56] N. Sannomiya and H. Katsura, "Supersymmetry breaking and nambu-goldstone fermions in interacting majorana chains", Phys. Rev. D **99**, 045002 (2019).

[57] E. O'Brien and P. Fendley, "Lattice supersymmetry and order-disorder coexistence in the tricritical ising model", Phys. Rev. Lett. **120**, 206403 (2018).

[58] R. Baxter, "A simple solvable Z_N hamiltonian", Phys. Lett. A **140**, 155–157 (1989).

[59] R. J. Baxter, "Superintegrable chiral potts model: thermodynamic properties, an "inverse" model, and a simple associated hamiltonian", J. Stat. Phys. **57**, 1–39 (1989).

[60] A. L. Retore, "Introduction to classical and quantum integrability", J. Phys. A: Math. Theor. **55**, 173001 (2022).

[61] J.-S. Caux and J. Mossel, "Remarks on the notion of quantum integrability", J. Stat. Mech: Theory Exp. **2011**, P02023 (2011).

[62] F. C. Alcaraz and R. A. Pimenta, "Integrable quantum spin chains with free fermionic and parafermionic spectrum", Phys. Rev. B **102**, 235170 (2020).

[63] E. M. Stein and R. Shakarchi, *Complex analysis*, Vol. 2 (Princeton University Press, 2010).

[64] U. Schollwöck, "The density-matrix renormalization group in the age of matrix product states", Ann. Phys. **326**, January 2011 Special Issue, 96–192 (2011).

[65] E. Altman, K. R. Brown, G. Carleo, L. D. Carr, E. Demler, C. Chin, B. DeMarco, S. E. Economou, M. A. Eriksson, K.-M. C. Fu, M. Greiner, K. R. Hazzard, R. G. Hulet, A. J. Kollár, B. L. Lev, M. D. Lukin, R. Ma, X. Mi, S. Misra, C. Monroe, K. Murch, Z. Nazario, K.-K. Ni, A. C. Potter, P. Roushan, M. Saffman, M. Schleier-Smith, I. Siddiqi, R. Simmonds, M. Singh, I. Spielman, K. Temme, D. S. Weiss, J. Vu čkovi ć, V. Vuleti ć, J. Ye, and M. Zwierlein, "Quantum simulators: architectures and opportunities", PRX Quantum **2**, 017003 (2021).

[66] J. L. Aurentz, T. Mach, R. Vandebril, and D. S. Watkins, "Fast and backward stable computation of roots of polynomials", SIAM J. Matrix Anal. Appl. **36**, 942–973 (2015).

[67] B. C. Hall, "Lie groups, lie algebras, and representations", in *Quantum theory for mathematicians* (Springer, 2013), pp. 333–366.

[68] W.-K. Tung, *Group theory in physics*, Vol. 1 (World Scientific, 1985).